Aalto University
School of Chemical Engineering
Master's Programme in Life Science Technologies

Sofia Julin

Electrostatic self-assembly of DNA origami and gold nanoparticles

Master's Thesis
Espoo, April 23, 2018

Supervisor: Professor Mauri Kostiainen
Advisor: Ph.D., Docent Veikko Linko

Aalto University
School of Chemical Engineering
Master's Programme in Life Science Technologies

ABSTRACT OF
MASTER'S THESIS

Author: Sofia Julin

Title:
Electrostatic self-assembly of DNA origami and gold nanoparticles

Date:	April 23, 2018	**Pages:**	ix + 111
Major:	Biosystems and Biomaterials Engineering	**Code:**	CHEM3028
Supervisor:	Professor Mauri Kostiainen		
Advisor:	Ph.D., Docent Veikko Linko		

Spatially well-ordered structures of gold nanoparticles (AuNPs) and other metal nanoparticles have unique electronic, magnetic and optical properties, and hence there is ever-increasing interest towards these kinds of nanomaterials. DNA and DNA nanostructures have successfully been used to direct the higher-ordered arrangement of AuNPs, but the programmable arrangement of them into larger, well-defined structures is still challenging.

The objective of this thesis is to establish a self-assembly method based on electrostatic interactions in which DNA origami nanostructures can be used to guide the higher ordered arrangement of cationic AuNPs in a controlled and programmable manner. The AuNP binding properties of different DNA origami structures were studied with UV/Vis spectroscopy and agarose gel electrophoretic mobility shift assay. DNA origami-AuNP assemblies were formed during dialysis against decreasing ionic strength, and the formed assemblies were characterized using small-angle X-ray scattering, transmission electron microscopy and cryogenic electron tomography.

Electrostatic self-assembly of DNA origami 6HB nanostructures and small AuNPs (D_{core} = 2.5 nm, $D_{\text{hydrodynamic diameter}}$ = 8.5 nm) yielded highly ordered superlattice structures with a 3D tetragonal lattice structure, whereas other studied combinations of DNA origami structures and AuNPs resulted in amorphous aggregates. These results suggest that both shape and charge complementarity between the building blocks are needed for well-ordered structures to be formed through electrostatic self-assembly. According to the results, electrostatic self-assembly guided by DNA origami structures seems promising for construction of novel, well-ordered structures with unique properties, such as lattice geometry, designed specifically for the chosen application.

Keywords: DNA nanotechnology, DNA origami, self-assembly, gold nanoparticles, functional materials, plasmonics

Language: English

Aalto-universitetet
Högskolan för kemiteknik
Master's Programme in Life Science Technologies

SAMMANDRAG AV
DIPLOMARBETET

Utfört av: Sofia Julin

Arbetets namn:
Elektrostatisk självorganisation av DNA origami och guldnanopartiklar

Datum:	23. april 2018	**Sidantal:**	ix + 111
Huvudämne:	Biosystems and Biomaterials Engineering	**Kod:**	CHEM3028
Övervakare:	Professor Mauri Kostiainen		
Handledare:	Fil.dr., Docent Veikko Linko		

Guldnanopartiklar och andra metallnanopartiklar organiserade i välordnade strukturer har unika elektroniska, magnetiska och optiska egenskaper och därför finns det ett ständigt växande intresse för dessa typer av nanomaterial. DNA och nanostrukturer av DNA har framgångsrikt använts för att framställa välordnade, förutbestämda tredimensionella guldnanopartikelstrukturer, men det finns fortfarande utmaningar att tackla.

Målet med detta diplomarbete är att utveckla en metod för självorganisation baserat på elektrostatiska interaktioner i vilken DNA-origaminanostrukturer på ett programmerbart och kontrollerat sätt kan användas för att styra hurudana strukturer som byggs upp av katjoniska guldnanopartiklar. De olika DNA-origamistrukturernas förmåga att binda guldnanopartiklar studerades med UV/Vis-spektroskopi och agarosgelelektrofores. DNA-origami-guldnanopartikelsystem byggdes upp genom dialys mot stegvis minskade jonkoncentrationer och de uppkomna strukturerna karaktäriserades med lågvinkelspridning, transmissionselektronmikroskopi och kryelektrontomografi.

Elektrostatisk självorganisation av DNA-origami 6HB nanostrukturer och små guldnanopartiklar ($D_{\text{kärna}} = 2.5$ nm, $D_{\text{hydrodynamisk diameter}} = 8.5$ nm) gav välordnade tredimensionella tetragonala kristallstrukturer, medan andra undersökta kombinationer av DNA origami strukturer och guldpartiklar endast resulterade i amorfa strukturer. Detta indikerar att de enskilda byggstenarna behöver kompletterande form och laddning för att välordnade strukturer skall kunna byggas upp genom elektrostatik självorganisation. Det förefaller dock finnas goda framtidsutsikter för elektrostatisk självorganisation som en metod att framställa välordnade strukturer med egenskaper, så som typ av kristallstruktur, lämpliga just för det önskade användningsområdet.

Nyckelord: DNA nanoteknologi, DNA origami, självorganisation, guldnanopartikar, funktionella material, plasmonik

Språk: Engelska

Aalto-yliopisto
Kemian tekniikan korkeakoulu
Master's Programme in Life Science Technologies

DIPLOMITYÖN
TIIVISTELMÄ

Tekijä: Sofia Julin

Työn nimi:
DNA-origamien ja kultananohiukkasten elektrostaattinen itsejärjestyminen

Päiväys:	23. huhtikuuta 2018	**Sivumäärä:**	ix + 111
Pääaine:	Biosystems and Biomaterials Engineering	**Koodi:**	CHEM3028
Valvoja:	Professori Mauri Kostiainen		
Ohjaaja:	FT, Dosentti Veikko Linko		

Hyvin järjestäytyneillä kultananohiukkasilla ja muilla metallisilla nanohiukkasilla on ainutlaatuisia sähköisiä, magneettisia ja optisia ominaisuuksia ja näin ollen näitä nanomateriaaleja kohtaan koetaan jatkuvasti kasvavaa kiinnostusta. DNA:ta ja DNA-nanorakenteita on menestyksekkäästi käytetty ohjaamaan kultananohiukkasten kolmiulotteista järjestymistä, mutta niiden hallittu järjestäminen suuriin ja hyvin määriteltyihin rakenteisiin on edelleen haastavaa.

Tämän diplomityön tarkoituksena on luoda sähköisiin vuorovaikutuksiin pohjautuva itsejärjestymismenetelmä, jossa DNA-origaminanorakenteita voidaan käyttää ohjamaan kationisten kultananohiukkasten järjestymistä hallitulla ja ohjattavalla tavalla. Erilaisten DNA-origamirakenteiden kultananohiukkasten sitomiskykyä tutkittiin ultravioletti- ja näkyvän valon spektroskopialla sekä agaroosielektroforeeesilla. DNA-origami-kultananohiukkasrakenteita muodostettiin dialyysin avulla, dialyysiliuosten ionivahvuutta hitaasti laskien, jonka jälkeen syntyneet rakenteet määritettiin pienkulmaröntgensironnalla, läpäisyelektronimikroskopialla sekä kryoelektronitomografialla.

DNA-origami 6HB nanorakenteiden ja pienien kultananohiukkasten ($D_{\text{sisus}} = 2.5$ nm, $D_{\text{hydrodyaaminen halkaisija}} = 8.5$ nm) elektrostaattinen itsejärjestyminen tuotti suorakulmaisen särmiön mukaisesti järjestyneitä hilarakenteita, kun taas muut tutkitut DNA-origamirakenteiden ja kultananohiukkasten yhdistelmät muodostivat amorfisia ja järjestymättömiä rakenteita. Nämä tulokset viittaavat siihen, että rakenneosasten on oltava yhteensopivia niin muodon kuin varauksenkin kannalla, jotta hyvin muodostuneita rakenteita voidaan saada aikaiseksi elektrostaattisella itsejärjestymisellä. Tulosten perusteella DNA origamirakenteiden ohjaama elektrostaattinen itsejärjestyminen vaikuttavaa lupaavalta menetelmältä muodostaa nanorakenteita, joilla on vaadittavia ominaisuuksia, kuten esimerkiksi tietynlainen hilarakenne.

Asiasanat:	DNA nanoteknologia, DNA origami, itsejärjestyminen, kultananohiukkaset, funktionaaliset materiaalit, plasmoniikka
Kieli:	Englanti

Acknowledgements

This master's thesis was carried out in the Research Group of Biohybrid Materials at the School of Chemical Engineering at Aalto University. This thesis project was maybe not as straightforward as I first expected, but shame on them giving up! Working on this project has been extremely intriguing and challenging, and on the way I have learned a lot and found a huge passion for self-assembled materials.

First of all, I would like to thank professor Mauri Kostiainen for the opportunity to join his research group and get introduced to the fascinating fields of DNA nanotechnology and self-assembly. I am grateful for all your valuable comments and suggestions during this thesis process. In addition, I owe a dept of gratitude to Docent Veikko Linko for advising this thesis and guiding me into the world of DNA origami nanostructures.

I would like to thank Ville Liljeström, Ari Ora, Jukka Hassinen, Maria Heilala and Mauri for providing the gold nanoparticles used in this study, Antti Korpi for helping me with both SAXS and DLS measurements, Nonappa for performing cryo-TEM imaging of the self-assembled structures, and Boxuan Shen for help with conventional TEM imaging. A special thank to Ville for helping also with the interpretation of the SAXS data. I would also like to thank Sami Nummelin, my co-author in the submitted review article about DNA nanostructure-directed self-assembly of AuNPs. Moreover, I want to thank all the members of the Biohybrid Materials Group, it has been and it is a pleasure working with you!

I would like to thank my parents for always supporting me through every choice I have made. Thanks also to all the friends at Teknologföreningen, you made my years of study to an enjoyable and memorable time of my life! Last but not least, I would like to thank Niklas, not for teaching me physics and helping me with the geometry in this thesis (even if you did that too), but for your endless support and for believing in my skills when I do not.

Espoo, April 23, 2018
Sofia Julin

Symbols and abbreviations

Symbols

A	Absorbance
c_{DNA}	DNA origami concentration
c_{i}	Number density of the electrolyte ion
e	Elementary charge
k_{B}	Boltzmann constant
l	Lenght of light path (in centimeters)
T	Absolute temperature (in Kelvin)
q	Magnitude of the scattering vector
z_{i}	Valency of the electrolyte ion
α	Wavelenght of the radiation
ε	Extinction coefficient
ε_0	Vacuum permittivity
ε_{r}	Dielectric constant of the solvent
κ^{-1}	Debye screening lenght
2θ	Scattering angle

Abbreviations

1D	One-dimensional
2D	Two-dimensional
3D	Three-dimensional
6HB	6-helix bundle
24HB	24-helix bundle
60HB	60-helix bundle
AgNP	Silver nanoparticle
AFM	Atomic force microcopy

Au	Gold
AuNP	Gold nanoparticle
AuNR	Gold nanorod
bcc	body-centered cubic
bct	body-centered tetragonal
bp	base pairs
CCMV	Cowpea chlorotic mottle virus
cryo-ET	Cryogenic electron tomography
cryo-TEM	Cryogenic transmission electron microscopy
DLS	Dynamic light scattering
DNA	Deoxyribonucleic acid
dsDNA	Double-stranded DNA
DX	Double-crossover
EDTA	Ethylenediamine tetraacetic acid
EMSA	Electrophoretic mobility shift assay
EtBr	Ethidium bromide
fcc	face-centered cubic
FOB	Folding buffer
hcp	hexagonal close-packed
LSPR	Localized surface plasmon resonance
$MgCl_2$	Magnesium chloride
MUTAB	(11-mercaptoundecyl)-*N,N,N*-trimethylammonium bromide
NaCl	Sodium chloride
NaOH	Sodium hydroxide
PCR	Polymerase chain reaction
PEG	Polyethylene glycol
PX	Paranemic crossover
RCA	Rolling circle amplification
SAXS	Small-angle X-ray scattering
SH	simple hexagonal
ssDNA	Single-stranded DNA
SWNT	Single-walled carbon nanotubes
TAE	Tris-acetate-EDTA
TEM	Transmission electron microscopy
TMV	Tobacco mosaic virus
Tris	Tris(hydroxymethyl)aminomethane
TX	Triple-crossover
UV	Ultraviolet
UV/Vis	Ultraviolet-visible (spectroscopy)

Contents

Chapter 1

Introduction

The past several decades have witnessed a fast growth of the field of nanotechnology, and impressive technological advances have been made in the area. As a result, a diverse toolbox of nanoscale objects with arbitrary shapes, sizes, and material properties is available for use. A full potential utilization of these nano-objects, however, requires their assembly into larger systems in which the individual nano-objects both interact with each other and are organized into predefined, ordered structures [1, 2]. With traditional top-down nanofabrication techniques, this is both hard and costly to achieve. Inspired by the biological systems in nature bottom-up techniques relying on self-assembly have emerged as an attractive low-cost method to construct higher-ordered structures with nanoscale precision [3, 4].

Self-assembly is a process by which components spontaneously, without human guidance or management, form ordered structures [5, 6]. Self-assembly is the method used by nature to create complicated architectures, and material scientists worldwide are therefore investigating the same strategy to organize nanoscale building blocks into completely novel materials with high complexity [7, 8]. A variety of biomolecules, such as DNA [9], proteins [10], peptides [8, 11] and lipids [12], have been used as self-assembling building blocks, and out of them DNA is, due to its unique properties, arguably the most promising one [13, 14].

The revolutionary idea of using DNA as a self-assembling building material to construct well-defined crystal structures was initiated by Nadrian "Ned" Seeman [15] in the early 1980s. Since this pioneering work of Seeman, the field of DNA nanotechnology has grown rapidly (Figure 1.1), and a large variety of different-sized two- and three-dimensional (2D and 3D) DNA nanostructures have been produced [16–18]. A major step forward occurred in 2006 when the DNA origami method was introduced by Paul Rothemund [19].

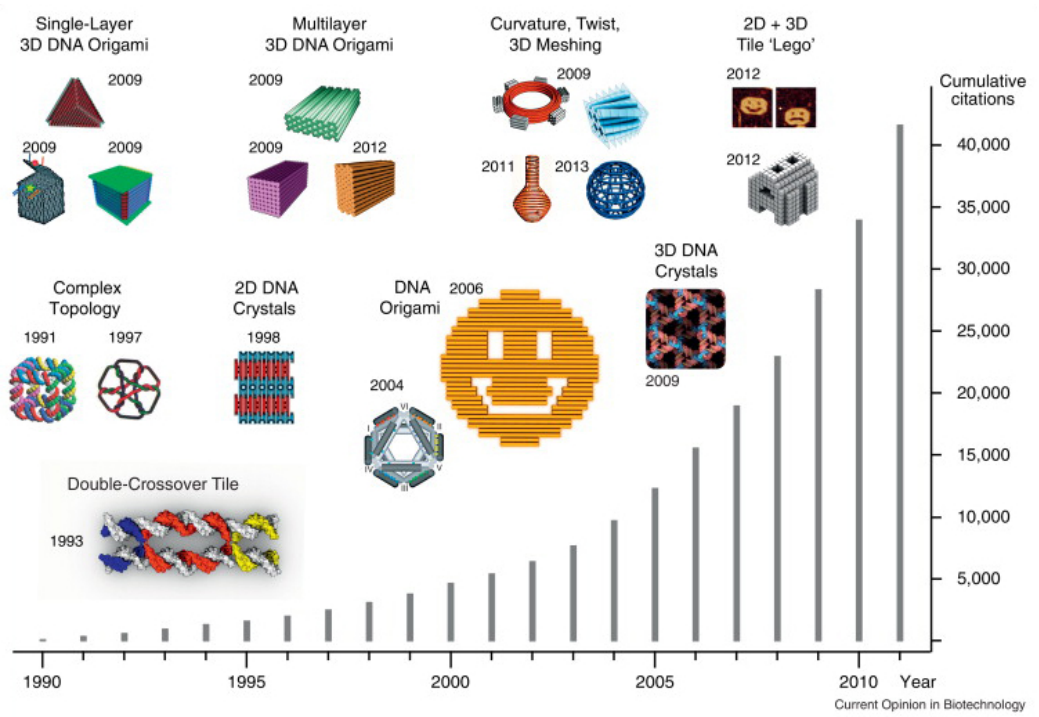

Figure 1.1: The last three decades have withnessed a fast development in the field of structural DNA nanotechnology, and an almost exponential growth in the interest towards structural DNA nanotechnology. Histogram describes the cumulative citations of a set of 1838 articles that handle structural DNA nanotechnology. Reprinted from reference [16].

Gold nanoparticles (AuNPs) have, due to their unique properties, aroused increasing interest in a wide variety of nanotechnology applications, but the programmable arrangement of them into larger, well-defined crystal structures is still challenging [2, 20]. DNA and DNA nanostructures have to some extent successfully been used to direct the higher-ordered lattice arrangement of AuNPs [21], but there are only a few studies [22, 23] reported taking advantage of the electrostatic interactions between the DNA nanostructures and AuNPs in the assembly process. The aim of this thesis is therefore to establish a novel self-assembly method based on electrostatic interactions in which DNA origami nanostructures can be used to guide the higher-ordered arrangement of gold nanoparticles in a controlled and programmable manner.

This thesis is divided into eight sections. Chapter 1, the introduction, presents the background and relevance of the study. Chapters 2 to 5 are the literature part of the thesis. First, the structure and properties of DNA, as

well as the fundamentals of structural DNA nanotechnology are presented in Chapter 2. The DNA origami method is introduced in Chapter 3, the design and synthesis of DNA origamis are discussed, and some utilization possibilities are presented. Chapter 4 gives an introduction to self-assembly and gives the theoretical background in electrostatic self-assembly essential for the self-assembly of DNA origami nanostructures and AuNPs. Chapter 5 focuses on the DNA-directed assembly of AuNPs, with the main focus laying on how DNA nanostructures can be used direct AuNPs into predefined nanostructures. The characteristics of AuNPs and their possible applications are also shortly discussed. The material in Chapter 5.3 draws heavily on a literature review [21] written together with colleagues. Chapters 6 and 7 constitute the experimental part of the thesis. Chapter 6 presents the materials and methods used in the study and explain the conducted experiments in detail. In Chapter 7, the results obtained in this work are presented. Finally, in Chapter 8, conclusions are drawn, and suggestions for future research are made.

Chapter 2

Deoxyribonucleic acid

Deoxyribonucleic acid (DNA) is widely known as the carrier of genetic information, but it is also an excellent building block for bottom-up construction of well-defined structures in the nanoscale regime [13, 17, 24, 25]. In this chapter, the structure and properties of DNA are presented, and the characteristics making DNA a suitable nanoscale building material are highlighted. In addition, self-assembled DNA nanostructures are briefly discussed.

2.1 Structure and properties of DNA

Deoxyribonucleic acid (DNA) is a polynucleotide build up from covalently linked deoxyribonucleotide units (nucleotides). Each nucleotide consists of a nitrogenous base, a five-carbon sugar, and a phosphate group. In the case of DNA, the sugar is 2'-deoxyribose, and the base a derivative of either bicyclic purine or monocyclic pyrimidine. The purine bases are adenine (A) and guanine (G), whereas the pyrimidine bases are cytosine (C) and thymine (T). The nucleotides are covalently linked together through 3',5'-phosphodiester bonds, i.e. the 5'-phosphate group of one nucleotide is bonded to the 3'-hydroxyl group of the adjacent nucleotide. As a result, a DNA strand with a backbone of alternating sugar and phosphate residues will be formed, and since the phosphate groups are negatively charged, the DNA strand will as a whole have a negative charge (Figure 2.1A). The DNA strand has also a polarity due to the free 5'-phosphate group at one end of the strand and the free 3'-hydroxyl group at the other end. [26, 27]

DNA hybridization is the process in which two DNA strands with complementary base sequences form a double helical structure, which is the principal secondary structure of DNA [26, 28]. The DNA double helix is mainly held together by hydrogen bonds between the complementary strands and base-

stacking interactions between the adjacent bases, but also electrostatic forces and hydrophobic interactions help stabilize the DNA structure [13, 29, 30]. As first proposed by James D. Watson and Francis Crick in 1953, adenine pairs efficiently only with thymine and guanine only with cytosine [31]. Two hydrogen bonds are formed between adenine and thymine and three between cytosine and guanine (depicted in Figure 2.1B). For the formation of well-aligned hydrogen bonds, the two DNA strands have to be antiparallel to each other, that is, the strands have to run in opposite directions [26].

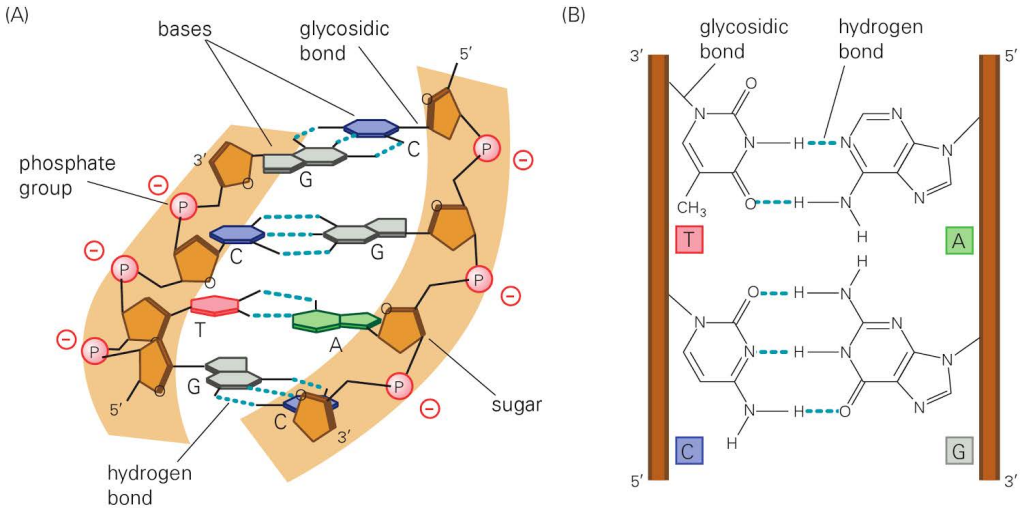

Figure 2.1: The structure of DNA. a) The DNA strand has a negatively charged backbone of alternating sugar and phosphate molecules. b) Hydrogen bonds between the Watson-Crick base pairs link the two single DNA strands together to a double helical structure. Reprinted from reference [28].

The base-stacking interactions are mainly van der Waals and dipole-dipole interactions, and they stabilize the structure by allowing the bases to stack on top of one another and thereby minimizing the contact of the bases with water [27, 32]. The hydrogen bonds are considerably weaker than the base-stacking interactions and the strength of the hydrogen bonds depends on the base pair. The three hydrogen bonds formed between cytosine and guanine have in vacuum a stabilization energy of $E_{\mathrm{C-G}} = 46$ kJ/mol, and the corresponding value for the two hydrogen bonds formed between adenine and thymine is $E_{\mathrm{A-T}} = 25$ kJ/mol [28]. Therefore, the more C-G base pairs the DNA double helix contains, the more stable it will be against thermal and pH-mediated denaturation into the initial two single strands [24, 33]. In addition, the base sequence and the chain length of the DNA duplex and the salt

concentration of the solvent also affect the denaturation and thereby also the melting temperature of double-stranded DNA [33].

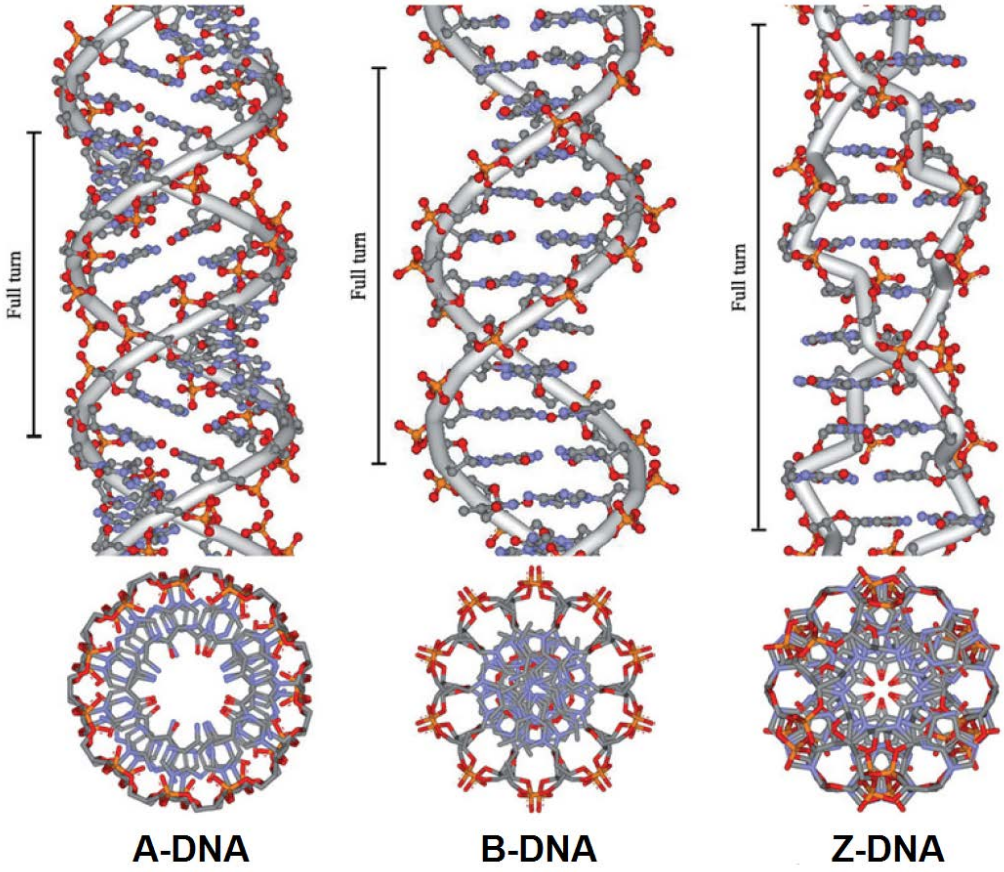

Figure 2.2: Models of A-, B-, and Z-DNA conformations. Reprinted from reference [34].

The DNA double helix is flexible, and its persistence length is only approximately 50 nm in physiological salt [35]. Therefore, the double-stranded DNA molecule can take different three-dimensional conformations depending on the environmental conditions. Figure 2.2 presents the three most important double helical conformations; A-DNA, B-DNA and Z-DNA. B-form DNA is the standard DNA double helical structure described by Watson and Crick [31], and this form is under physiological conditions the most stable conformation. B-DNA is a right-handed helix with a diameter of approximately 2 nm. One complete turn is on average 10.5 base pairs, which corresponds to a helix rise of 0.34 nm per base pair. A-DNA is commonly

found under dehydrating conditions and forms like B-DNA a right-handed double helix. The A-DNA is though more compact than the B-DNA, the diameter is approximately 2.6 nm and there is on average 11 base pairs per helical turn, which gives a helix rise of 0.26 nm per base-pair. Z-DNA has on the other hand a quite different structure, it is in contrast to A- and B-DNA left-handed. One helical turn is on average 12 base pairs, which is equivalent to a helix rise of 0.37 nm per base-pair. The diameter of the Z-DNA helix is approximately 1.8 nm and the backbone has a zigzag appearance. [27, 32]

2.2 DNA as a building material

DNA is widely known to store and transfer genetic information from one generation to the next, but due to its distinctive properties, it can also be used in a nonbiological context as a building material to produce structures with nanoscale precision [13, 17, 24, 25]. As already discussed, DNA is a well-known nanometer-scale structure composed of only four different building blocks (nucleotides). The Watson-Crick base pairing makes the hybridization between the two DNA strands both predictable and tunable, and the flexibility and structural stiffness can be altered by changing the numbers of base-pairs [24, 25, 30, 36, 37]. Additionally, many of the tools needed for the manipulation, modification, and synthesis of DNA are already provided by biotechnology, organic chemistry and molecular biology [24, 30, 36, 37]. DNA is further both biocompatible and biodegradable, which makes it promising for use as biomaterial also *in vivo* [24, 30].

The revolutionary idea of using DNA to construct well-defined 2D and 3D crystal structures was initiated by Nadrian Seeman in 1982 [15]. Inspired by the Holliday junction found in the natural genetic recombination, he proposed that single-stranded DNA (ssDNA) could be designed to hybridize together to form immobile four-armed junction. Further, as illustrated in Figure 2.3a, these junctions could be connected together to more complex crystal structures trough complementary ssDNA overhangs, so called sticky-ends, placed at the end of each arm of the junctions. The first DNA motif to be synthesized indeed contained this immobile four-armed junction [38], and was later followed by motif containing three-arm [39], five-arm [40], six-arm [40], eight-arm [41] and twelve-arm [41] junctions. However, these multi-arm junctions are rather flexible, and the assembly of these motifs into larger, stable arrays are problematic due to the flexibility of the junction region [3, 24].

Therefore, Fu and Seeman [42] introduced a more robust motif, the double-cross (DX) molecule, in which two parallel DNA double helices are

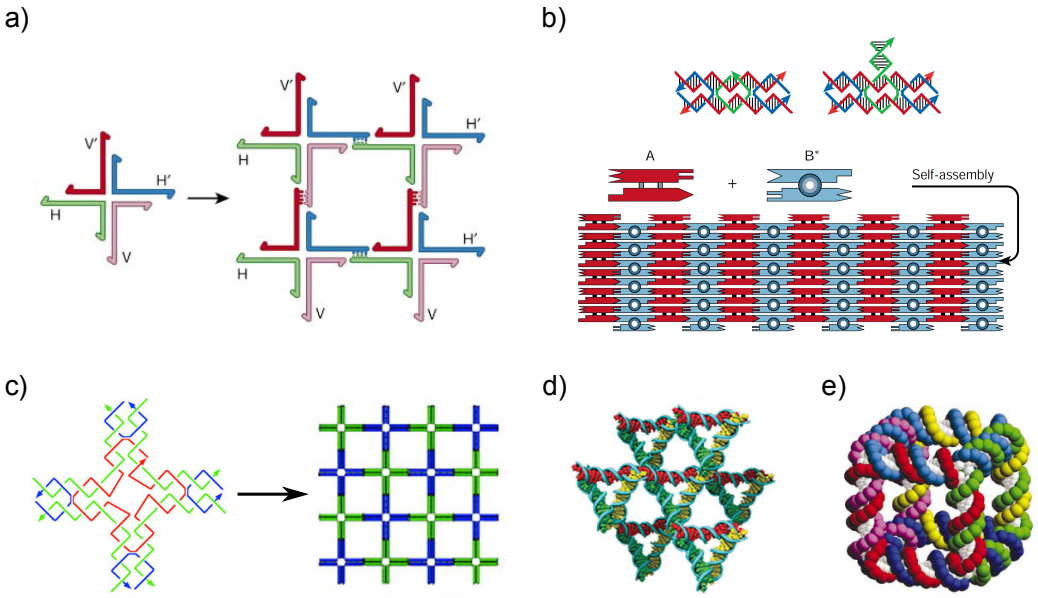

Figure 2.3: DNA structures and lattices constructed using branched DNA motifs and sticky ends. a) Seemans's original idea of using immobile four-arm junctions to construct larger structures through self-assembly. Reprinted from reference [9]. b) Larger arrays can be assembled using double-crossover (DX) tiles with sticky-ends. Reprinted from reference [9]. c) A 2D DNA nanogrid structure constructed from 4 × 4 DNA tiles. Reprinted from reference [48]. d) A 3D DNA crystal constructed from the tensegrity triangle motifs. Reprinted from reference [53]. e) A cube-like 3D object constructed using DNA. Reprinted from reference [9].

linked together by two crossover junctions (Figure 2.3b). These antiparallel DX molecules provided the rigidity and stability needed for the construction of crystal structures [43], and the first well-defined 2D DNA arrays were later assembled using DX molecules with complementary sticky ends, i.e. DNA tiles [44]. To enable the construction of more versatile 2D (and 3D) DNA lattice structures, a large variety of different DNA tiles have been designed and experimentally synthesized. These include for instance triple-crossover (TX) tiles [45], paranemic crossover (PX) tiles [46], double-double crossover tiles [47], 4 × 4 DNA tiles [48] (Figure 2.3c), three-point- star DNA motifs [49], five-point-star motifs [50], six-point-star motifs [51] and T-junction motifs [52]. The tensegrity triangle motif is constructed from three double-helical domains connected pairwise by three four-arm junctions, and the helix axes of this motif span, unlike previously mentioned motifs, 3-space [53]. This is

advantageous in construction of 3D crystals, and the tensegrity triangles have de facto been assembled into both well-ordered 3D rhombohedral crystals [54] and 2D arrays [53] using sticky-end cohesion. (Figure 2.3d)

During the past decades, a wide range of 2D and 3D lattices have been assembled using branched DNA motifs and sticky end cohesion [3, 24, 55]. Using the same approach, also discrete 3D nanoobjects, such as a DNA cube [56] (Figure 2.3e), a truncated DNA octahedron [57] and a DNA tetrahedron [58], have been designed and synthesized. However, the sticky-end assembly of branched DNA motifs has certain limitations and disadvantages. A strict stoichiometric control and purification of the strands used in the assembly is needed, and the yields are often low due to sensitive assembly processes [18, 55, 59]. Since the structures are assembled using the same basic building blocks, the structures that can be constructed are also limited to basic geometric shapes with low complexity [59]. These methods for construction of DNA structures have therefore partially been replaced by the DNA origami technique [19] that a decade ago revolutionized the field of structural DNA nanotechnology. The DNA origami technique will be discussed in more detail in Chapter 3.

Chapter 3

DNA origami

An important advance in the field of structural nanotechnology occurred in 2006 when the DNA origami self-assembly technique was introduced by Paul Rothemund [19]. This chapter gives an introduction to the DNA origami method, as well as the techniques used for DNA origami design and synthesis. In addition, possible applications of DNA origami are shortly discussed with the main focus laying on the material organization properties of the DNA origami structures.

3.1 The DNA origami method

DNA origami method is a bottom-up technique that can be used to construct almost any desired two- or three-dimensional DNA nanostructure with nanometer precision [60]. In the DNA origami technique, a long single-stranded DNA (ssDNA) molecule, the so called 'scaffold', is folded into arbitrary shapes through the action of many complementary single-stranded oligonucleotides, 'staple strands' [19]. The scaffold is usually a 7249 nucleotides long ssDNA molecule derived from the bacteriophage M13mp18, but also other scaffolds are possible. The staples, on the other hand, are shorter synthetically produced single-stranded oligonucleotides with lengths from 18 nucleotides to 50 nucleotides. For the folding of a normally sized DNA origami, some hundred staple strands are typically needed. [60–62] The principle of the DNA origami technique is illustrated in Figure 3.1.

The DNA origami technique has many advantages compared to other methods used for DNA nanoconstruction. First of all, the same scaffold can be used to construct a large number of two- and three-dimensional nanostructures since it is the short ssDNA staples that define the shape of the object [16, 63]. The use of a long ssDNA scaffold that is folded through

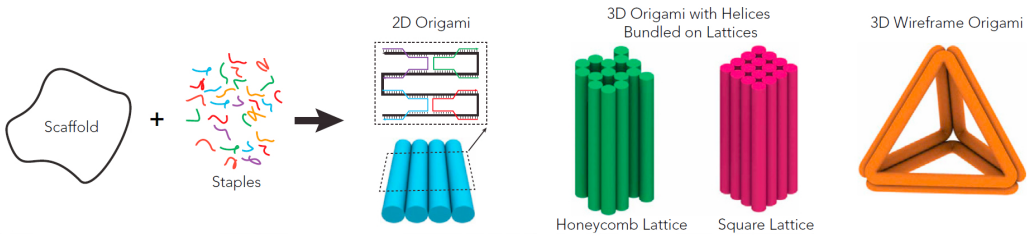

Figure 3.1: The DNA origami technique. A long single-stranded DNA scaffold is folded desired shapes through the action of many complementary staple strands. Reprinted from reference [60].

the action of shorter ssDNA staples is in itself also advantageous as the staple strands favor hybridization with a common scaffold strand rather than with each other. Each correct binding of a staple to the scaffold will further promote the right addition of the remaining staple strands and as a result, the error rate and synthesis time will be significantly reduced, and the yield increased. In the DNA origami method, the staples are not designed to hybridize to each other, so there will not be any need for stoichiometric control and purification of the staple strands. In fact, an excess amount of staple strands will facilitate correct folding and displacement of incorrect strands through strand invasion and exchange mechanisms. [19, 59, 64]

A major drawback of the DNA origami method is the limitation of the size of the nanostructures by the length of the ssDNA scaffold [63, 65, 66]. The structures achieved with the commercially available M13mp18 scaffold have a maximum area of 78 $\times$ 78 nm^2 or a maximum volume of 24.7 $\times$ 24.7 $\times$ 24.7 nm^3 [65]. The M13mp18 scaffold is reliable and therefore the commonly used one, but basically, any ssDNA molecule can be used as scaffold and various methods to create differently sized scaffolds have been investigated [16, 62]. Shorter ssDNA scaffolds (756 to 4808 nucleotides) have been amplified from M13mp18 and lambda DNA sources by polymerase chain reaction (PCR) followed by strand separation via streptavidin-coated magnetic beads [67]. Lambda DNA is also suitable for longer scaffolds, and a 26182 nucleotides long scaffold has been obtained by PCR and selective enzymatic digestion of one of the DNA strands [68]. Further, strategies using restriction enzymes [69] and asymmetric PCR [70] have been used to create shorter scaffold fragments from the original M13mp18 scaffold. DNA normally exists as a double-stranded molecule in living organisms and the successful initial attempts to use double-stranded DNA (dsDNA) as scaffold are therefore promising for the creation of larger and more complex DNA nanostructures.

Högberg *et al.* [71] showed that two discrete nanoscale objects can be synthesized from a dsDNA molecule in the same reaction process if the dsDNA as the first step in the synthesis are separated into two ssDNA strands using the denaturant formamide. Later, Yang *et al.* [65] reported a method in which different DNA origami structures can be folded from dsDNA without the need for a denaturating agent. DNA origami superstructures have also been achieved using folded DNA origami tiles as staple strands instead of usually used short oligonucleotides [72]. Even larger "superorigamis" have been produced by replacing the scaffold strand with a prefolded DNA origami framework and the staple strands with DNA origami tiles [73].

Additionally, larger DNA origami structures can be constructed connecting together individual DNA origami units through sticky end associations, shape complementarity and nonsequence specific blunt end base stacking interactions. Complementary sticky-ends extending from the DNA origami structure have been used to connect individual DNA origami units into micrometer-sized 2D DNA origami arrays [74, 75] and large, discrete 3D polyhedrons [79, 80]. Individual DNA origami tile units have also been assembled into larger 2D arrays using the "jigsaw pieces" approach in which shape complementarity is combined with sticky end hybridization to direct the assembly [76–78]. Further, larger 2D [81] and 3D [82, 83] DNA origami objects with up to gigadalton-scale sizes have been constructed utilizing only shape complementarity and the possibility of base stacking interactions between the blunt ends of the DNA origami helices. Recently, Qian and coworkers developed an algorithm with certain design and hybridization rules for the construction of micrometre-size 2D DNA origami structures with arbitrary patterns on the surface from the same specific set of unique staple strands [84, 85].

In addition to the problems in scaling up the size of the DNA origami structures, there are also other obstacles that need to be tackled to fully realize the potential of the DNA origami method. For example, with the current design principle, a complete new set of staple strands are needed for each new DNA origami shape [86, 87]. The prices of synthetic oligonucleotides have decreased remarkably during the last years, but still the staples needed to test a new DNA origami design cost several hundreds of euros [88]. Commercially available DNA origami applications will most likely be the reality in the future, but it is still a long way to go. Most commercial applications require both a reduction in the cost of the starting materials and a scaling-up in the production from micro-/milligram quantities to gram/kilogram quantities [16, 89, 90]. A promising method for reducing the DNA origami production costs is the scalable biotechnological method for mass production of DNA origami recently developed by the research group of Dietz [91].

3.2 Principles of DNA origami design

The first step in the preparation of a DNA origami nanostructure is to make a geometrical model of the desired shape of the structure. This structure is then filled from top to bottom by parallel double-helical domains, and the single-stranded DNA scaffold strand is folded back and forth through the structure in such a way that it comprises one of the two strands in every helical domain. Shorter staple strands with unique sequences are further designed to bind complementary to the scaffold in accordance with the Watson-Crick base pairing rules. The staple strands hold the structure together by binding to multiple parts of the scaffold and connecting adjacent double-helical domains to each other via interhelical connections (immobilized Holliday junctions). [19] These interhelical connections are usually formed by antiparallel strand crossovers between adjacent DNA double-helical domains, and both the staples and the scaffold strand can form these crossovers. As will be discussed later in this section, the position of the crossovers depends on the packing lattice for the desired DNA origami structure. [62] In addition to double-helical domains also single-stranded domains can be included in the DNA origami design. Single-stranded domains can prevent unwanted base-stacking interactions between the interfaces of the DNA origami structures [79], function as entropic springs to support tensegrity structures [92], or provide attachment sites for other DNA origami structures or biomolecules [62]. A combined scaffold-staple layout for a DNA origami design showing the path for the scaffold and the staples, as well as the interhelical crossover points is illustrated in Figure 3.2.

The first DNA origami structures, designed and synthesized by Rothemund, were planar 2D structures, e.g. rectangular shapes, stars, triangles and smiley faces. In this design, adjacent helices are connected to each other via crossovers taking place every 1.5 helical turns, which for B-DNA corresponds to 16 base pairs (bp). This design principle results in interhelical connections every 180°, which gives a single-layer of helices that forms a planar 2D structure. [19] Such 2D DNA origami sheets can further be extended to hollow 3D structures by connecting the edges of the sheets with interconnecting strands [59, 63]. A variety of 3D nanostructures with an internal cavity have been designed using this approach, such as DNA box with a controllable lid [93] and a tetrahedron [94]. (Figure 3.3a) Han *et al.* [95] have also developed a design strategy for the construction of single-layer DNA origami structures with complex curvatures, such as concentric rings, spheres, hemispheres and ellipsoids (Figure 3.3b).

Single-layer DNA origami structures have a rather weak resistance to

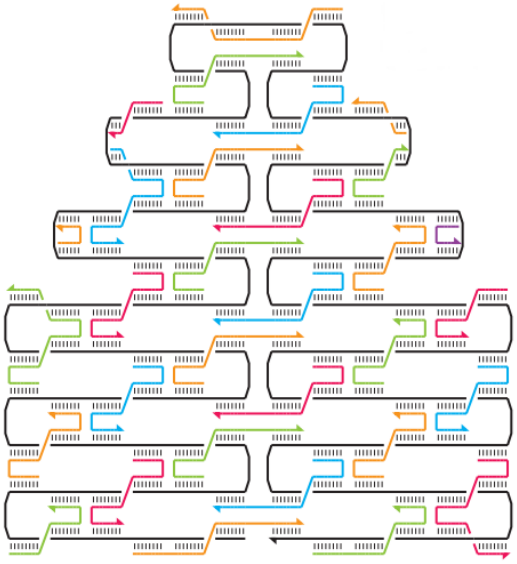

Figure 3.2: Principle of DNA origami design. The scaffold strand (black) is folded back and forth throughout the whole area of the desired structure, and the short staple strands hold the structure together by binding to multiple parts in the scaffold and forming crossovers. Reprinted from reference [19].

mechanical stress, and multilayered 3D DNA origami objects have therefore been developed to get more stable and rigid structures [59]. More densely packed tubular and multilayered DNA origami structures can be constructed by interconnecting adjacent dsDNA helices through a precisely 3D arrangement of crossovers. The relative distance between the crossovers along the helical axis determines the packing of the lattice formed by the dsDNA helices and thereby how densely packed the DNA origami structure is. [59, 62] Multilayer DNA origami structures can be obtained by arranging the dsDNA helices in parallel onto honeycomb [79], square [96], or less common, onto hexagonal lattices [97].

On the honeycomb lattice, each dsDNA helix is connected to up to three adjacent helices in a threefold symmetry where the potential adjacent helices are separated by an angle of 120°. This gives a structure with a hexagonal cross-section. The potential crossovers along the helical axis are separated by 7 bp, which results in a distance of 21 bp between the crossovers of the same pair of adjacent dsDNA helices. [59, 62] (Figure 3.3c) Dietz *et al.* [98] further demonstrated that twisting and bending can be introduced to the structure by deviating from the constant 7-bp crossover distance rule. The deletion of one base pair in a selected unit of helices results in a local overtwisting of the

DNA helices, whereas the addition of one base pair in a selected unit of helices results in a local undertwisting (Figure 3.3e-f). Furthermore, global bending of the helices can be introduced by a combination of base pair deletions and and base pair additions (Figure 3.3g).

On the square lattice, the dsDNA helices are more densely packed, each double helix is connected to up to four neighboring helices in a fourfold symmetry where the potential neighboring helices are separated by an angle of 90°. There is an interval of 8 bp between the crossovers, which gives a distance of 32 bp between the crossovers of the same two neighbors. [59, 62] (Figure 3.3d) An even more densely packed multi-layer DNA origami structure is obtained if the dsDNA helices are arranged onto a hexagonal lattice. Each double helix is then connected to up to six adjacent helices with the potential adjacent helices separated by an angle of 60°. In this case there is a distance of either 13 bp or 9 bp between the crossovers along the helical axis. [97]

There are several computational tools available for designing and predicting the shape of DNA origami structures. SARSE [99] was the first publicly accessible software for DNA origami design, but it is nowadays rarely used due to the availability of other more advanced tools. Today, researchers working with DNA origami structures commonly use the caDNAno by Douglas *et al.* [100] combined with CanDo by Castro *et al.* [62] and Kim *et al.* [101]. caDNAno is used to construct the routing of the scaffold strand through the structure and to generate the sequences for the complementary staple strands, while CanDo is used to computationally predict the shape, mechanical fluctuations, and flexibility of the structure in aqueous solution [18]. Even though caDNAno simplifies the process of designing DNA origami structures, it is a bottom-up approach that requires some understanding of the structural properties of the DNA molecule. It is the user himself/herself that routes the scaffold strand through the structure and the sequences for the staple strand have to some extent be manually designed. [102]

vHelix by the research group of Högberg [103] and DAEDALUS (DNA Origami Sequence Design Algorithm for User-defined Structures) by the research group of Bathe [70] are two recently developed top-down softwares for DNA origami design. The aim of these two softwares is to simplify the process of designing DNA origami structures by automating both the routing of the scaffold strand through the target structure and the design of the needed staple strands. vHelix uses a routing algorithm based on graph theory, whereas DAEDALUS uses a spanning three algorithm to direct the scaffold strand through the polyhedral meshwork of the desired 3D structure, which have been given as input. DAEDALUS can be used to design DNA origami structures with a great diversity of sizes and topologies, but vHe-

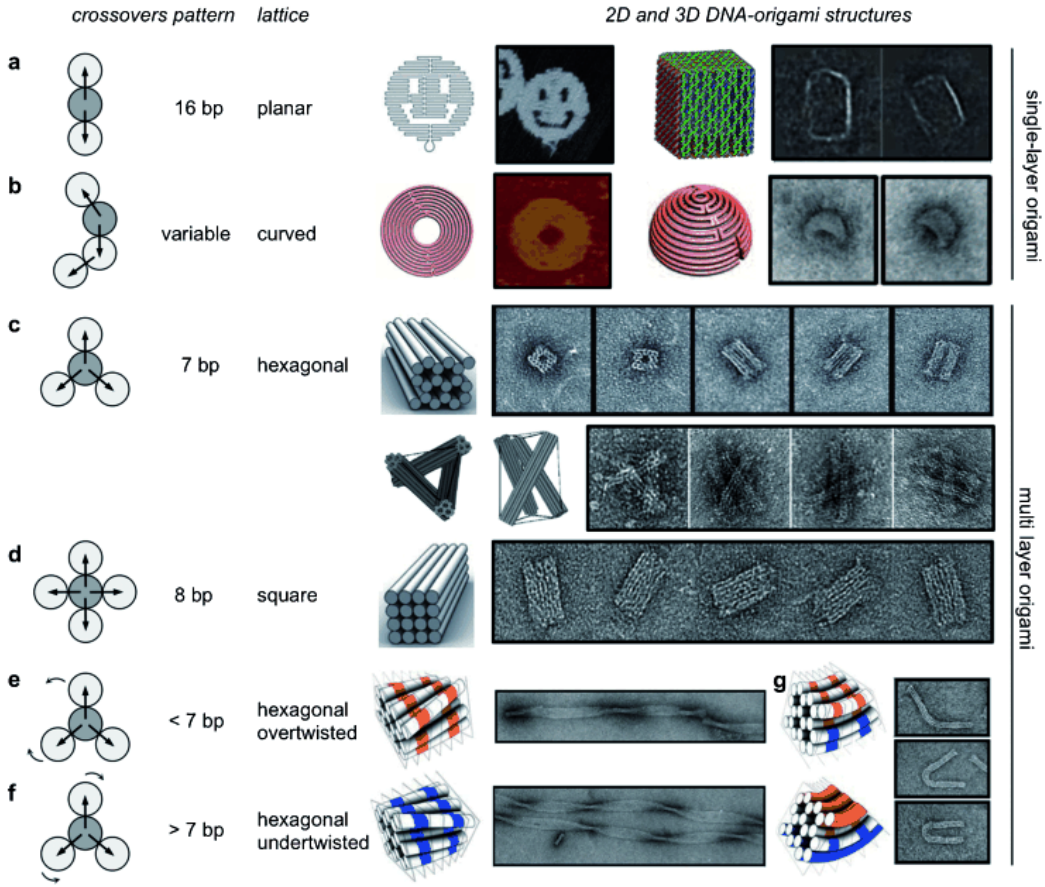

Figure 3.3: By adjusting the number of base pairs between adjacent interhelical crossovers along the same helical axis different single-layer (A,B) and multilayer (C-G) DNA origami structures can be designed. Reprinted from reference [59].

lix is still limited to only spherical topologies. DAEDALUS further enables rigid double-crossover edges, which gives more robust structures compared to those designed with vHelix that only enables single duplex edges. [18, 102]

3.3 Principles of DNA origami synthesis

The folding of the DNA origami structures is done in a one-pot reaction by mixing the ssDNA scaffold with staple strands in a buffer solution containing additional ions. Staple strands are typically added in five- to ten-fold excess amount relative to the scaffold, but depending on the DNA origami

structure other scaffold to staple strand ratios are also possible. [61, 62] The buffer solution for the folding is usually Tris-acetate-EDTA (TAE) containing additional magnesium ions [104]. The magnesium ions stabilize the DNA origami structure by neutralizing the negatively charged phosphate groups in the DNA backbone and thereby allowing adjacent double helices to come closer to each other at the crossovers [61, 104]. The yield of especially multilayer DNA origami structures is further highly dependent on the magnesium concentration and inadequate concentration often results in undesired misfolded and aggregated byproducts [62, 79]. DNA origami structures have successfully been folded also in a buffer containing monovalent sodium ions instead of divalent magnesium ions, but noticeably higher sodium concentrations (up to 100 times higher than the magnesium ion concentration) were needed [105].

For the actual DNA origami folding to occur, the reaction mixture is subjected to a thermal denaturation and annealing process. Initially, the reaction mixture is rapidly heated above the melting temperature of DNA (60-90 °C) to separate dsDNA into ssDNA, after which the temperature of the mixture is slowly decreased to room temperature. The slow cooling allows the staple strands to hybridize to the scaffold in accordance with the Watson-Crick base-pairing rules, and as a result, the desired DNA origami structure is formed. [106] Single-layer DNA origami structures can usually be synthesized within a few hours [19], while multi-layer structures require considerably longer folding times [59]. It has also been demonstrated that DNA origami structures can be folded at constant temperatures by slowly decreasing the concentration of a denaturant (formamide or urea) by dialysis [107] or by carrying out the folding at a structure-specific temperature after a denaturating heat shock [108]. DNA nanostructures have also been assembled isothermally over a wide range of temperatures and salt concentrations, including physiological conditions, using either single-stranded tiles or single-stranded tiles containing single-stranded linker regions, both with adjustable sequence, length and GC content [109]. The commonly used thermal-based folding technique is not suitable for all applications, and efficient methods for folding of DNA origami nanostructures also at constant temperatures would be important for a full potential utilization of the DNA origami method [107, 109].

A purification step to remove the excess amount of staple strands and misfolded structures is typically needed before the folded DNA origami structures can be further utilized. Possible purification methods include poly(ethylene glycol) (PEG) precipitation [110], rate zonal ultracentrifugation [111], agarose gel extraction using electroelution [112] or homogenization [79], spin filtering [113] and gel filtration through size exclusion columns

[114]. Agarose gel electrophoresis can be used to qualitatively analyze the DNA origami folding [79], but also to confirm that the purification method is feasible. Moreover, the DNA origami nanostructure can be analyzed and imaged using either negative-staining or cryogenic transmission electron microscopy or atomic force microscopy (AFM) [62].

3.4 Applications

The ability to precisely control matter at the nanoscale level is one of the major challenges in the field of nanotechnology. As discussed in previous sections, the DNA origami technique is a promising self-assembly method that allows the construction of almost any arbitrary nanostructure with nanometer-scale resolution and high complexity. The DNA origami nanostructures have further a highly addressable surface that can be both chemically modified and selectively functionalized with other nanomaterials and biomolecules [14, 17]. The DNA origami technique has therefore found uses in a variety of applications, ranging from plasmonics [4, 115] and optical devices [116] to enzymatic nanoreactors [117] and drug-delivery applications [90, 118].

3.4.1 Material organization on DNA origami

DNA origami nanostructures have custom-designed shapes and a unique addressability, which makes them promising platforms for the nanoscale level organization of materials. Due to the Watson-Crick base pairing, each staple has a unique position in the DNA origami structure, and selective functionalization is therefore possible with a wide range of materials and a few nanometer accuracy. [59, 61, 76] The DNA origami structures themselves have limited chemical, optical and electronic properties, and hence the addition of other components with the desired functionality is necessary for many applications [59].

DNA origami nanostructures are excellent templates for the organization of gold nanoparticles (AuNPs) and other metallic nanoparticles [4, 115]. Nanoparticles are commonly attached to the DNA origami structures through complementary DNA strand hybridization. The nanoparticles are functionalized with one or more ssDNA oligonucleotides (generally using thiol chemistry), which allows them to hybridize to complementary ssDNA sequences at specific positions on the DNA origami structure. [59] The DNA origami-directed assembly of metal nanoparticle superlattices will be discussed in detail in Chapter 5.3, while this chapter will focus on the attachment of

nanoparticles to individual DNA origami objects. DNA origami structures can be used as templates for the construction of plasmonic architectures with new optical properties [4, 115], but are also useful for the study of the plasmonic coupling of metal nanoparticles [59, 64]. These DNA origami-metal nanoparticle hybrid materials posses great potential for applications in e.g. sensing and optical devices [59, 64, 115].

One of the first approaches to utilize DNA origami templates for the positioning of AuNPs was reported by Sharma *et al.* [119] that selectively arranged one or two AuNPs at predefined positions on a rectangular DNA origami template. Ding *et al.* [120] on the other hand positioned 5, 10 and 15 nm AuNPs in a six-nanoparticle chain on a triangular-shaped DNA origami (Figure 3.4a). The AuNPs were functionalized with different ssDNA oligonucleotides designed to hybridize to complementary ssDNA overhangs at specific positions on the DNA origami triangle, which allowed for a precisely placement of the AuNPs into a linear array. Since these early works, a variety of DNA-origami templated AuNP architechtures have been assembled, including different AuNP arrangements on a rectangular DNA origami template [121] and a linear AuNP chain on a DNA origami nanotube [122]. Chiral plasmonic AuNP superstructures have also been constructed. For instance by rolling up a rectangular DNA origami sheet, decorated with two diagonally well-aligned AuNP rows, into a hollow DNA origami tube [123] (Figure 3.4b), and by assembling AuNPs into left- and right-handed helical conformations using rod-like DNA origami structures [124]. Urban *et al.* [125] constructed a plasmonic toroidal AuNP structure from four identical curved DNA origami blocks, with six helically arranged AuNP binding sites (Figure 3.4c). AuNPs [126] and gold nanorods (AuNRs) [127] have also successfully been encapsulated into DNA origami structures.

Beside AuNPs, DNA origami nanostructures can be used to precisely and programmable organize also other inorganic compounds. Silver nanoparticles (AgNPs) have been arranged into different discrete architectures on a triangular-shaped DNA origami [128] and into a bow-tie antenna configuration on a rectangular DNA origami [129]. Further, quantum dots, i.e. semiconductor nanocrystals, have been positioned on DNA origami templates using both streptavidin-biotin interactions [130] (Figure 3.4d) and complementary DNA strand hybridization [131]. Similarly, also single-walled carbon nanotubes (SWNTs) have successfully been assembled on DNA origami templates utilizing both complementary DNA strand hybrdidization [132] and streptavidin-biotin interactions [133]. Quantum dots and SWNTs have unique electronic and optical properties, and precisely positioned they could have uses in nanoelectronic devices [132, 134].

DNA origami structures are also promising platforms for the preciely

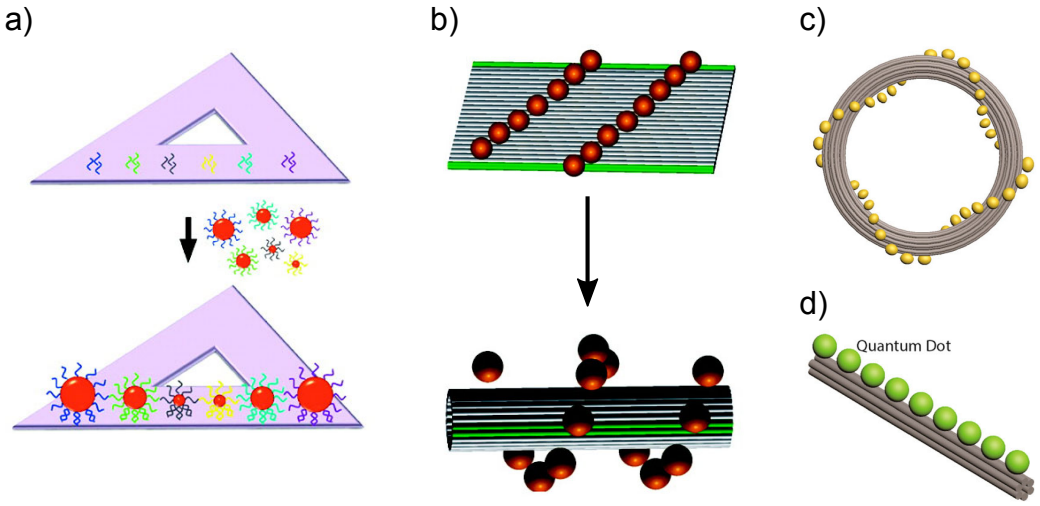

Figure 3.4: Material organization on DNA origami structures. a) Different sized AuNPs positioned in a controlled manner on a triangular-shaped DNA origami. Reprinted from reference [120]. b) Assembly of AuNPs into a chiral helical structure by bending a AuNP-decorated 2D DNA origami sheet into a tube. Reprinted from reference [123]. c) A plasmonic toroidal AuNP structure was constructed using a DNA origami template. Reprinted from reference [14]. d) Quantum dots positioned into a well-ordered linear array on a DNA origami nanotube. Reprinted from reference [14].

positioning of biological materials including proteins [64, 135], enzymes [117, 137] and virus capsids [138]. Complementary DNA strand hybridization is usually used to attach the proteins to the DNA origami structures, and a variety of strategies are available for the protein-DNA conjugation [239]. Well-definied arrangement of proteins at the nanoscale level can be used to study protein-protein interactions and construct novel biomaterials for applications in e.g. tissue engineering [64]. A programmable organization of enzymes on and inside DNA origami structures allow enzyme-mediated reactions to be controlled and regulated, and may found uses in biosensors, drug delivery systems and other functional devices [117, 137].

3.4.2 Other applications

The application possibilities of the DNA origami method cover a wide range of areas, and new applications are constantly being developed. It is impossible to cover all these applications within the scope of this thesis, but in

the next section some interesting applications of the DNA origami technique will be shortly discussed. A recently published review article by Yan and coworkers [14] can be recommended for readers who wish for a more extensive summary of the applications achieved thus far.

DNA origami nanostructures are promising for use in medicine as nanocarriers for smart and target drug delivery and as functional molecular devices that can perform tasks in living cells [90]. DNA origami nanostructures are biocompatible and biodegradable, have structural stability under physiological conditions and can be taken up by the cell. In addition, the DNA origamis have a predefined shape and size, and the addressable surface allows for site-specific loading of cargo molecules. Different biomolecules, such as nucleic acids and proteins, and small molecules, e.g. fluorescent dyes and doxorubicin, have been successfully loaded into/onto DNA origami structures. [118] Implemented DNA origami delivery systems (in research only, no commercial applications yet) include a tubular DNA origami for delivery of cytosine-phosphate-guanine (CpG) sequences [139], a DNA origami box with an adaptamer-encoded logic gate that enables controlled release of antibody fragments [79] and a tubular DNA origami structure with tunable encapsulation efficiency and release rate of doxorubicin [140]. To increase the cellular uptake and biocompatibility, DNA origami delivery systems have been coated with a variety of materials, e.g. lipid membranes [141], virus proteins [142], cationic polymers [143] and protein-dendron conjugates [144].

DNA origami nanostructures can also be used for the fabrication of custom-shaped inorganic nanoobjects with nanometer precision. For example, a variety of differently shaped nanoparticles have been synthesized using rigid and hollow DNA origami structures as molds [145, 146]. These molds contain a single anchored nucleating nanoparticle seed that under suitable chemical conditions can grow into a shape defined by the DNA origami structure. Further, micrometer long conductive gold nanowires have succesfully been fabricated by linking multiple of these DNA origami molds utilizing attractive and repulsive ssDNA overhangs [147]. Customized metallic nanostructures have also been achieved using DNA-assisted lithography (DALI) in which the structural diversity and high accuracy of DNA origami is combined with conventional lithography techniques to construct well-defined nanoobjects with feature sizes of about 10 nm [148, 149]. In the DALI method, stencil openings with the shape of the DNA origami structures are formed on a silicon oxide layer, and these openings are used as masks in the following conventional microfabrication steps.

In addition, DNA origami structures can find applications in nanometrology and super-resolution imaging. DNA origami nanoobjects are excellent

calibration standards for scanning probe microscopy, as they have precisely defined dimensions, are relatively stable over time and can be designed in such a way that defect structures easily can be distinguished from correctly folded structures. [150] As an example, cross-shaped DNA origami structures have successfully been used as a repeatable calibration technique for atomic force microscopes (AFMs) [151]. Further, combined with the DNA-PAINT approach, DNA origami nanostructures can also be used as templates and calibration standards for super-resolution microscopy [152, 153]. Worth mentioning is also that nanorulers for super-resolution systems, developed by GATTAquant DNA Nanotechnologies, are the first commercial available applications utilizing the DNA origami technique [150, 154, 155].

Chapter 4

Self-assembly of nanoparticles

Self-assembly is the method used by nature to create complicated architectures, and material scientists worldwide are therefore investigating the same strategy to organize nanoscale building blocks into well-ordered materials with high complexity [7, 8]. This chapter gives an introduction to self-assembly and the basic principles of electrostatic self-assembly of nanoparticles.

4.1 Principles of self-assembly

Self-assembly is a process by which elementary components spontaneously, without human guidance or management, form ordered structures [5, 6]. Self-assembly plays a key role in many biological processes at both the molecular and macroscopic levels, and for instance lipid membranes, folded proteins and protein capsids of viruses are all results of self-assembly [8]. Self-assembly has during the past years also emerged as a promising and low-cost route towards well-defined nanoscale structures [2, 5, 6].

For formation of ordered structures through self-assembly, the attractive and repulsive forces between the self-assembling components have to be in balance [6]. These forces are typically weak non-covalent or covalent interactions, such as van der Waals forces, electrostatic and hydrophobic interactions, and hydrogen and coordination bonds [5]. It is also important that the building blocks have shapes complementary with each other [6].

Normally, self-assembly takes place in solution or on smooth surfaces, since the individual components have to be mobile and come into contact with each other for self-assembly to occur. Usually, ordered self-assembled structures are formed at the equilibrium state, and the self-assembly process requires either that the interactions between the components are reversible

or that the components can adjust their positions within the structure also after it has been formed. If the components irreversibly attach to each other during the self-assembly process, a glass is produced instead of a crystal structure. [5, 6]

4.2 Electrostatic self-assembly of nanoparticles

Electrostatic self-assemblies are formed via electrostatic interactions, i.e. Coulombic forces, between the individual charged components. This is advantageous, as the distance over which these interactions are effective in a solution, the Debye screening length, can be controllably tuned [1]. The Debye screening length is given by

$$\kappa^{-1} = \sqrt{\frac{\varepsilon_0 \varepsilon_\mathrm{r} k_\mathrm{B} T}{e^2 \sum_\mathrm{i} c_\mathrm{i} {z_\mathrm{i}}^2}}, \tag{4.1}$$

where ε_0 is vacuum permittivity, ε_r is the dielectric constant of the solvent, k_B is the Boltzmann constant, T is the absolute temperature (in Kelvin), e is the elementary charge, and c_i and z_i are the number densities and valencies of the electrolyte ions [156]. As can be seen from the equation above, the strength of the electrostatic interactions can be adjusted by the selection of solvent (dielectric constant) and the concentration and chemical properties (number densities and valencies) of the ions in the electrolyte. Notably is also that the electrostatic interactions will be effective over longer distances in a dilute solution than in a concentrated solution and thereby considerably more important [157].

Formation of well-ordered self-assembled structures requires control over both the assembly conditions and the assembly kinetics [158, 159]. For electrostatic self-assemblies this is particularly done by adjusting the electrostatic interactions between the building blocks, e.g. tuning the ionic strength of the solution. If the attractive interactions between the building blocks are too strong, gel-like aggregates with only short range order are formed. On the other hand, if the interactions are too weak no assemblies at all are produced. [156, 160] The formation of highly periodic structures with a long range order occurs when there is a balance between electrostatic attraction and repulsion. The components are then tightly bound to each other, the attraction between oppositely charged components are maximized and the repulsion of like-charged components minimized. [161] (Figure 4.1)

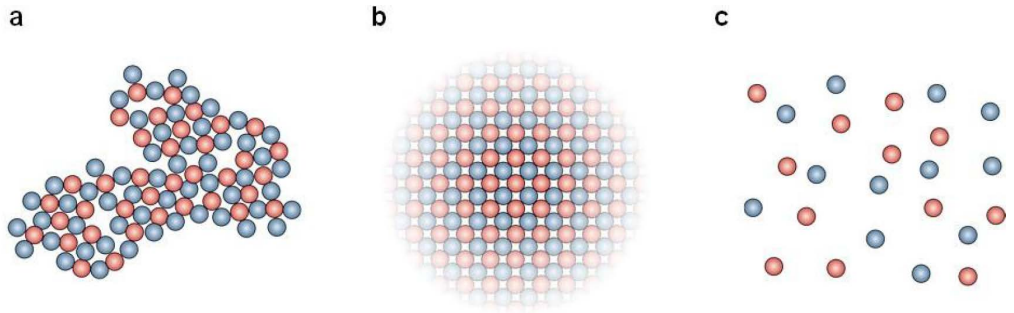

Figure 4.1: Electrostatic self-assembly of nanoparticles under different conditions. a) Too strong attraction between the components leads to kinetically trapped structures. b) Highly periodic structures are formed when there is balance between attraction and repulsion. c) No structures at all are formed if the attraction between the components are too weak and particle-solvent interactions dominate. Reprinted from reference [161].

In biological systems, however, also the pH of the solvent may affect the electrostatic interactions between the building blocks. Many biological particles, such as protein cages, are build up from protein subunits consisting of chains of amino acids that undergo pH-dependent protonation and deprotonation. [161] Therefore, the magnitude and sign of the charge of many biological building blocks are highly pH dependent, and for instance the electrostatic self-assembly of protein cages have successfully been introduced or inhibited by adjusting the pH [156, 162].

A prerequisite for self-assembly of well-ordered structures is that the formed structures are dynamic and that the components can adjust their positions within the structure also after the initial self-assembly [5, 6]. This applies for electrostatically self-assembled systems as well, and the particle configurations and the dynamics of these systems can be adjusted by altering the ionic strength. Well-ordered structures with long range order cannot be formed if kinetically trapped structures, in which the building blocks are locked in poorly ordered configurations, dominate the assembly. Non-spherical compounds readily form these kinetically trapped configurations if they are simply mixed together at low ionic strength. However, the alignment and order of non-spherical compounds can be improved using an assembly process in which the ionic strength is gradually decreased and the compounds slowly can self-assembly into larger structures with optimal particle configurations. [161]

Chapter 5

DNA-directed gold nanostructures

Spatially well-ordered structures of metal nanoparticles have unique electronic, magnetic and optical properties, and hence there is ever-increasing interest towards these kinds of nanomaterials [2, 20]. In general, the construction of materials with nanometer-scale precision is rather challenging, but owing to the predictable and programmable DNA hybridization (i.e. Watson-Crick base pairing), the precise arrangement of molecular components at the nanoscale becomes feasible [25, 115]. The techniques for DNA-directed self-assembly of nanoparticles have therefore traditionally relied on the superior molecular recognition properties of the DNA, but there are also strategies taking advantage of electrostatic or other non-specific interactions. In this chapter, the unique properties of gold nanoparticles (AuNPs) are presented, and some interesting application possibilities are highlighted. The DNA-directed self-assembly of AuNPs into larger, ordered structures are discussed with the main focus laying on the DNA nanostructure-directed self-assembly.

5.1 Gold nanoparticles

Colloidal gold nanoparticles (AuNPs) have fascinated scientists for a long time already, actually the first uses of AuNPs are dated back to the fourth century when the Romans used AuNPs in the production of "gold ruby" glass. During the last decades, AuNPs have attracted increasing interest in the field of nanotechnology. AuNPs have namely unique optical, electronic, physical and chemical properties, and these properties are remarkably different from those of individual gold (Au) atoms and bulk gold. [164, 165]

The intriguing optical properties of gold and other metal nanoparticles arise from their localized surface plasmon resonance (LSPR), which is the coherent oscillation of the conduction electrons induced by interaction with electromagnetic radiation, i.e. light. When a dispersion of AuNPs is illuminated with visible light, the light will be strongly absorbed at a certain wavelength, which can be seen as a peak in the absorption spectrum (the surface plasmon band). The origin of this strong absorption is the collective oscillation of the free surface electrons induced by the incoming light (Figure 5.1). [164–168] The particle size and shape, the interparticle distance, the presence and nature of a supporting or stabilizing ligand shell, and the dielectric constant of the dispersion medium have shown to affect the position of the absorption peak, and thus the color of the AuNP dispersion [164–167]. For instance, AuNPs with a diameter of 10-15 nm typically have an absorption peak in the region of 520 nm due to a strong absorption of green light, which gives the colloidal gold its distinctive ruby red color [164–170]. Mie [171] originally described the LSPR by solving Maxwell's equation for the absorption and scattering of electromagnetic radiation by homogeneous spherical particles, and for readers who wish for a more extensive introduction to the physics behind LSPR a review article by Ghosh *et al.* [164] can be recommended.

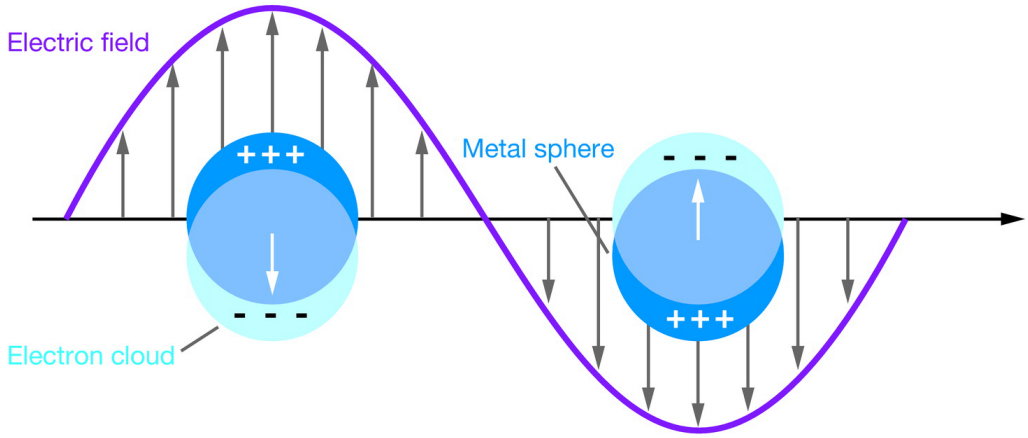

Figure 5.1: A schematic illustrating the localized surface plasmon resonance of metal nanoparticles. Reprinted from reference [176].

AuNPs can be synthesized using both top-down and bottom-up approaches, and in recent years many efforts have been made to develop new,

optimized synthesis routes [165, 172–175]. These include approaches for synthesis of AuNPs with different size and shape, narrow size distributions and surface functionalities suitable for the target application. To date, AuNPs have found uses in a variety of nanotechnology applications ranging from biomedical analysis tools [174, 177] and drug-delivery systems [174, 178] to nanophotonic [179] and electronic [180] devices. AuNPs are particularly promising for use in optical, electronic, catalytic and sensing applications, and AuNPs are in the future expected to be found in solar cells, high-capacity drug delivery agents and theranostic materials among other applications [181]. The optical and electronic properties of the AuNPs are though highly dependent on their geometrical arrangements, and efficient strategies for controlling and directing their arrangements and positions at the nanoscale level will be needed [2, 17, 20].

5.2 DNA molecule-directed assembly

The first uses of DNA to direct the assembly of gold nanoparticles was simultaneously reported in 1996 by the research groups of Mirkin [182] and Alivisatos [183]. Both groups used thiols to conjugate the DNA strands to the AuNPs, but they came up with two very different strategies for the use of DNA to arrange the AuNPs into assemblies. The group of Mirkin prepared two sets of AuNPs with several DNA linker strands on the surface, and these AuNPs reversibly self-assembled into macroscopic aggregates in solution when hybridized with a complementary linking DNA duplex. The group of Alvisatos on the other hand linked only a single DNA strand to the AuNP surface, and when a complementary single-stranded DNA template was added, these AuNPs assembled into discrete dimers and trimers. These pioneering works by Mirkin, Alivisatos and co-workers served as the starting point for DNA-based assembly of AuNPs, and later the same strategies have been used to a assemble a variety of discrete clusters of AuNPs with controllable spatial arrangements [115, 184, 185].

The ultimate goal of the DNA molecule-directed assembly of AuNPs was for a long time 3D crystals with long-range periodicity, and in 2008, the research groups of Mirkin [186] and Gang [187] independently constructed the first well-ordered AuNP superlattices using DNA molecules with complementary sequences as linkers. In these studies, the AuNPs were assembled into either face-centered cubic (fcc) crystal structures, body-centered cubic (bcc) crystal structures, or amorphous aggregates depending on which kind of DNA linking molecules (e.g. length and flexibility) that were used in the assembly. Later, these works by Mirkin, Gang and colleagues have been ex-

tended and built upon in subsequent studies by several research groups, and a wide spectra of different superlattice arrangement of AuNPs have been achieved using DNA molecules as linking elements [25, 188]. Design rules for synthesizing well-ordered nanoparticle crystal structures using DNA have also been established [188, 189].

5.3 DNA nanostructure-directed assembly

As discussed earlier in Chapter 2.2 and Chapter 3, the advances in the field of structural DNA nanotechnology and in particular the development of the DNA origami method have given rise to an extensive collection of structurally versatile micro- and nanoscale DNA structures. These structures can act as templates onto which nanoparticles can be precisely positioned or as linkers that connect several nanoparticles to larger superlattices [4]. Utilizing the molecular recognition properties of the DNA, DNA-based structures can serve as scaffolds for the assembly of nanoparticles using two different strategies [179]. In the first strategy, the nanoparticles are functionalized with one or more single-stranded DNA (ssDNA) oligonucleotides, which allows them to hybridize to complementary ssDNA sequences on specific positions on a pre-assembled DNA template. In the other strategy, each nanoparticle is first conjugated to a ssDNA sequence. These DNA-nanoparticle conjugates are then used to construct the tiles making up the lattice, and thus nanoparticles are incorporated into the larger lattice structure during its assembly process.

5.3.1 One-dimensional arrays

One of the first approaches to use self-assembled DNA nanostructures to precisely organize AuNPs into linear one-dimensional (1D) arrays was reported by Li *et al.* [190]. In this study streptavidin-conjugated AuNPs were controllable positioned on a linear DNA template constructed from DNA triple crossover molecules (TX). The TX molecules contained two additional hairpin loops that were modified to incorporate biotin groups, and using streptavidin-biotin interactions the AuNPs were assembled on the template with an interparticle spacing of 17 nm. Beyer *et al.* [191] also used streptavidin-biotin interactions to construct periodic 1D arrays of 5 nm AuNPs. Rolling circle amplification (RCA) was employed to produce a long ssDNA that formed a dsDNA template with complementary biotinylated ssDNA oligonucleotides. Incubation of this DNA template with streptavidin-coated AuNPs resulted in well-ordered arrangements of the AuNPs along the template.

Sharma *et al.* [192] constructed complex 1D helical arrays of AuNPs using a DNA template formed from four double crossover (DX) DNA tiles, similar to that originally reported by Liu *et al.* [193]. 5 nm AuNPs were positioned on the DNA template in parallel lines with ca. 64 nm periodicity using a thiol-conjugated DNA strand as the central strand in one of the tiles (Figure 5.2a). The close proximity of the AuNPs on the template induced strong electrostatic and steric repulsion between the neighboring AuNPs, which forced the 2D template to bend into tubes displaying stacked rings, single spirals, double spirals and nested spirals of AuNPs. When larger AuNPs (10 and 15 nm) were assembled onto the 2D template, nearly all of the tubules were in stacked-ring conformations, indicating that the AuNPs plays an important role in directing the tube formation.

The research group of Sleiman adopted a different strategy for the construction of well-defined linear arrays of AuNPs by encapsulating them into triangular DNA nanotubes with longitudinal structural variations [194] (Figure 5.2b). 1D nanotubes of alternating small and large capsules were constructed from small (7 nm) and large (14 nm) DNA triangles and additional DNA strands that connected the triangles. When citrate-coated AuNPs were added during the assembly of these tubes, the AuNPs were size-selectively encapsulated into specific pockets of the tube, resulting in "nanopepod" arrays of AuNPs with controlled interparticle distances. Furthermore, the encapsulated AuNPs could be released from the nanotube by adding ssDNA sequences, "eraser strands", that bound complementary to the linking strands and thus selectively opened the capsules. In a subsequent study, the design was improved, which allowed for construction of DNA nanotubes with controllable lengths [195]. Later, the same research group have reported an alternative DNA nanotube design that can be used to position AuNPs into well-defined 1D arrays [196] (Figure 5.2c). This nanotube structure is constructed from repeating triangular rung units [197] to which a double stranded overhang with two terminal AuNPs binding sites (cyclic dithiols) have been added. Furthermore, since the rung units have a single-stranded binding region that is complementary to a templating RCA backbone strand, linear 1D arrays of AuNPs can be fabricated in a controlled manner.

In addition to these works, AuNP "ripples" have been organized into 1D arrays with well-defined interparticle distances using different DNA motifs. The AuNP ripples were prepared by coating 10 nm AuNPs with a binary mixture of thiol-ligands, using the method described by Stellacci and co-workers [198]. The AuNP "rippers" were further functionalized with two thiolated ssDNA sequences (5'SH-DNA 20mer, 5'SH-DNA 42mer or 5'SH-DNA 60mer) to form divalent DNA/AuNP conjugates that could self-assembly with complementary DNA strands into different formations. Assembly of divalent

DNA/AuNP conjugates with complementary 5'SH-DNA 20 mer sequences resulted in flexible worm-like DNA nanoparticle arrays, whereas more rigid, linear arrays were obtained using 60mer DNA/AuNP conjugates and T-motif forming DNA strands or 42mer DNA/AuNP conjugates and DX motif forming DNA strands. [199] (Figure 5.2d)

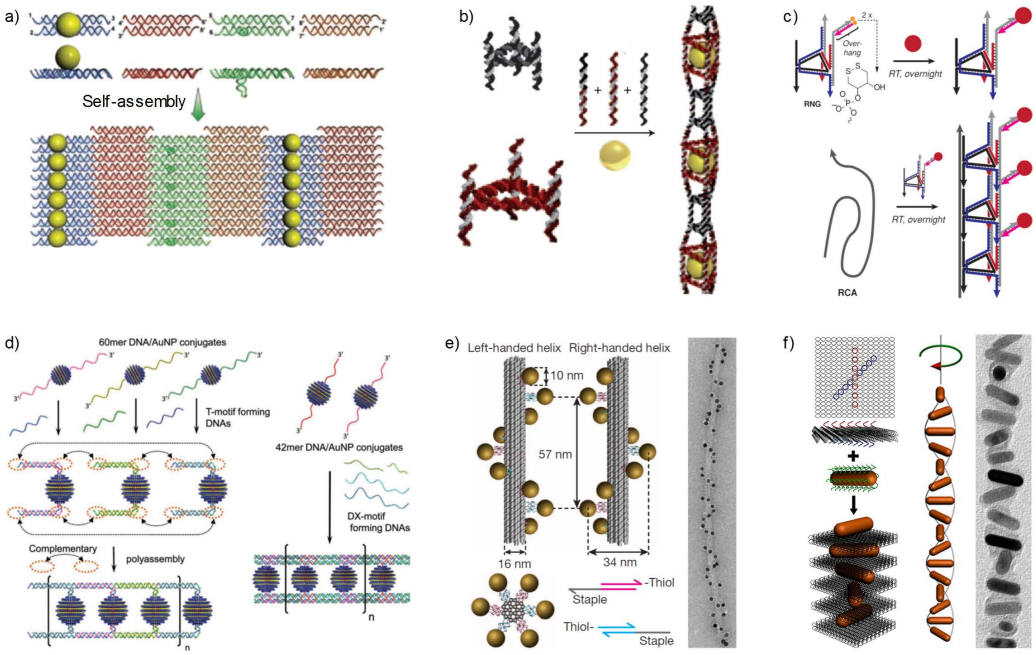

Figure 5.2: One-dimensional arrays of nanoparticles and extensions to more complex configurations. a) AuNPs positioned in parallel lines on a double-crossover (DX) template. Further, the close proximity of the AuNPs will force the 2D template to bend into tubules. b) Size-selective encapsulation of AuNPs into triangular DNA nanotubes. c) Linear chains of AuNPs assembled using repeating triangular rung units. d) Rigid, linear chains of AuNP "ripples" assembled using divalent DNA/AuNP conjugates and T- or DX motifs. e) Assembly of AuNPs into left- and right-handed helical conformations using rod-like DNA origami structures. f) Assembly of gold nanorods (AuNRs) into right-handed helical superstructure using 2D rectangular DNA origami templates. Reprinted from reference [21].

The DNA origami technique can be used to construct almost any arbitrary DNA nanostructure with nanometer precision, structures that can readily be connected to each other through sticky-end associations, and to which nanoparticles can be attached with thiol-modified oligonucleotides.

Liedl and co-workers were among the first to utilize DNA origami structures to precisely arrange nanoparticles into 1D arrays [124]. In this work, 10 nm AuNPs were assembled into left- and right-handed nanoscale helices that act as optical polarizers using DNA origami 24-helix bundles (24HB) with precisely positioned attachment sites for ssDNA-functionalized AuNPs (Figure 5.2e). Additionally, longer 1D helical arrays of AuNPs were obtained by connecting the left-handed nanohelices using complementary polymerization oligonucleotides. Lan *et al.* [200] on the other hand arranged gold nanorods (AuNRs) into left- and right-handed helical superstructures utilizing 2D rectangular DNA origami templates (Figure 5.2f). The AuNRs were functionalized with ssDNA sequences and complementary ssDNA overhangs were designed on both sides of the DNA origami template in a "X"-shape manner, which allowed controlled positioning of the AuNRs with an inter-rod spacing of 14 nm an an inter-rod angle of 45°.

Furthermore, DNA origami structures have been used to arrange AuNPs into linear 1D arrays. Tian *et al.* [201] constructed an octahedral DNA origami structure with AuNP attachment sites on two oppositely located vertices and used this structure as a rigid linker to connect AuNPs into well-aligned 1D arrays. Chains of AuNPs were obtained using AuNPs wrapped with DNA origami bundles into flower-shaped structures [202]. The outer ends of two bundles, separated by 180° in the nanoflower, were further functionalized with complementary ssDNA linkers, which enabled the "nanoflowers" to assemble into 1D arrays. Liu et al. [203] used cross-shaped DNA origami tiles to program the 1D arrangement of AuNPs. The tiles had an AuNP attachment site in the middle, and ssDNA connector strands were added to two of the four arms. If the connector strands were added to two oppositely located arms of the structure, a linear 1D array of AuNPs was obtained, whereas a zigzag 1D array was achieved when the connector strands were added to two adjacent arms.

5.3.2 Two-dimensional arrays

One of the first approaches to utilize DNA templates in the construction of two-dimensional (2D) assemblies of gold nanoparticles (AuNPs) was reported by Maeda *et al.* [204]. Although only a limited ordering of AuNPs was obtained on the DNA network template, the study still demonstrated the power of using 2D DNA scaffolds for the precise and programmed arrangement of metal NPs. Since this early work, a number of ordered 2D arrays of AuNPs have been reported, and particularly Kiehl, Seeman, Yan and co-workers have made significant advances towards specific arrangements of AuNPs on 2D lattices.

In an initial study by Kiehl and colleagues, small AuNPs (1.4 nm) were organized into well-aligned 2D arrays on a DNA scaffold, originally reported by Liu *et al.* [193], and constructed from four different double-crossover (DX) tiles with complementary ssDNA overhangs (sticky ends) [205]. Prior to the growth of the DNA crystal, the AuNPs were covalently linked to the DNA within one of the tiles, which enabled a controlled positioning of the AuNPs with interparticle spacings of 4 and 64 nm. The same research group also reported a method for controllable alignment of AuNPs on a pre-assembled 2D DNA template attached to a mica surface [206]. Similarly to the previous study, the template was constructed from four different DX tiles using a design closely to one described by Liu *et al.* [193], but one of the tiles contained an extended ssDNA overhang (dA_{15}) instead of a covalently linked AuNP. Further, 6-nm AuNPs were functionalized with multiple strands of 3'-thiolated DNA (dT_{15}) designed to hybridize to the complementary ssDNA overhangs on the DNA template, which allowed precise arrangement of AuNPs in large micrometer-sized rows with a spacing of 63 nm between adjacent rows. Kiehl and co-workers later extended this work, showing that the same principle can be used to precisely arrange 5 and 10 nm AuNPs into parallel, alternating rows with a spacing of 32 nm [207] (Figure 5.3a). By coating the two types of AuNPs with different 3'-thiolated DNA strands, the sequence selectivity of DNA was effectively exploited to position the AuNPs with remote cross-contamination between the AuNP rows. Later, similar self-assembled DX DNA-tile templates have been used to arrange streptavidin-coated quantum dots into regular 2D arrays [208]. Yet another approach has been presented by Ke *et al.* [209], where parallel chains of AuNPs and parallel AuNP monolayers have been assembled on DNA crystals based on the ssDNA tile strategy [210].

In addition to these works, AuNPs have been organized into periodic square lattices on 4×4 cross tile based 2D DNA nanogrids [211, 212]. Adopting the previously described strategies of AuNPs functionalized with ssDNA (dT_{15}) that hybridize to complementary "target" sequences (dA_{15}) on the DNA template and construction of 2D nanogrids [48, 213], Zhang *et al.* [211] positioned 5 nm AuNPs into 2D square lattices in a controlled manner with a center-to-center interparticle spacing of 38 nm. Carter and LaBean [212] utilized a different strategy and arranged 5 nm AuNPs on the nanogrid in which a high-affinity gold binding peptide was covalently conjugated to one of the oligonucleotides used to construct the nanogrid tiles. This work clearly demonstrated that peptide-directed assembly is viable alternative to thiol chemistry in DNA-templated assembly of AuNPs.

Yan and colleagues demonstrated that well-defined periodic arrays of 5 nm AuNPs can be constructed also in a one-pot reaction by incorporating

the AuNPs into the nanogrid lattice during its assembly [214] (Figure 5.3b). In this strategy, an AuNP-bearing ssDNA sequence is first used as a building material for the construction of a single DNA tile, which is subsequently assembled with other DNA tiles to form a lattice structure. The spacing between adjacent AuNPs can be precisely controlled by altering the dimensions of the DNA tile. A more complex, well-ordered pattern of AuNPs was achieved by Seeman and co-workers by conjugating AuNPs to ssDNA used in the assembly of two different three-dimensional double crossover (3D DX) triangle motifs [215] (Figure 5.3c). Three different periodic 2D arrays of 5 nm AuNPs, and 5 and 10 nm AuNPs were obtained by connecting the triangle motifs by specific sticky end associations using the approach by Liu *et al.* [53].

Schreiber *et al.* [202] demonstrated the feasibility of using DNA origami structures in fabrication of 2D lattices with different symmetries using the already mentioned "nanoflowers" in which the AuNPs are wrapped with DNA origami bundles into flower-shaped structures (Figure 5.3d). ssDNA linkers were selectively added to the outer ends of chosen bundles of these "nanoflowers", which allowed the "nanoflowers" to assemble into different 2D lattices depending on the number of attachment sites and their position. Likewise, Liu *et al.* [203] used the mentioned cross-shaped DNA origami tiles with AuNP capturing strands in the middle to program the 2D arrangement of AuNPs (Figure 5.3e). A large variety of well-defined planar architectures and arrays were fabricated using a lock-and-key mechanism and with different combinations of these cross-shaped DNA origami tiles having ssDNA connector sequences at one, two, three or all of the four arms. AuNPs have also been controllably arranged onto 2D honeycomb lattices that have been assembled from DNA origami hexagon tiles [75].

A different method for constructing higher-ordered lattice arrangement of nanoparticles is to use DNA origami nanostructures as rigid linking elements that connect the nanoparticles with each other. Schreiber *et al.* [216] used DNA origami nanotubes with attachment sites at the ends to assemble metal nanoparticles and quantum dots into hierarchical nanoclusters with a "planet-satellite"-type structure. They further demonstrated that the nanoclusters formed closed-packed lattices upon slow drying on solid faces, indicating that the nanoclusters were uniform in size. Tian *et al.* [201] later constructed an octahedral DNA origami frame with AuNP attachment sites on the vertices, which allowed enhanced control over positioning the AuNPs (Figure 5.3f). Utilizing this octahedral DNA origami structure as linking element, ordered 2D arrays were assembled by attaching AuNPs only to specific vertices of the octahedra as connecting sites.

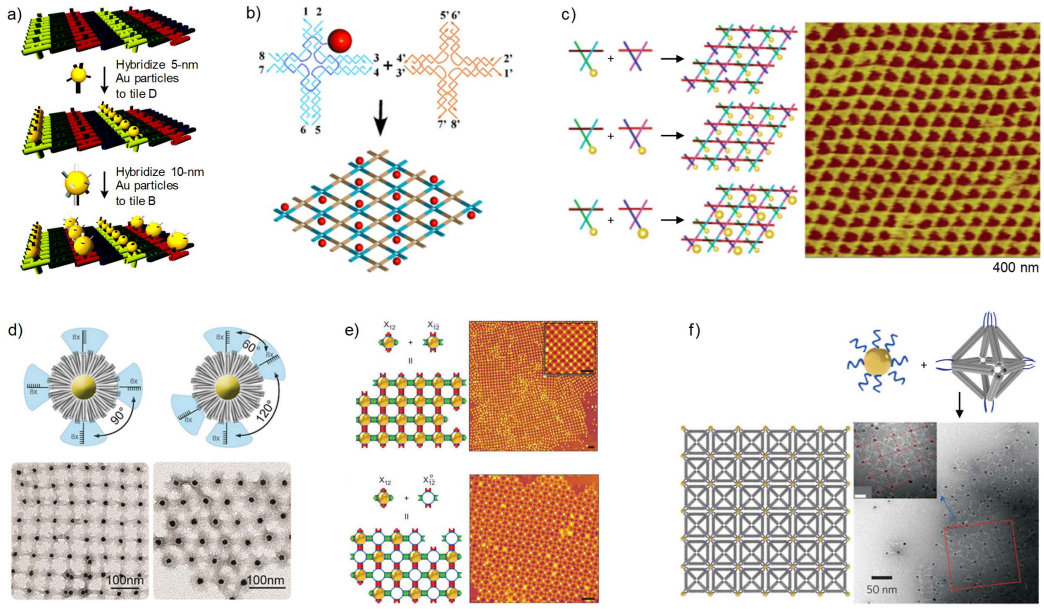

Figure 5.3: Two-dimensional nanoparticle arrays. a) A 2D DX DNA-tile template was used to arrange 5 and 10 nm AuNPs into parallel, alternating rows. b) Assembly of a 2D square array using AuNP-bearing DNA tiles. c) AuNPs were incorporated into "tensegrity triangles" used in the assembly of 2D arrays. d) AuNPs wrapped with DNA origami bundles formed different lattices depending on the position of the ssDNA linkers. e) 2D square lattices assembled using cross-shaped DNA origami tiles with AuNP attachment sites in the middle. f) Octahedral DNA origami structures connected AuNPs into 2D square arrays. Reprinted from reference [21].

5.3.3 Three-dimensional arrays

The self-assembly of nanoparticles into predefined three-dimensional (3D) lattices is a formidable challenge. However, the use of DNA origami frames have emerged as a promising solution. DNA origami frames are rigid and have well-defined geometries. ssDNA strands extending from the structures provide essential connecting points for nanoparticles needed for the crystal growth. The research group of Gang constructed different 3D AuNP superlattices using a tetrahedron-shaped DNA origami frame with AuNP attachment sites at the vertices and inside the tetrahedron [217] (Figure 5.4a). If the AuNPs, with a core diameter of 14.5 nm, were attached only to the connecting sites at the four vertices, an ordered open face-centered cubic (fcc) lattice was obtained whereas AuNPs placed inside the tetrahedron results

in a cubic diamond lattice formation. Further, an interchange to smaller AuNPs (core diameter of 8.7 nm) at the connection sites or both at the connection sites and inside the structure resulted in a zinc blende respective "wandering" zinc blende type of lattice. In a subsequent study the same group constructed a variety of 3D AuNP superlattices using different polyhedron DNA origami frames with AuNP connecting sites at their vertices [218] (Figure 5.4b). A fcc lattice was obtained when an octahedral DNA origami frame and ssDNA-coated AuNPs (core diameter of 10 nm) were employed. Accordingly, a simple cubic lattice was obtained from a cubic DNA origami frame, a body-centered tetragonal (bct) lattice from an elongated square bipyramidic DNA origami frame, and a simple hexagonal (sh) lattice from a prism-shaped DNA origami frame. Moreover, Zhang *et al.* [219] demonstrated that a crystalline 3D rhombohedral lattice can be assembled from DNA origami-based "tensegrity triangles" in addition to a 3D rhombohedral AuNP lattice obtained by a site-specific positioning of AuNPs on the tensegrity triangles before lattice growth (Figure 5.4c).

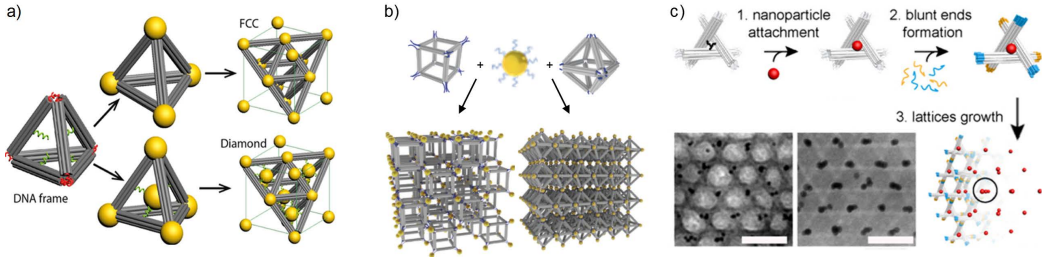

Figure 5.4: Three-dimensional AuNP superlattices assembled using DNA origami frames. a) Face-centered cubic (fcc) and diamond lattices obtained from a tetrahedron-shaped DNA origami frame. b) Varous superlattices constructed using different polyhedron DNA origami frames. c) Rhombohedral lattice constructed using DNA origami "tensegrity triangles". Reprinted from reference [21].

Recently, Liu *et al.* [220] reported a construction of ordered 3D lattices of AuNPs without rigid DNA origami frameworks. In this study, short 6-helix bundle (6HB) DNA structures (21 nm in length) with ssDNA attachment sites at both ends, were used to assemble ssDNA-coated AuNPs into different configurations depending on the effective size of the AuNPs. For a small effective AuNP sizes and low stoichiometric ratios of 6HB DNA rods to AuNPs, only disordered arrangements were formed. However, an unexpected transition from disorder to hexagonal close-packed (hcp) and further

to face-centered cubic (fcc) lattices occured when the effective AuNP size was gradually increased, and the 6HB rod to AuNP ratio was at least 5:1.

5.4 Electrostatic self-assembly of DNA and AuNPs

As discussed in the previous sections, DNA molecules and DNA nanostructures have widely been used to direct the higher-ordered lattice arrangement of AuNPs, but there is only a few studies reported taking advantage of the electrostatic interactions between the DNA nanostructures and AuNPs during the assembly process. This is rather suprising, since DNA molecules and DNA nanostructures are polyanions that, at least in theory, readily should form electrostatic self-assemblies with cationic AuNPs.

The first use of DNA molecules as templates for electrostatic self-assembly of cationic AuNPs was reported by Kumar *et al.* [22]. By first capping the gold nanoparticles with lysine they used the attractive electrostatic interactions between the negatively charged phosphate backbone of the DNA double helix and the positively charged gold nanoparticles to form linear and close-packed lamellar structures. Warner *et al.* [23] also demonstrated that AuNPs functionalized with a cationic ligand form close-packed structures with DNA. Electrostatic self-assembly of the cationic AuNPs onto the DNA resulted in linear, ribbon-like and branched AuNP assemblies that was readily visible by TEM. Electrostatic self-assembly has also been used to construct linear 1D chains of AuNPs on DNA molecule templates, but the control over the positioning of the AuNPs and the interparticle distances have often been quite limited [221–224].

Different biological building blocks, e.g. cowpea chlorotic mottle virus (CCMV) [156, 225] and ferritin [156] protein cages and tobacco mosaic virus (TMV) rods [158], have successfully been used to guide the formation of well-defined AuNP crystalline superlattice structures through electrostatic self-assembly. Recently, Jiang *et al.* [226] also reported that well-ordered 1D and 2D peptide-DNA hybrid materials can be constructed by electrostatic self-assembly of positively charged collagen-mimetic peptides and DNA origami nanosheets or bricks. These studies, taken together, demonstrate great possibilities to use electrostatic self-assembly as an alternative to the conventional techniques relying on the molecular recognition properties of the DNA, when constructing nanoparticle superlattices with DNA origami structures as templates.

Chapter 6

Materials and methods

In this thesis, the electrostatic self-assembly of negatively charged DNA origami nanostructures and cationic gold nanoparticles (AuNPs) is studied in order to establish a method based on electrostatic interactions in which DNA origami nanoobjects can be used to direct the two- and three-dimensional arrangement of AuNPs. This chapter presents the DNA origami nanostructures and AuNPs used in the study, as well as the methods used for their preparation and characterization. The experimental approach used for the electrostatic self-assembly of the DNA origami nanoobjects and AuNPs is discussed in detail, and the techniques used to characterize the self-assembled DNA origami-AuNP complexes are presented.

6.1 DNA origami preparation and analysis

For this study, three different DNA origami nanostructures (6HB, 24HB and 60HB) were prepared. The fabrication process varied slightly between the structures, but for all structures the same purification method and analysis techniques were used.

6.1.1 Synthesis of DNA origami 6HB

The 6-helix bundle (6HB) DNA origami nanostructure is a tube with approximately a length of 412 nm and a diameter of 6 nm (Figure 6.1). The DNA origami design and folding conditions are with some adjustments adapted from Bui *et al.* [130]. In the DNA origami 6HB design used in this study, the extended staple strands in the original design have been replaced with shorter staple strands of normal length. A complete list of all the 170 staple strands required for the DNA origami 6HB structure can be found in

Appendix A.

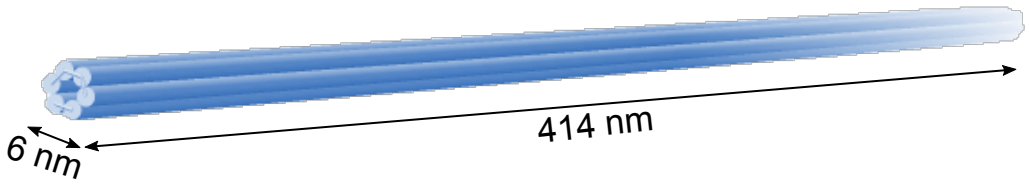

Figure 6.1: CanDo-simulated shape and dimensions of the 6-helix bundle (6HB).

The DNA origami 6HB was folded in 100 µl quantities in a one-pot reaction by mixing a 7249 nucleotides long single-stranded scaffold derived from bacteriophage M13mp18 (Tilibit Nanosystems) with ten times excess of staple strands (Integrated DNA Technologies). The folding took place in a buffer containing 1× TAE (40 mM tris(hydroxymethyl)aminomethane (Tris), 1 mM ethylenediamine tetraacetic acid (EDTA), and acetic acid for adjusting the pH to 8.0, purchased from VWR International) and 12.5 mM magnesium chloride ($MgCl_2$). The reagents and quantities used for the folding of the DNA origami 60HB are listed in Table 6.1. The origami folding mixture was subjected to a thermal-annealing ramp (G-storm G1 Thermal Cycler) that first cooled from 90 °C to 70 °C over the course of 13.2 minutes, from 70 °C to 60 °C over 13.2 minutes and then slowly cooled from 60 °to 27 °C over 10 hours and 52 minutes. After the annealing, the origamis were stored at 12 °C until the program was manually stopped. After the folding process, the DNA origami nanostructures were refrigerated at 4 °C.

Table 6.1: Reagents used in the folding of the DNA origami 6HB. Final concentration is the concentration of the reagents in the DNA origami folding mixture.

Component	**Volume**	**Concentration**	**Final concentration**
Scaffold, p7249	20 µl	100 nM	20 nM
Staples	40 µl	500 nM	200 nM
Folding buffer	40 µl	2.5×	1×
TAE buffer		2.5×	1×
$MgCl_2$		31.25 mM	12.5 mM

6.1.2 Synthesis of DNA origami 24HB

The 24-helix bundle (24HB) DNA origami nanostructure is a cylinder-formed object with approximately a length of 100 nm and a diameter of 16 nm (Figure 6.2). The DNA origami design and folding conditions are with some small adjustments adapted from Kuzyk *et al.* [124], and all of the 175 oligonucleotide staple strands used for the DNA origami 24HB structure are listed in the same reference.

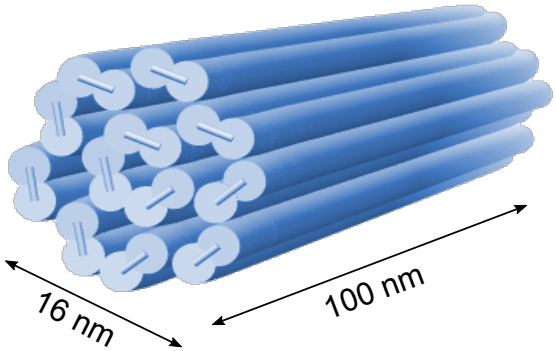

Figure 6.2: CanDo-simulated shape and dimensions of the 24-helix bundle (24HB).

Table 6.2: Reagents used in the folding of the DNA origami 24HB. Final concentration is the concentration of the reagents in the DNA origami folding mixture.

Component	**Volume**	**Concentration**	**Final concentration**
Scaffold, p7560	10 µl	100 nM	10 nM
Staples	20 µl	500 nM	100 nM
Folding buffer	40 µl	2.5×	1×
TAE buffer		2.5×	1×
$MgCl_2$		35 mM	14 mM
Distilled H_2O	30 µl	-	-

The DNA origami 24HB was folded in 100 µl quantities in a one-pot reaction by mixing a 7560 nucleotides long single-stranded scaffold derived from bacteriophage M13mp18 (Tilibit Nanosystems) with ten times excess of staple strands (Integrated DNA Technologies). The folding took place in a

buffer containing 1× TAE (40 mM tris(hydroxymethyl)aminomethane (Tris), 1 mM ethylenediamine tetraacetic acid (EDTA), and acetic acid for adjusting the pH to 8.0, purchased from VWR International) and 14 mM magnesium chloride ($MgCl_2$). The reagents and quantities used for the folding of the DNA origami 24HB are listed in Table 6.2. The origami folding mixture was subjected to a thermal-annealing ramp (G-storm G1 Thermal Cycler) that first cooled from 65 °C to 60 °C over the course of 90 minutes and then slowly cooled from 60 °C to 39 °C over 60 hours. After the annealing, the origamis were stored at 12 °C until the program was manually stopped. After the folding process, the DNA origami nanostructures were refrigerated at 4 °C.

6.1.3 Synthesis of DNA origami 60HB

The 60-helix bundle (60HB) DNA origami nanostructure is a rectangular cuboid with dimensions of approximately 20 nm × 20 nm × 40 nm (Figure 6.3). The origami was prepared as earlier reported by Linko *et al.* [227] and all of the 141 oligonucleotide staple strands used for the DNA origami 60HB structure are listed in the same reference.

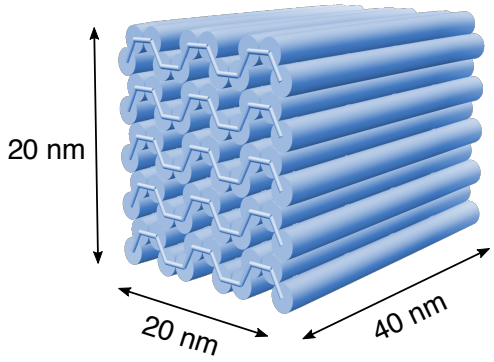

Figure 6.3: CanDo-simulated shape and dimensions of the 60-helix bundle (60HB).

The DNA origami 60HB was folded in 100 µl quantities in a one-pot reaction by mixing a 7249 nucleotides long single-stranded scaffold derived from bacteriophage M13mp18 (Tilibit Nanosystems) with ten times excess of staple strands (Integrated DNA Technologies). The folding took place in a buffer containing 1× TAE (40 mM tris(hydroxymethyl)aminomethane (Tris), 1 mM ethylenediamine tetraacetic acid (EDTA), and acetic acid for adjusting the pH to 8.0, purchased from VWR International), 20 mM magnesium chloride ($MgCl_2$) and 5 mM sodium chloride (NaCl). The reagents

and quantities used for the folding of the DNA origami 60HB are listed in Table 6.3. The origami folding mixture was subjected to a thermal-annealing ramp (G-storm G1 Thermal Cycler) that first cooled from 65 °C to 60 °C over the course of 90 minutes and then slowly cooled from 60 °C to 39 °C over 60 hours. After the annealing, the origamis were stored at 12 °C until the program was manually stopped. After the folding process, the DNA origami nanostructures were refrigerated at 4 °C.

Table 6.3: Reagents used in the folding of the DNA origami 60HB. Final concentration is the concentration of the reagents in the DNA origami folding mixture.

Component	**Volume**	**Concentration**	**Final concentration**
Scaffold, p7249	20 µl	100 nM	20 nM
Staples	40 µl	500 nM	200 nM
Folding buffer	40 µl	2.5×	1×
TAE buffer		2.5×	1×
NaCl		12.5 mM	5 mM
$MgCl_2$		50 mM	20 mM

6.1.4 Purification of synthesized DNA origamis

A non-destructive PEG purification method adapted from the research group of Dietz [110] was used to remove the excess amount of non-integrated staple strands from the synthesized DNA origami structures. This technique utilizes macromolecular crowding and the fact that high molecular weight DNA origamis are sterically excluded from the hydrodynamic volume of polyethylene glycol (PEG). When PEG is added as a crowding agent to the reaction mixture after the DNA origami synthesis, the DNA origamis will precipitate out of solution, but the excess staple strands will remain in solution.

200 µl of the DNA origami reaction mixture was diluted four-fold in 1× folding buffer (FOB) to obtain a starting volume of 800 µl. The solution was mixed 1:1 with precipitation buffer (15 % PEG 8000 (w/v), 1× TAE and 505 mM NaCl) and centrifuged at 14000 g for 30 minutes at room temperature using an Eppendorf 5420 microcentrifuge. The supernatant was discarded and the DNA origami precipitate was resuspended in 1× FOB. Depending on the wanted concentration, the DNA origami precipitate was resuspended to 0.12-1 times of the initial reaction volume. The PEG purified samples were incubated overnight at room temperature before refrigerated at 4 °C.

6.1.5 Analysing DNA origamis

The concentrations of the prepared DNA origami structures were estimated using UV/Vis spectroscopy. The absorbance at a wavelength of 260 nm was measured with a BioTek Eon Microplate spectrophotometer using a Take3^{TM} micro-volume plate and a sample size of 2 µl. When the absorbance at a wavelength of 260 nm (A_{260}) is known, the DNA origami concentration (c_{DNA}) can be calculated using Beer-Lambert law

$$A_{260} = \varepsilon_{260} c_{DNA} l, \tag{6.1}$$

where ε_{260} is the approximated molar extinction coefficient and l is the path length through the solution in centimetres (0.05 cm) [228]. The extinction coefficient is approximated by the number of hybridized respective non-hybridized nucleotides in the DNA origami structure [229], and the extinction coefficient is estimated to 0.8×10^8 $M^{-1}cm^{-1}$ for the DNA origami 24HB shape, 0.9×10^8 $M^{-1}cm^{-1}$ for the DNA origami 60HB shape and 1.0×10^8 $M^{-1}cm^{-1}$ for the DNA origami 6HB shape.

Agarose gel electrophoresis was used to qualitatively analyze the DNA origami folding and confirm the removal of excess amount of non-integrated staple strands. Gel electrophoresis is a widely used technique to separate nucleic acid fragments by size. When an external electric field is applied, the negatively charged DNA fragments will migrate through the agarose gel matrix towards the anode with the same mobility, but since larger fragments will be retarded by the pores in the gel matrix the fragments will be size separated. Wilson. In this case, the gel electrophoresis will separate the correctly folded DNA origami structures with lower electrophoretic mobility from the staple strands. Ethidium bromide (EtBr) was used as a fluorescent tag during the gel electrophoresis. EtBr binds to DNA by intercalating between stacked base pairs and fluoresces with an intense orange-red color when exposed to ultraviolet (UV) light [228].

For the agarose gel electrophoresis, a 2 % (w/v) agarose gel was made by dissolving 2 g of agarose (Bioline) in 90 ml of 1× TAE buffer and 10 ml of 110 mM $MgCl_2$ solution. The gel was stained with 80 µl of EtBr solution (0.58 mg/l). The samples were prepared by mixing 10 µl of DNA origami solution with 2 µl of 6× Gel Loading Dye Blue (New England Biolabs), and the whole sample of 12 µl was loaded into the gel well. The M13mp18 scaffold strand was used as reference sample after first diluted 2:3 in 1× FOB. The gel electrophoresis was performed in an ice bath at a constant voltage of 95 V for 40 minutes using a BioRad PowerPac^{TM} Basic. 1× TAE buffer containing

11 mM $MgCl_2$ was used as running buffer. The gel was visualized under UV light using a BioRad Gel Doc Ez Imager.

Additionally, the folded and purified DNA origami nanostructures were imaged using transmission electron microscopy (TEM) to verify that they were correctly folded. The TEM images were obtained using a FEI Tecnai 12 Bio-Twin instrument operated at an acceleration voltage of 120 kV. The samples were prepared on plasma cleaned (30 seconds oxygen plasma flash) Formvar carbon coated copper grids (Electron Microscopy Science) mainly following the protocol described earlier by Castro *et al.* [62]. 3 µl of DNA origami solution was applied onto the carbon-coated side of the TEM grid and excess sample solution was blotted away with filter paper after an incubation of 2 minutes. The samples were further negatively stained using a 2 % uranyl formate stain solution containing 25 mM sodium hydroxide (NaOH). First, the sample-side of the grid was immersed into a 5 µl stain solution droplet. The stain was blotted away with filter paper immediately and the sample-side of the grid was immersed into another droplet of 20 µl of stain solution. Excess stain solution was blotted away with filter paper after 45 seconds. After these procedures, the samples were left to dry under ambient conditions for at least one hour before imaging.

6.2 Cationic gold nanoparticles

In this study, the electrostatic self-assembly of DNA origami nanostructures and cationic gold nanoparticles (AuNPs) is studied. In order to demonstrate the importance of size complementarity between the AuNP and the DNA origami structure, AuNPs of three different sizes are used, all with a narrow size distribution. The larger two AuNPs were synthesized as previously described by Hassinen *et al.* [225] and Liljeström *et al.* [158] and had an average core diameter (D_{core}) of 10.9 nm respective 12.4 nm. These AuNPs were functionalized with a covalently linked (11-mercaptoundecyl)-*N,N,N*-trimethylammonium bromide (MUTAB) ligand, which due to the quaternary ammonium group gives the AuNPs a cationic surface over a wide pH range (Figure 6.4a). The small AuNP with an average core diameter of 2.5 nm was on the other hand synthesized as previously described by Kostiainen *et al.* [156] taking advantage of the biphasic Brust-Schiffrin method [230]. This AuNP is not functionalized with a MUTAB ligand, but with an other ligand (for structure see Figure 6.4b) also containing a quarternary ammonium group.

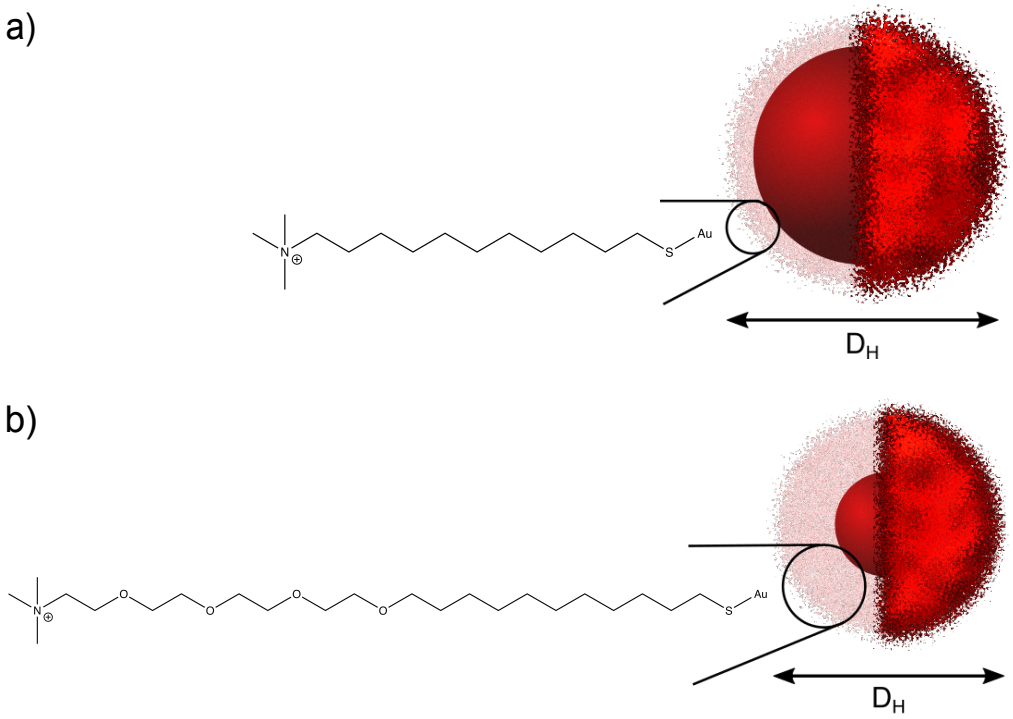

Figure 6.4: Schematic of the gold nanoparticles used in the study including the chemical structure of the cationic ligand. a) The larger two AuNPs (D_{core} = 10.9 nm and D_{core} = 12.4 nm). b) The small AuNP (D_{core} = 2.5 nm).

6.2.1 Characterization

The hydrodynamic diameter, D_{H}, of the AuNPs was determined by dynamic light scattering (DLS) using a Zetasizer Nano ZS (Malvern Instruments Ltd) equipped with a He-Ne ion laser at a wavelength of 633 nm. The measurements were carried out at 25 °C and the scattered light was detected at an angle of 173° (backscattering) with laser attenuation and measurement position adjusted automatically by the Malvern software. The hydrodynamic diameter was determined from the volume-based particle size distribution, and a refractive index of 0.18 and an absorption index of 3.4 were used for the distribution estimation [225]. The measurements were done in disposable Brand® micro UV-cuvettes, and each sample consisted of 100 µl of neutral aqueous AuNP solution (2-17 x 10^{12} AuNPs/ml). Three measurements of 10 runs with 5 s duration was performed for each sample, and the hydrodynamic diameter was obtained as the average of at least three samples with different concentrations.

For the larger two AuNPs, the colloidal stability of the AuNPs in solutions of different ionic strength was studied using UV/Vis spectroscopy. AuNPs with a diameter of 10-15 nm typically have an absorption peak in the region of 520 nm due to the surface plasmon resonance and a strong absorption of green light [164–170]. When the AuNPs aggregate, their oscillating electric fields starts to interact with each other and the surface plasmons of the AuNPs will be coupled. As a result there will be a significant shift to longer wavelengths and a broadening of the surface plasmon band. [169, 170, 231] Depending on AuNP size and concentration as well as the degree of aggregation this can also be seen with the naked eye as a color change from the distinctive ruby red for colloidal gold to blue-grey [182, 231]. Due to this change in the surface plasmon band, the colloidal stability of the AuNPs can be determined as a function of ionic strength by the aggregation index $A_{800\text{nm}}/A_{522\text{nm}}$, where $A_{800\text{nm}}$ and $A_{522\text{nm}}$ are the absorbances at a wavelength of 800 nm respective 522 nm measured by UV/Vis spectroscopy.

The UV/Vis absorption spectra were recorded at 2 nm intervals in the wavelength range of 400 nm to 850 nm using a BioTek Cytation 3 microplate reader. The measurements were done at 37 °C from 96-well polystyrene microplates without a lid (Thermo Scientific$^{\text{TM}}$ Nunc$^{\text{TM}}$ MicroWell$^{\text{TM}}$), and a sample size of 70 µl was used. For the measurements a series of samples with different NaCl concentration was prepared, but the AuNP concentration was kept constant at 6 nM for all samples.

6.3 Electrostatic self-assembly of DNA origami and gold nanoparticles

To better understand the formation of DNA origami-AuNP complexes through electrostatic self-assembly, different combinations of DNA origami structures and AuNPs were studied. The following combinations of DNA origami structures and AuNPs have been investigated within this study:

- DNA origami 6HB + small AuNP ($D_{\text{core}} = 2.5$ nm)
- DNA origami 6HB + middle-sized AuNP ($D_{\text{core}} = 10.9$ nm)
- DNA origami 6HB + large AuNP ($D_{\text{core}} = 12.4$ nm)
- DNA origami 24HB + small AuNP ($D_{\text{core}} = 2.5$ nm)
- DNA origami 24HB + middle-sized AuNP ($D_{\text{core}}= 2.5$ nm)
- DNA origami 60HB + large AuNP ($D_{\text{core}} = 12.4$ nm)

In addition, the effect of the stoichiometric ratio between the AuNPs and the DNA origami structures was studied. The electrostatic binding of the cationic AuNPs to the negatively charged DNA origami structures was first studied with electrophoretic mobility shift assay (combinations with the smallest AuNP) or UV/Vis spectroscopy (combinations with the larger two AuNPs) in order to find a limited range of possible fruitful AuNP to DNA origami ratios. When this range was found, DNA origami-AuNP assemblies were formed during dialysis, and characterized using small-angle X-ray scattering (SAXS) and transmission electron microscopy (TEM). SAXS was also used to determine the optimal stoichiometric ratio between the AuNPs and the DNA origami structures.

6.3.1 Electrophoretic mobility shift assay

For the the smallest AuNPs ($D_{\text{core}} = 2.5$ nm), agarose gel electrophoretic mobility shift assay (EMSA) was used to study the electrostatic binding of the cationic AuNPs to the negatively charged DNA origami structures. EMSA is usually used to study protein binding to a specific DNA sequence, but the same technique can also be used to identify efficient binding of the AuNPs to the DNA origami structures. As the AuNPs bind to the DNA origami structures and assemblies are formed, the DNA origami structures will be located in the assemblies rather than as free DNA origami structures in the solution, which will affect their electrophoretic mobility. The assemblies have larger size and a different charge compared to the individual DNA origamis, and a decrease in the electrophoretic mobility could therefore indicate a successful binding of the AuNPs to the DNA origami structures.

For the EMSA, a 2 % (w/v) agarose gel was prepared, electrophoresed and visualized under UV light as earlier described in Section 6.1.5. In the samples for the EMSA, the DNA origami concentration was kept constant at 6.3 nM, but the AuNP concentration varied between the samples. After mixing the DNA origami solution with AuNP solution and distilled H_2O, the samples were incubated for 20 minutes at room temperature to allow the formation of complexes. 3 µl of Gel Loading Dye Blue (New England Biolabs) was then added to the samples (volume of 15 µl), and the whole sample of 18 µl was loaded into the gel well.

6.3.2 Aggregation of DNA origami and AuNP

For the larger two AuNPs, the electrostatic binding of the cationic AuNPs to the negatively charged DNA origami nanostructures was studied in solutions of different ionic strength using UV/Vis spectroscopy. When the AuNPs

bind to the DNA origami structures, their surface plasmons will be coupled in a manner similar to when the AuNPs aggregate with each other at high ionic strength. The changes in the surface plasmon band and in the colloidal stability of the AuNPs when also DNA origami structures are present in the solution could therefore give some indications of the electrostatic binding of the AuNPs to the DNA origami structures.

The UV/Vis absorption sepctra were also in this case recorded at 2 nm intervals in the wavelength range of 400 nm to 850 nm using a BioTek Cytation 3 microplate reader. The measurements were done at 37 °C from 96-well polystyrene microplates without a lid (Thermo Scientific™ Nunc™ MicroWell™), and a sample size of 70 µl was used. For the measurements a series of samples with different NaCl and DNA origami concentrations was prepared, but the AuNP concentration was kept constant at 6 nM for all samples. The colloidal stability of the AuNPs was determined as a function of ionic strength by the aggregation index $A_{800\text{nm}}/A_{522\text{nm}}$, where $A_{800\text{nm}}$ and $A_{522\text{nm}}$ is the absorbance at a wavelength of 800 nm respective 522 nm measured by UV/Vis spectroscopy.

6.3.3 Formation of DNA origami-AuNP assemblies

As already discussed in Section 4.2, oppositely charged components readily form kinetically trapped configurations when mixed together at low ionic strengths. The DNA origami nanostructures and the AuNPs are therefore mixed together at such a high ionic strength (c_{NaCl} = 500-750 mM depending on the size of the AuNP), where the electrostatic interaction between the different charged components are efficiently screened and the AuNPs to some extent aggregated with each other. Then, by slowly dialysing the mixture against decreasing ionic strength, the electrostatic attraction between the AuNPs and the DNA origami structures can be tuned, and ordered assemblies can be formed. (Figure 6.5) A similar approach have previously been used to construct well-ordered superlattice structures of TMV nanorods and AuNPs [158].

The DNA origami-AuNP assemblies were formed during dialysis with floating dialysis cups (Slide-A-Lyzer® MINI Dialysis Units, 3500 MVCO, Thermo Scientific) that floated on the dialysate during continuous stirring. The dialysate consisted of 5 mM $MgCl_2$ and a specific NaCl concentration (c_{NaCl}). Depending on the size of the AuNP, the c_{NaCl} was 500-750 mM in the beginning of the dialysis and the c_{NaCl} was decreased by 50 mM every 30 minutes until a final c_{NaCl} = 0 mM was reached. The dialysate was then changed one more time (to c_{NaCl} = 0 mM and c_{MgCl_2} = 5 mM) and the dialysis was continued for two hours. The DNA origami solution and

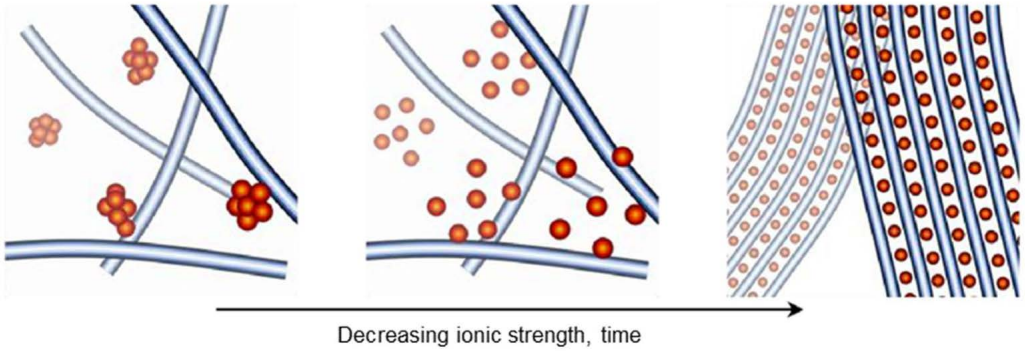

Figure 6.5: The DNA origami-AuNP assemblies were formed during dialysis against decreasing ionic strength. Reprinted from [161].

the AuNP solution were mixed, and the NaCl concentration of the mixture adjusted to the initial c_{NaCl} of the dialysate before placed into the dialysis cup.

6.4 Characterization of self-assembled structures

The DNA origami-AuNP complexes formed through electrostatic self-assembly were characterized using small-angle X-ray scattering, transmission electron microscopy and cryogenic electron tomography as described below.

6.4.1 Small-angle X-ray scattering

The formed DNA origami-AuNP assemblies were studied with small-angle X-ray scattering (SAXS) in order to gain information about their structural geometries. SAXS is a noninvasive and reliable technique to decide whether a sample is crystalline or amorphous, but also to determine the geometry of the crystal structure. In a crystal structure the building blocks have a well-ordered arrangement, and each crystal plane in this arrangement will reflect incident X-rays differently. By studying the reflection of the incident X-rays from different crystal orientations, the crystal structure and the lattice constant(s) can be determined. During SAXS measurements, the sample is irradiated with monochromated X-rays, and the intensity of the X-rays scattered by the sample are measured by the detector as a 2D interference

pattern. This scattering pattern is usually presented as the magnitude of the scattering vector, q,

$$q = \frac{4\pi sin\theta}{\lambda}, \tag{6.2}$$

where 2θ is the scattering angle and λ the wavelength of the radiation. [232]

For the SAXS measurements, 10 µl of the aqueous sample from the dialysis was placed in a metal ring and tightly sealed by Kapton tape on both sides, resulting in a sample with a liquid thickness of approximately 0.9 mm. To reduce background scattering from air, vacuum was applied in the sample environment. The measurements were carried out using a Bruker Microstar microfocus rotating anode X-ray source (Cu Kα radiation, $\lambda = 1.54$ Å). The X-ray beam was monochromated and focused by a Montel multilayer focusing monochromator (Incotec). The beam was further collimated with four sets of collimation slits (JJ X-ray) resulting in a final spot size of approximately 1 mm in diameter at the sample position. The scattered intensity was collected using a Hi-Star 2D area detector (Bruker). Depending on the sample, the sample-to-detector distance was 0.59 m and/or 1.59 m, and a silver behenate standard sample was used for the calibration of the length of the scattering vector q. One-dimensional SAXS data were obtained by azimuthally averaging the 2D scattering data.

6.4.2 Transmission electron microscopy and cryogenic electron tomography

The DNA origami-AuNP assemblies were imaged using both conventional transmission electron microscopy (TEM) and cryogenic transmission electron microscopy (cryo-TEM) in order to gain additional information about the structure and composition of the DNA origami-AuNP complexes. Further, cryogenic electron tomography (cryo-ET) reconstruction was used to visualize DNA origami-AuNP assemblies from different orientations.

The conventional TEM images were obtained using a FEI Tecnai 12 BioTwin instrument operated at an acceleration voltage of 120 kV. The samples were prepared by applying 3 µl of sample solution on plasma cleaned (30 seconds oxygen plasma flash) Formvar carbon coated copper grids (Electron Microscopy Science). The samples were incubated for 2.5 minutes before excess sample solution was blotted away with filter paper. The samples were left to dry under ambient conditions for at least one hour before imagning.

The cryo-TEM images were obtained using a JEM 3200FSC field emission cryo-TEM (JEOL) operated at 300 kV in bright field mode with an Omega-

type Zero-loss energy filter. The images were acquired with Gatan Digital Micrograph software while the specimen temperature was maintained at -187 °C. The cryo-TEM samples were prepared by applying 3 μl of sample solution (diluted 1:5 or 1:10 in distilled water) on plasma cleaned (30 seconds oxygen plasma flash) 300-mesh copper grids with lacey carbon support film and plunge freezed in 1:1 liquid propane/ethane mixture using vitrobot with 2.5 s blotting time under 55 % humidity.

Tilt series for the cryo-ET reconstruction were obtained using above mentioned sample preparation techniques for cryo-TEM and the JEM 3200FSC field emission cryo-TEM (JEOL) under above mentioned conditions. The tilt series between ±69° angles with 2-3° increment steps were acquired with the SerialEM-software package [233]. Prealignment, fine alignment and the cropping of the tilt series was executed with IMOD [234]. The images were binned 2-4 times to reduce noise and computation time. Maximum entropy method (MEM) reconstruction scheme was carried out with custom made program on Mac or Linux cluster with regularization parameter value of $\lambda = 0.001$ [235].

Chapter 7

Results and discussion

This chapter outline the main results obtained within the scope of this thesis.

7.1 DNA origami folding

Agarose gel electrophoresis and transmission electron microscopy (TEM) were used to verify the correct folding of all three DNA origami structures. Furthermore, the removal of excess amount of non-integrated staple strands by the PEG-purification method was confirmed with agarose gel electrophoresis. Both agarose gel electrophoresis and TEM indicated a correct folding and effecient PEG-purification of all three structures, as can be seen in Figure 7.1-7.3.

In the gel electrophoresis, the electrophoretic mobility of the folded DNA origami structure is compared to the electrophoretic mobility of the scaffold strand. The agarose gel electrophoresis images show that the folded DNA origami (middle and right lane) in moves faster in the gel than the scaffold strand (left lane), which indicates that the DNA origami structure has been successfully folded. The DNA origami structure is compared to the scaffold more compact and have therefore a higher electrophoretic mobility. The bright area at the bottom of the gel lane for unpurified DNA origami (middle lane) is excess staple strands. They are smaller in size than the DNA origami structure and have thus a higher electrophoretic mobility. This bright area disappears in the gel lane for PEG-purified DNA origami (right lane), which demonstrates that the excess staple strands have been successfully removed. The gel lanes for the DNA origami 24HB structure (Figure 7.2, middle and right lane) have additional bands above the leading band for the single DNA origami structure, which indicates that these DNA origami nanostructures easily interact with each other and form dimers and trimers.

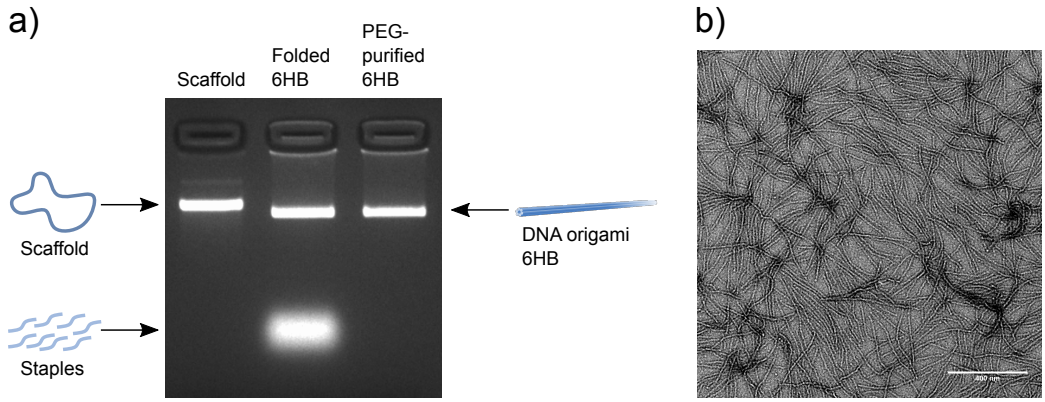

Figure 7.1: a) Agarose gel electrophoresis of the DNA origami 6HB structure before and after PEG-purification. The 7249 bp long single-stranded scaffold was used as reference sample. b) TEM image of the DNA origami 6HB structure (negatively stained with uranyl formate).

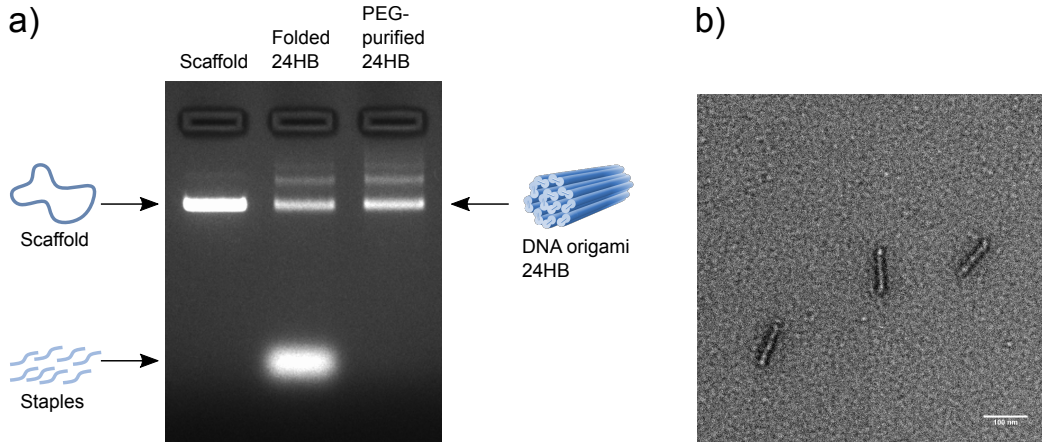

Figure 7.2: Agarose gel electrophoresis of the DNA origami 24HB structure before and after PEG-purification. The 7560 bp long single-stranded scaffold was used as reference sample. b) TEM image of the DNA origami 24HB structure (negatively stained with uranyl formate).

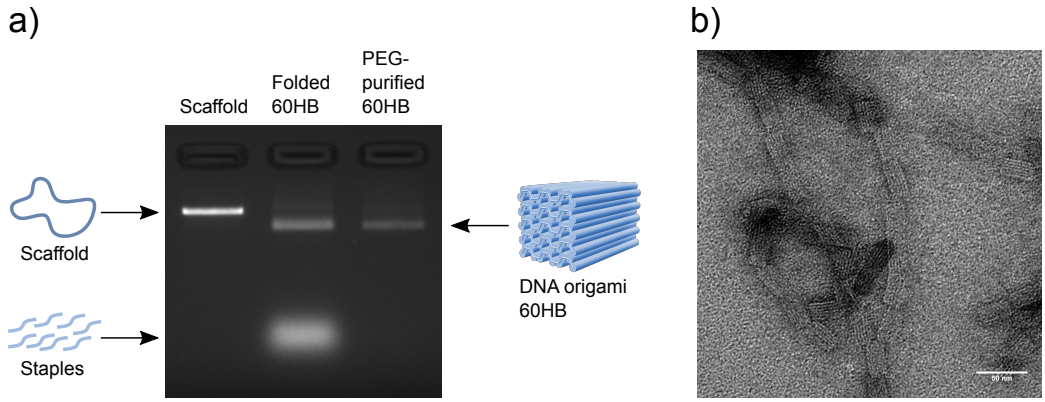

Figure 7.3: Agarose gel electrophoresis of the DNA origami 60HB structure before and after PEG-purification. The 7249 bp long single-stranded scaffold was used as reference sample. b) TEM image of the DNA origami 60HB structure (negatively stained with uranyl formate).

7.2 Properties of cationic gold nanoparticles

Dynamic light scattering (DLS) was used to study and characterize the cationic gold nanoparticles before the electrostatic self-assembly with the DNA origami nanostructures. The hydrodynamic diameter, D_{H}, was determined from the volume-based particle size distribution as an average of multiple measurements. A D_{H} of 8.5 nm was obtained for the AuNPs with a core diameter, D_{core}, of 2.5 nm, a D_{H} of 14.7 nm for the AuNPs with a D_{core} of 10.9 nm, and a D_{H} of 15.8 nm for the AuNPs with a D_{core} of 12.4 nm. In additions, the DLS measurements indicated that the AuNPs had a narrow size distribution and that there was nearly no aggregation of the AuNPs.

The small AuNPs ($D_{\mathrm{core}} = 2.5$ nm) will not aggregate in the presence of NaCl, but for the larger two AuNPs the colloidal stability in a wide range of ionic strength was studied. The large AuNPs ($D_{\mathrm{core}} = 12.4$ nm) were observed to aggregate at a ionic strength, c_{NaCl}, of about 500 mM (Figure 7.4a), whereas the middle-sized AuNPs ($D_{\mathrm{core}} = 10.9$ nm) aggregated at a $c_{\mathrm{NaCl}} \approx$ 750 mM (Figure 7.4b). The aggregation is reversible, and the AuNPs will detach from each other if the ionic strength is decreased. Similar behaviour have been demonstrated also before for like-charged AuNPs [158, 236].

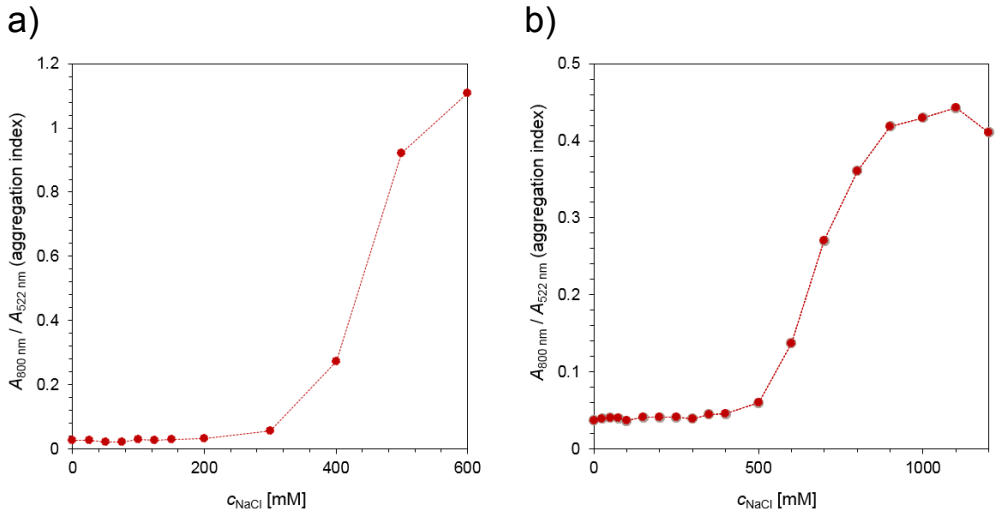

Figure 7.4: Colloidal stability of the AuNPs measured by UV/Vis spectroscopy. The colloidal stability is determined as a function of the ionic strength by the aggregation index, $A_{800\text{nm}}/A_{520\text{nm}}$. a) Large AuNPs ($D_{\text{core}}$ = 12.4 nm). b) Small AuNPs (D_{core} = 10.9 nm.)

7.3 AuNP binding properties of DNA origami nanostructures

The electrostatic binding of the cationic AuNPs to the negatively charged DNA origami structures was studied with agarose gel electrophoretic mobility shift assay (EMSA) or UV/Vis spectroscopy. For the small AuNPs (D_{core} = 2.5 nm), the absorption peak related to the localized surface plasmon resonance can not be readily seen with UV/Vis spectroscopy, and EMSA was therefore used as an alternative method for studing the binding affinity. A change in the surface plasmon band and the colloidal stability of the AuNPs can be an indication of a successful binding of the AuNPs to the DNA origami structures, but, moreover, also a decrease in the electrophoretic mobility can demonstrate that DNA origami-AuNP assemblies are formed. Furthermore, the results obtained from the EMSA and UV/Vis spectroscopy measurements formed together with dimension calculations the basis for the stoichiometric ratios between the AuNPs and the DNA origami structures ($n_{\text{AuNP}}/n_{\text{origami}}$) used in the study.

For the DNA origami 6HB structure, the EMSA clearly indicates that the small AuNPs bind to the DNA origami structures and form large complexes

with them (Figure 7.5). A $n_{\mathrm{AuNP}}/n_{\mathrm{origami}} \sim 200$ is needed to completely immobilize the DNA origami structures, but most of the DNA origami structures are bound to the DNA origami-AuNP complexes already at $n_{\mathrm{AuNP}}/n_{\mathrm{origami}} \sim 150$. Theoretically, each DNA origami 6HB structure can bind up to approximately 200 small AuNPs, and if well-ordered structures are formed even less AuNPs are needed. As most of the DNA origami structures are bound to the DNA origami-AuNP complexes already at $n_{\mathrm{AuNP}}/n_{\mathrm{origami}} \sim 150$, the same AuNP will most likely bind to multiple DNA origami structures, which further supports that large complexes are formed. The gel lanes for $n_{\mathrm{AuNP}}/n_{\mathrm{origami}} \sim 300$ and $n_{\mathrm{AuNP}}/n_{\mathrm{origami}} \sim 350$ have a faint band in front of the gel well. These bands are most likely a result of a partial detachment of the AuNPs from some of the DNA origami structures when the loading dye is mixed with the sample or when the sample is loaded into the gel well, which in turn alter the charge and the mobility of the complexes.

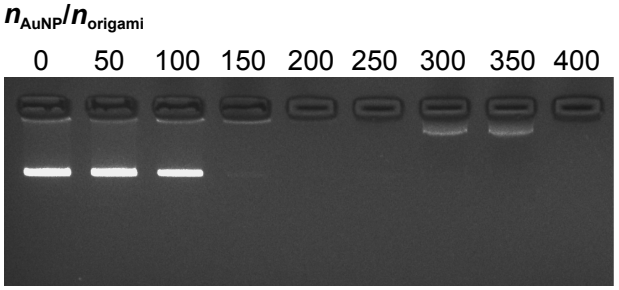

Figure 7.5: Agarose gel electrophoretic mobility shift assay (EMSA) of the DNA origami 6HB structure mixed with increasing amount of small AuNPs ($D_{\mathrm{core}} = 2.5$ nm). The DNA origami concentration was kept constant at 6.3 nM. The EMSA indicates that the AuNPs bind to the DNA origami structures and form large complexes with them at a stoichiometric ratio $n_{\mathrm{AuNP}}/n_{\mathrm{origami}}$ of 200 or higher.

For the DNA origami 24HB structure, however, the EMSA indicates that the small AuNPs do not even at high concentrations form large complexes with the DNA origami structures (Figure 7.6). Theoretically, each DNA origami 24HB structure can bind up to approximately 50 small AuNPs. Therefore, if large DNA origami-AuNP assemblies are formed, a shift in the electrophoretic mobility or at least a weakening of the leading band readily should be seen at $n_{\mathrm{AuNP}}/n_{\mathrm{origami}} \sim 120$. The intensity of the leading band is though not remarkably changing over time. This indicates that the AuNPs

only form loose complexes with the DNA origami structures, which does not affect the charge and mobility of the DNA origami structures.

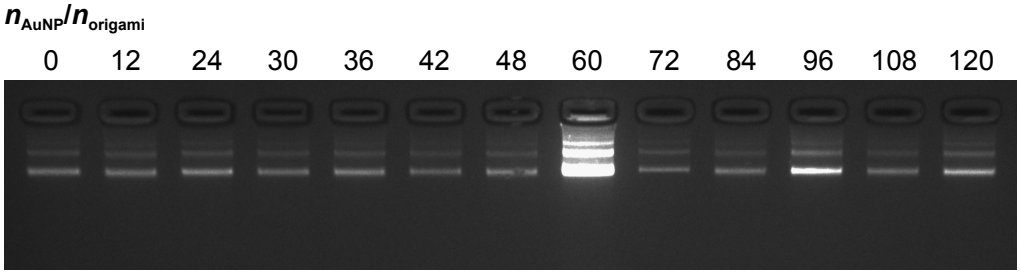

Figure 7.6: Agarose gel EMSA of the DNA origami 24HB structure mixed with increasing amount of small AuNPs ($D_{core} = 2.5$ nm). The DNA origami concentration was kept constant at 6.3 nM. The EMSA indicates that the AuNPs do not form large complexes with the DNA origami structures as there is no clear shift in the electrophoretic mobility.

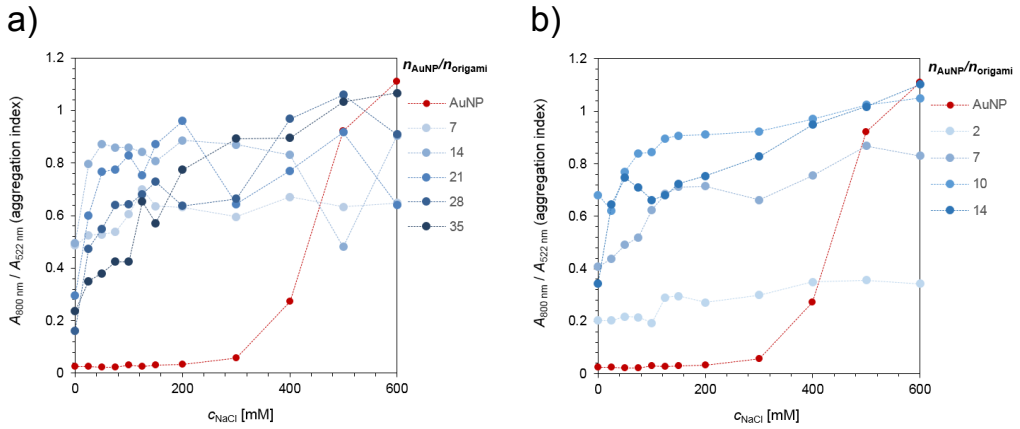

Figure 7.7: Colloidal stability of the AuNPs when also DNA origami structures are present in the solution. The colloidal stability is measured by UV/Vis spectroscopy and determined as a function of the ionic strength by the aggregation index, A_{800nm}/A_{520nm}. The AuNP concentration is kept constant ($c_{AuNP} = 6$ nM), but the DNA origami concentration varied between the series and is given as the AuNP to DNA origami ratio ($n_{AuNP}/n_{origami}$) in the legend. a) DNA origami 6HB and large AuNPs ($D_{core} = 12.4$ nm) b) DNA origami 24HB and large AuNPs ($D_{core} = 12.4$ nm).

The UV/Vis spectroscopy measurements done for the middle-sized (D_{core} = 10.9 nm) and large (D_{core} = 12.4 nm) AuNPs suggest that the AuNPs and the DNA origami structure interact with each other and form some kind of complexes. (Figure 7.7 and Appendix B). If DNA origami structures are present in the solution, the aggregation index is generally high already at low NaCl concentrations indicating that the AuNPs bind to the DNA origami structures. For the large AuNPs and the DNA origami 6HB structure (Figure 7.7a), the change in the colloidal stability suggest that $n_{\text{AuNP}}/n_{\text{origami}} \sim 21$ would be optimal for formation of DNA origami-AuNP complexes, whereas a $n_{\text{AuNP}}/n_{\text{origami}} \sim 7$ would be necessary for formation of DNA origami-AuNP complexes with middle-sized AuNPs and DNA origami 24HB structures (Figure 7.7). Provided that the AuNPs can bind to four DNA origami structures each, these results are in quite good agreement with the theoretical values (26 respective 6). For the other AuNP and DNA origami structure combinations, it is though difficult to predict suitable $n_{\text{AuNP}}/n_{\text{origami}}$ from the obtained results.

7.4 Characterization of formed assemblies

To better understand the formation of DNA-origami complexes through electrostatic self-assembly, different combinations of DNA origami structures and AuNPs were studied. In additon, the effect of the stoichiometric ratio between the AuNPs and the DNA origami structures was investigated. The DNA origami-AuNP assemblies were formed during dialysis against decreasing ionic strength, and all studied combinations yielded assemblies that were visible as a dark precipitate in the bottom of the dialysis cup. The formed assemblies were characterized using small-angle X-ray scattering (SAXS) and transmission electron microscopy (TEM).

Out of all studied combinations of DNA origami structures and AuNPs, well-ordered superlattice structures were formed for only one combination, DNA origami 6HB and small AuNP (D_{core} = 2.5 nm). Both the SAXS data (Figure 7.8) and the TEM images (Figure 7.9) suggest that highly ordered superlattice structures are formed for this combination. Further, clear diffraction peaks can be found for a wide range of stoichiometric ratios between the AuNPs and the DNA origami 6HB structures ($n_{\text{AuNP}}/n_{\text{origami}}$), which indicates that ordered structures are likely to be formed regardless of the $n_{\text{AuNP}}/n_{\text{origami}}$. The best resolved diffraction peaks were observed for the sample with $n_{\text{AuNP}}/n_{\text{origami}} \sim 150$, whereas the diffraction peaks were less evident with increasing/decreasing $n_{\text{AuNP}}/n_{\text{origami}}$. The optimal $n_{\text{AuNP}}/n_{\text{origami}}$ ~ 150 is also in excellent agreement with the obtained EMSA results (Fig-

ure 7.5).

A similar self-assembly behavior with clear diffraction peaks for a wide range of stoichiometric ratios has been reported earlier for tobacco mosaic virus (TMV) nanorods and AuNPs [158]. It was in this study proposed that the superlattice formation is cooperative self-assembly process in which the nucleation of the superlattice occurs when the TMV rods are cross-linked by AuNPs. As it will be energetically more favorable for the AuNPs to be in the cross-linked assemblies, bundles of AuNPs and TMV rods, forming large superlattice structures, will be present already at low $n_{\mathrm{AuNP}}/n_{\mathrm{origami}}$. In addition to the SAXS data, TEM images at different $n_{\mathrm{AuNP}}/n_{\mathrm{origami}}$ (Figure 7.9, additional images in Appendix C) support that this superlattice formation mechanism apply also for the formation of AuNP-DNA origami 6HB superlattices. For samples with excess amounts of DNA origami structures (Figure 7.9a), ordered AuNP-DNA origami 6HB structures were formed, but each intersitial channel between the DNA origami 6HB structure contained only a few AuNPs. At optimal $n_{\mathrm{AuNP}}/n_{\mathrm{origami}}$, large close-packed superlattices of AuNPs and DNA origami 6HB structures were formed, and no free AuNPs or DNA origami 6HB structures were observed (Figure 7.9b). Moreover, also for samples with excess amounts of AuNPs (Figure 7.9c), well-ordered superlattice structures were formed, but unbound AuNPs were present in the sample.

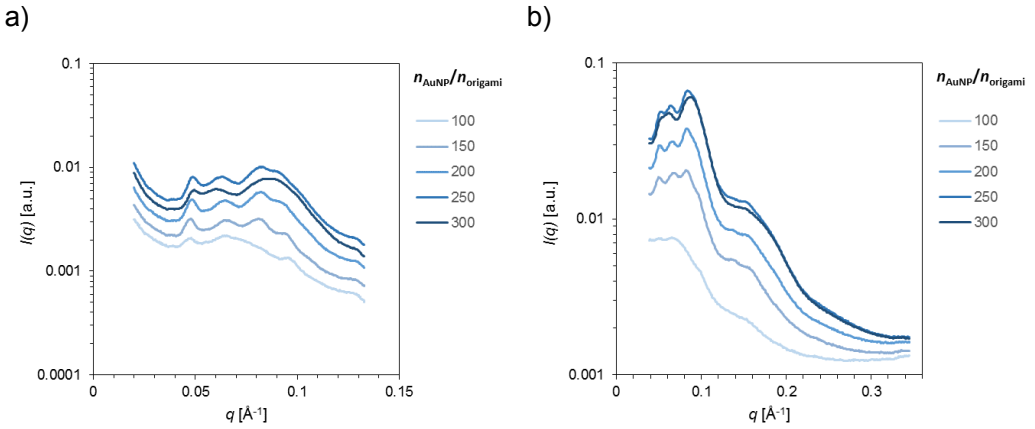

Figure 7.8: SAXS data measured from samples having different stoichiometric ratios between small AuNPs (D_{core} = 2.5 nm) and DNA origami 6HB structures ($n_{\mathrm{AuNP}}/n_{\mathrm{origami}}$). a) SAXS data measured at sample-to-detector distance of a) 1.59 m and b) 0.59 m.

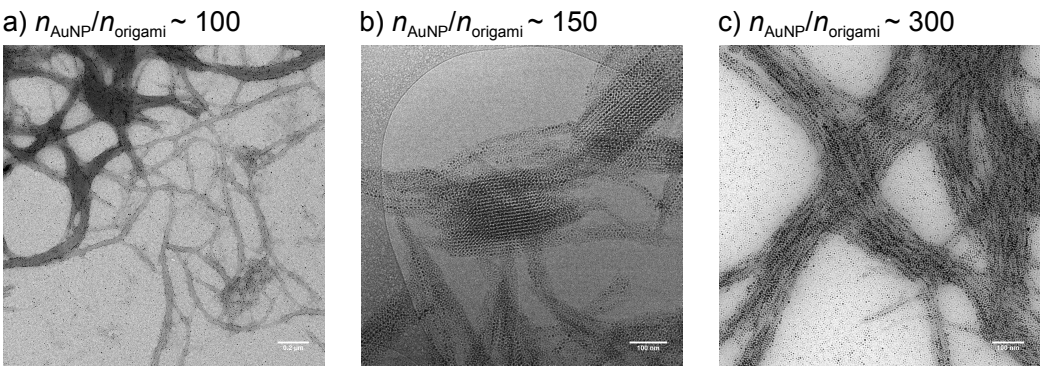

Figure 7.9: Electrostatic self-assembly of DNA origami 6HB structure and small AuNPs (D_{core} = 2.5 nm) yielded well-ordered superlattice structures. a) Conventional TEM image of a sample with excess amounts of DNA origami structures. b) Cryo-TEM image of a sample with optimal stoichiometric ratio between AuNPs and DNA origami structures. c) Conventional TEM image of a sample with excess amounts of AuNPs.

The DNA origami 6HB structure combined with small AuNPs yielded highly ordered superlattice structures, but combined with large AuNPs (D_{core} = 12.4 nm) only amorphous aggregates with short range order were formed (Figure 7.10a and Figure 7.11a). Further, small AuNPs combined with the DNA origami 24HB structure with significant different dimensions, gave also only amorphous aggregates (Figure 7.10b and Figure 7.11b-c). Similar amorphous aggregates were obtained also for all the other studied DNA origami and AuNP combinations: DNA origami 6HB and middle-sized (D_{core} = 10.9 nm) AuNPs, DNA origami 24HB and middle-sized AuNPs, and DNA origami 60HB and large AuNPs (See Appendix D - F for SAXS data and TEM images). Taken together, these results provide strong evidence of the importance of shape and charge complementarity between the building blocks for well-ordered structures to be formed through electrostatic self-assembly. Taking only dimensions into account, the DNA origami 6HB structure should form well-ordered structures with all the three sizes of AuNPs. The DNA origami 6HB structures are though rather flexible, and when combined with large, highly cationic AuNPs, they will most likely wrap around the AuNPs instead of forming well-ordered close-packed superlattices with them. The attraction to the cationic surface of the AuNPs will be so high that the flexible DNA origami 6HB structure will start to bend, which will preclude the formation of ordered structures. For the DNA origami 24HB structure, the short length (100 nm) is most likely the reason to why only amorphous

aggregates were formed. The dimension of its cross-section should be ideal for construction of ordered superlattices with all three AuNP sizes, but its short length compared to the AuNP dimensions is problematic. The DNA origami 24HB structure is not long enough to direct the growth of an ordered superlattice structure, and the next DNA origami to be cross-linked to the DNA origami 24HB-AuNP-complex can take more or less any orientation. The DNA origami 60HB structure was assembled with large AuNPs, which yielded only large amorphous aggregates. This was to some extent expected, since there is no kind of shape complementarity between the two building blocks. Further, the dimensions of the DNA origami 60HB structure are almost the same in all directions, allowing the DNA origami 60HB to bind to the DNA origami 60HB-AuNP complexes in any orientation.

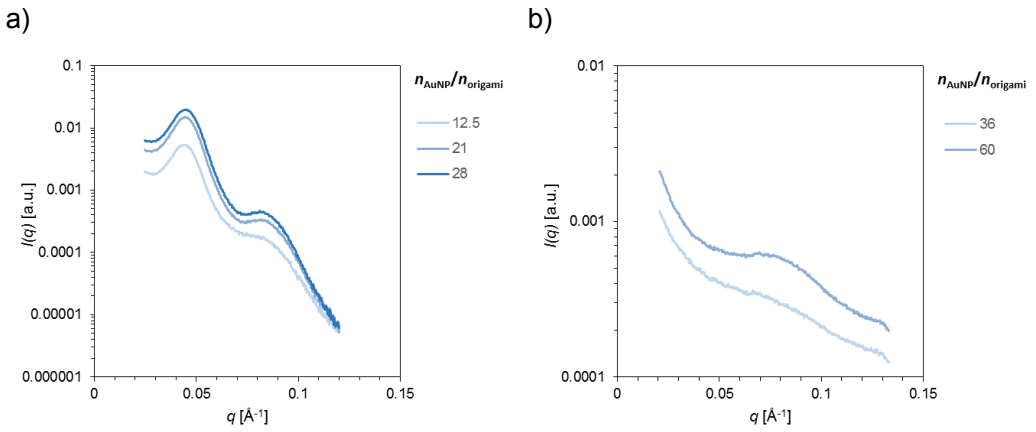

Figure 7.10: SAXS data measured from samples having different stoichiometric ratios between AuNPs and DNA origami structures ($n_{\mathrm{AuNP}}/n_{\mathrm{origami}}$). a) DNA origami 6HB structure and large AuNPs ($D_{\mathrm{core}} = 12.4$ nm). b) DNA origami 24HB structure and small AuNPs ($D_{\mathrm{core}} = 2.5$ nm).

7.5 Structure determination of formed assemblies

The DNA origami 6HB structure combined with small AuNPs ($D_{\mathrm{core}} = 2.5$ nm) yielded highly ordered superlattice structures with an optimal stoichiometric ratio between AuNPs and DNA origami 6HB structures ($n_{\mathrm{AuNP}}/n_{\mathrm{origami}}$) of 150. Additional analysis of the SAXS data for

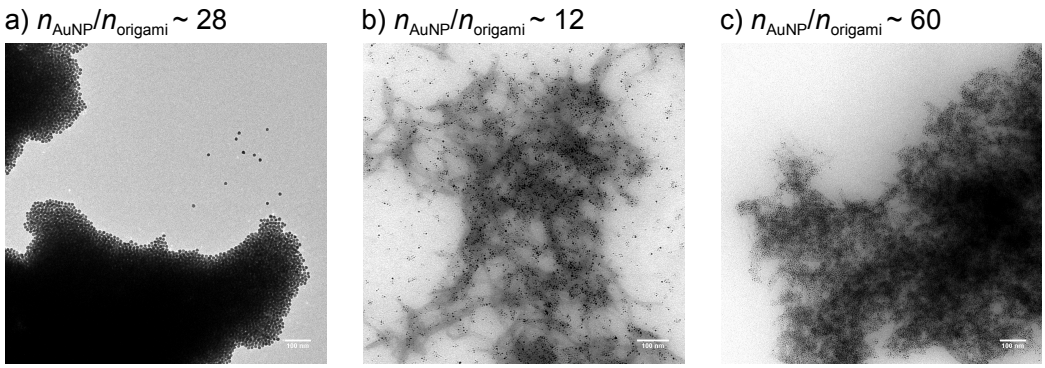

Figure 7.11: Electrostatic self-assembly of most of the combinations of DNA origami structures and AuNPs yielded amorphous aggregates with only short range order. a) Conventional TEM image of a sample containing DNA origami 6HB structures and large AuNPs ($D_{\text{core}} = 12.4$ nm). b)-c) Conventional TEM images of a sample containing DNA origami 24HB structures and small AuNPs ($D_{\text{core}} = 2.5$ nm).

$n_{\text{AuNP}}/n_{\text{origami}} \sim 150$ was therefore done to determine the hierarchical structure of the formed assemblies (Figure 7.12a). The structure factor, $S(q)$, was obtained by dividing the scattering intensity $I(q)$ by the $I(q)$ measured from AuNPs in solution using the local monodisperse approximation [238], whereas the theoretical $S(q)$ was calculated using PowderCell [237]. Unexpectedly, the peak positions of the structure factor, $S(q)$, corresponds to Bragg reflections from a 3D tetragonal crystal system (space group *p4mm*, number 99) with lattice constants $a = 9.25$ nm and $c = 12.5$ nm. The heights and peak positions of the experimental data is also in excellent agreement with calculated theoretical SAXS data for a 3D tetragonal crystal system with similar dimensions. In addition, the quadratic Miller indices of assigned reflections plotted as a function of the measured q-vaules demonstrate that a 3D tetragonal crystal structure is consistent with the experimental data.

Further, to confirm the SAXS data analysis and to visualize the superlattice structures from different orientations, cryo-TEM imaging and cryogenic electron tomography (cryo-ET) reconstruction were carried out. Both the cryo-TEM images (Figure 7.13) and the cryo-ET 3D reconstructions (data not shown) also clearly demonstrated that a 3D crystal structure was formed. The constant interparticle distance along the DNA origami 6HB structure and the 3D crystalline arrangement of the AuNPs were rather unexpected. The earlier reported superlattice structure of AuNPs and TMV rods, also

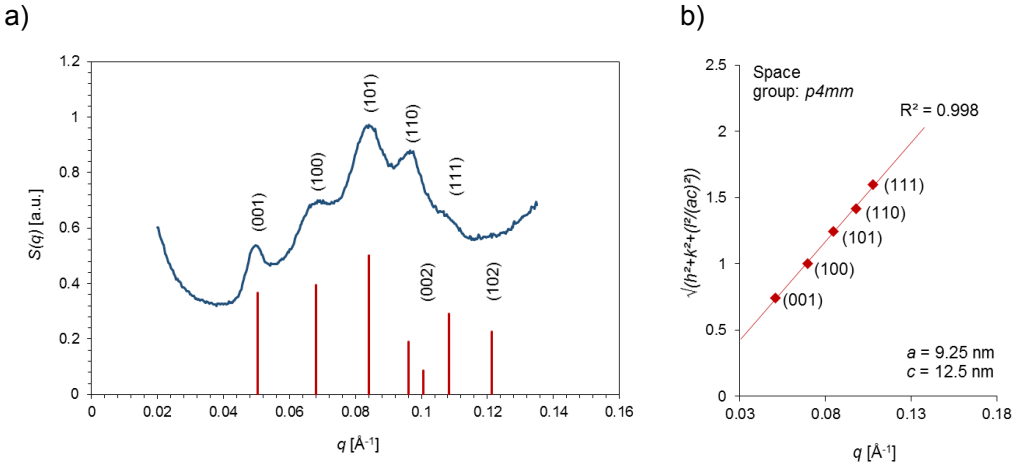

Figure 7.12: Structure determination of formed DNA origami 6HB-AuNP (D_{core} = 2.5 nm) assemblies. a) Measured calculated structure factor *S(q)* for $n_{\text{AuNP}}/n_{\text{origami}} \sim 150$. a = 9.25 nm and c = 12.5 nm are assumed in the theoretical *S(q)* calculated using PowderCell [237]. b) Quadratic Miller indices of assigned reflections plotted as a function of measured q-values.

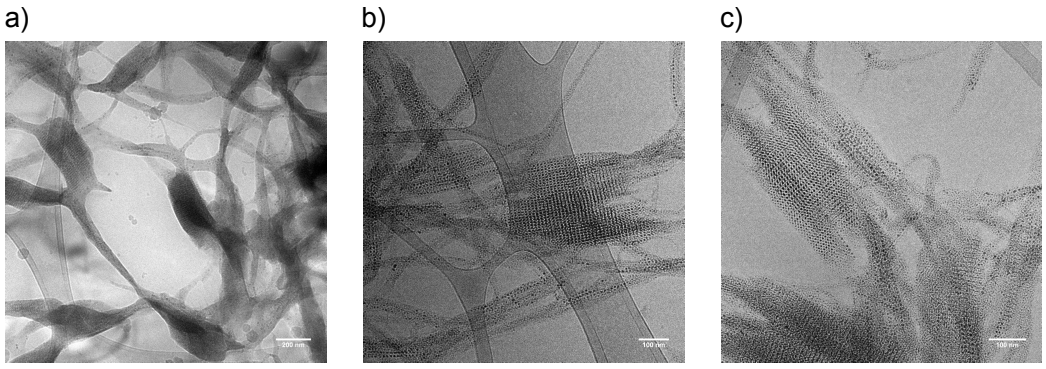

Figure 7.13: Electrostatic self-assembly of DNA origami 6HB structure and small AuNPs (D_{core} = 2.5 nm) yielded well-ordered superlattice structures. a) Cryo-TEM image of a dialysed sample at $n_{\text{AuNP}}/n_{\text{origami}} \sim 150$. b)-c) Cryo-TEM image of samples mixed togehter at $n_{\text{AuNP}}/n_{\text{origami}} \sim 150$ without dialysis.

formed through electrostatic self-assembly, had a 2D square lattice or 2D hexagonal lattice structure without any ordering of AuNPs along the TMV

structure [158]. The relative dimensions of the DNA origami 6HB and small AuNPs are quite similar, and a 2D lattice structure was therefore expected also for this combination.

Chapter 8

Conclusions and future perspectives

The results presented in this thesis demonstrate that a self-assembly method based on electrostatic interactions can be used to construct higher-ordered structures of gold nanoparticles (AuNPs) in a controlled and programmable manner. Electrostatic self-assembly of DNA origami 6HB nanostructures and small AuNPs ($D_{\text{core}} = 2.5$ nm, $D_{\text{H}} = 8.5$ nm) yielded highly ordered superlattice structures with a 3D tetragonal lattice structure, characterized by SAXS and TEM. The other studied combinations of DNA origami structures and AuNPs resulted in amorphous aggregates with only short range order, which suggest that both shape and charge complementarity between the building blocks are needed for well-ordered structures to be formed through electrostatic self-assembly.

The advances in the field of nanotechnology have given rise to a diverse toolbox of nanoscale objects with arbitrary shapes, sizes and material properties, but a full potential utilization of these nanoobjects requires strategies for controlling and and directing their arrangements and positions at the nanoscale level [1, 2]. Using AuNPs as a model of these nanoobjects, the results in this thesis demonstrate that electrostatic self-assembly guided by DNA origami structures provide a possible solution to this issue. The DNA origami technique can be used to construct almost any arbitrary 2D or 3D nanoobject with nanometer precision, and the new production techniques [91] make their synthesis rather inexpensive. DNA origami structures are therefore promising self-assembling building blocks for construction of well-ordered structures with properties, such as lattice geometry, designed specifically for the chosen application.

The limits of the traditional top-down nanofabrication techniques, such as lithography, will most likely be reached in the near future, and to keep

up with the Moore's law new effective techniques is needed [239]. Moreover, construction of 3D architectures using lithographic methods is both costly and challenging [6, 124]. Effective bottom-up fabrication techniques relying on self-assembly are therefore required, but the mechanisms behind the self-assembly are still not completely understood, which slows down the development process. The DNA origami structures with their precise, but tunable sizes are excellent tools for studying the wide range of interactions involved in the self-assembly, and how they contribute to the outcome of the self-assembly. A continuation of this study, and the next step in developing effective self-assembly strategies based on electrostatic interactions could therefore be to more systematically study how the size of the DNA origami structure affect how effective it is in guiding the electrostatic self-assembly of other nanoobjects.

Bibliography

[1] Bishop, K. J. M., Wilmer, C. E., Soh, S. & Grzybowski, B. A. *Nanoscale Forces and Their Uses in Self-Assembly.* Small. Vol. 5:14. 2009. pp. 1600-1630. DOI: 10.1002/smll.200900358.

[2] Nie, Z., Petukhova, A. & Kumacheva, E. *Properties and emerging applications of self-assembled structures made from inorganic nanoparticles.* Nature Nanotechnology. Vol. 5:1. 2010. pp. 15-25. DOI: 10.1038/nnano.2009.453.

[3] Li, H., Carter, J. D., LaBean, T. H. *Nanofabrication by DNA self-assembly.* Materials Today. Vol. 12:5. 2009. pp. 24-32. DOI: 10.1016/S1369-7021(09)70157-9.

[4] Chao, J., Lin, Y., Liu, H., Wang, L. & Fan, C. *DNA-based plasmonic nanostructures.* Materials Today. Vol. 18:6. 2015. pp. 326-335. DOI: 10.1016/j.mattod.2015.01.018.

[5] Whitesides, G. M. & Grzybowski, B. *Self-Assembly at All Scales.* Science. Vol. 295:5564. 2002. pp. 2418-2421. DOI: 10.1126/science.1070821.

[6] Whitesides, G. M. & Boncheva, M. *Beyond molecules: Self-assembly of mesoscopic and macroscopic components.* Proceedings of the National Academy of Sciences of the United States of America. Vol. 99:8. 2002. pp. 4769-4774. DOI: 10.1073/pnas.082065899.

[7] Zhang, S. *Fabrication of novel biomaterials through molecular self-assembly.* Nature Biotechnology. Vol. 21:10. 2003. pp. 1171-1178. DOI: 10.1038/nbt874.

[8] Mendes, A. C., Baran, E. T., Reis, R. L. & Azevedo, H. S. *Self-assembly in nature: using the principles of nature to create complex nanobiomaterials.* Wiley Interdisciplinary Reviews:

Nanomedicine and Nanobiotechnology. Vol. 5:6. 2013. pp. 582-612. DOI: 10.1002/wnan.1238.

[9] Seeman, N. C. *DNA in a material world.* Nature. Vol. 421:6921. 2003. pp. 427-431. DOI: 10.1038/nature01406.

[10] King, N. P. & Lai, Y-T. *Practical approaches to designing novel protein assemblies.* Current Opinion in Structural Biology. Vol. 23:4. 2013. pp. 632-638. DOI: 10.1016/j.sbi.2013.06.002.

[11] De Santis, E. & Ryadnov, M. G. *Peptide self-assembly for nanomaterials: the old new kid on the block.* Chemical Society Reviews. Vol. 44:22. 2015. pp. 8288-8300. DOI: 10.1039/c5cs00470e.

[12] Antonietti, M. & Förster, S. *Vesicles and Liposomes: A Self-Assembly Principle Beyond Lipids.* Advanced Materials. Vol. 15:16. 2003. pp. 1323-1333. DOI: 10.1002/adma.200300010.

[13] Aldaye, F. A., Palmer, A. L. & Sleiman, H. F. *Assembling Materials with DNA as the Guide.* Science. Vol. 321:5897. 2008. pp. 1795-1799. DOI: 10.1126/science.1154533.

[14] Hong, F., Zhang, F., Liu, Y. & Yan, H. *DNA Origami: Scaffolds for Creating Higher Order Structures.* Chemical Reviews. Vol. 117:20. 2017. pp. 12584-12640. DOI: 10.1021/acs.chemrev.6b00825.

[15] Seeman, N. C. *Nucleic acid junctions and lattices.* Journal of Theoretical Biology. Vol. 99:2. 1982. pp. 237-247. DOI: 10.1016/0022-5193(82)90002-9.

[16] Linko, V. & Dietz, H. *The enabled state of DNA nanotechnology.* Current Opinion in Biotechnology. Vol. 24:4. 2013. pp. 555-561. DOI: 10.1016/j.copbio.2013.02.001.

[17] Seeman, N. C. & Sleiman, H. F. *DNA nanotechnology.* Nature Reviews Materials. Vol. 3. 2017. no. 17068. DOI: 10.1038/natrevmats.2017.68.

[18] Nummelin, S., Kommeri, J., Kostiainen, M. A. & Linko, V. *Evolution of Structural DNA Nanotechnology.* Advanced Materials. Vol. 30. 2018. no. 1703721. DOI: 10.1002/adma.201703721.

[19] Rothemund, P. W. K. *Folding DNA to create nanoscale shapes and patterns.* Nature. Vol. 440:7082. 2006. pp. 297-302. DOI: 10.1038/nature04586.

[20] Ofir, Y., Samanta, B. & Rotello, V. M. *Polymer and biopolymer mediated self-assembly of gold nanoparticles.* Chemical Society Reviews. Vol. 37:9. 2008. pp. 1814-1825. DOI: 10.1039/B712689C.

[21] Julin, S., Nummelin, S., Linko, V. & Kostiainen, M. A. *DNA nanostructure-directed assembly of metal nanoparticle superlattices.* Journal of Nanoparticle Research. Vol. 20. 2018. DOI: 10.1007/s11051-018-4225-3. Accepted for publication.

[22] Kumar, A., Pattarkine, M., Bhadbhade, M., Mandale, A. B., Ganesh, K. N., Datar, S. S., Dharmadhikari, C. V. & Sastry, M. *Linear Superclusters of Colloidal Gold Particles by Electrostatic Assembly on DNA Templates.* Advanced Materials. Vol. 13:5. 2001. pp. 341-344. DOI: 10.1002/1521-4095(200103)13:5¡341::AID-ADMA341¿3.0.CO;2-X

[23] Warner, M. G. & Hutchison, J. E. *Linear assemblies of nanoparticles electrostatically organized on DNA scaffolds.* Nature Materials. Vol. 2:4. 2003. pp. 272-277. DOI: 10.1038/nmat853.

[24] Yang, D., Campolongo, M. J., Nhi Tran, T. N., Ruiz, R. C. H., Kahn, J. S. & Luo, D. *Novel DNA materials and their applications.* Wiley Interdisciplinary Reviews: Nanomedicine and Nanobiotechnology. Vol. 2:6. 2010. pp. 648-669. DOI: 10.1002/wnan.111.

[25] Jones, M. R., Seeman, N. C. & Mirkin, C. A. *Programmable materials and the nature of the DNA bond.* Science. Vol. 347:6224. 2015. no. 1260901. DOI: 10.1126/science.1260901.

[26] Alberts, B., Johnson, A., Lewis, J., Morgan, D., Raff, M., Robers, K. & Walter, P. *Molecular Biology of the Cell.* 6th ed. New York: Garland Science, 2014. 1342 pp. ISBN: 978-0-8153-4464-3.

[27] Nelson, D. L. & Cox, M. M. *Lehninger principles of biochemistry.* 4th ed. New York: W. H. Freeman and Company, 2005. 1119 pp. ISBN: 0-7167-4339-6.

[28] Kuriyan, J., Konforti, B. & Wemmer, D. *The Molecules of Life: Physical and Chemical Principles.* New York: Garland Science, 2013. 1008 pp. ISBN: 978-0-8153-4188-8.

[29] Yakovchuk, P., Protozanova, E. & Frank-Kamenetskii, M. D. *Base-stacking and base-pairing contributions into thermal stability of the DNA double helix.* Nucleic Acids Research. Vol. 34:2. 2006. pp. 564-574. DOI: 10.1093/nar/gkj454.

[30] Lin, C., Liu, Y. & Yan, H. *Designer DNA Nanoarchitectures.* Biochemistry. Vol. 48:4. 2009. pp. 1663-1674. DOI: 10.1021/bi802324w.

[31] Watson, J. D. & Crick, F. H. C. *Molecular Structure of Nucleic Acids: A Structure for Deoxyribose Nucleic Acid.* Nature. Vol. 171:4356. 1953. pp. 737-738. DOI: 10.1038/171737a0.

[32] Berg, J. M., Tymoczko, J. L. & Stryer, L. *Biochemistry.* 7th ed. New York: W. H. Freeman and Company, 2012. 1098 pp. ISBN: 978-1-4292-7635-1.

[33] Blackburn, G. M., Gait, M. J., Loakes, M. & Williams, D. M. *Nucleic acids in chemistry and biology.* 3rd ed. Oxford: The Royal Society of Chemistry, 2006. 470 pp. ISBN: 0-85404-654-2.

[34] Carcía-Ramos, J. C., Galindo-Murillo, R., Cortés-Guzmán, F. & Ruiz-Azuara, L. *Metal-based drug-DNA interactions.* Journal of the Mexican Chemical Society. Vol. 57:3. 2013. pp. 245-259. ISSN: 1870-249X.

[35] Bustamante, C., Smith, S. B., Liphardt, J. & Smith, D. *Single-molecule studies of DNA mechanics.* Current Opinion in Structural Biology. Vol 10:3. 2000. pp. 279-285. DOI: 10.1016/S0959-440X(00)00085-3.

[36] Gothelf, K., V. & LaBean, T. H. *DNA-programmed assembly of nanostructures.* Organic & Biomolecular Chemistry. Vol: 3:22. 2005. pp. 4023-4037. DOI: 10.1039/b510551j.

[37] Lin, C., Liu, Y., Rinker, S. & Yan, H. *DNA Tile Based Self-Assembly: Building Complex Nanoarchitectures.* ChemPhysChem. Vol. 7:8. 2006. pp. 1641-1647. DOI: 10.1002/cphc.200600260.

[38] Kallenbach, N. R., Ma, R-I. & Seeman, N. C. *An immobile nucleic acid junction constructed from oligonucleotides.* Nature. Vol. 305:5937. 1983. pp. 829-831. DOI: 10.1038/305829a0.

[39] Ma, R-I., Kallenbach, N. R., Sheardy, R. D., Petrillo, M. L., Seeman, N. C. *Three-arm nucleic acid junctions are flexible.* Nucleic Acids Research. Vol. 14:24. 1986. pp. 9745-9753. DOI: 10.1093/nar/14.24.9745.

[40] Wang, Y., Mueller, J. E., Kemper, B. & Seeman, N. C. *Assembly and Characterization of Five-Arm and Six-Arm DNA Branched Junctions.* Biochemistry. Vol. 30:23. 1991. pp. 5667-5674. DOI: 10.1021/bi00237a005.

[41] Wang, X. & Seeman, N. C. *Assembly and Characterization of 8-Arm and 12-Arm DNA Branched Junctions.* Journal of the American Chemical Society. Vol. 129:26. 2007. pp. 8169-8176. DOI: 10.1021/ja0693441.

[42] Fu, T-J. & Seeman, N. C. *DNA Double-Crossover Molecules.* Biochemistry. Vol. 32:13. 1993. pp. 3211-3220. DOI: 10.1021/bi00064a003.

[43] Li, X., Yang, X., Qi, J. & Seeman, N. C. *Antiparallel DNA Double Crossover Molecules As Components for Nanoconstruction.* Journal of the American Chemical Society. Vol. 118:26. 1996. pp. 6131-6140. DOI: 10.1021/ja960162o.

[44] Winfree, E., Liu, F., Wenzler, L. A. & Seeman, N. C. *Design and self-assembly of two-dimensional DNA crystals.* Nature. Vol. 394:6693. 1998. pp. 539-544. DOI: 10.1038/28998.

[45] LaBean, T. H., Yan, H., Kopatsch, J., Liu, F., Winfree, E., Reif, J. H. & Seeman, N. C. *Construction, Analysis, Ligation, and Self-Assembly of DNA Triple Crossover Complexes.* Journal of the American Chemical Society. Vol. 122:9. 2000. pp. 1848-1860. DOI: 10.1021/ja993393e.

[46] Shen, Z., Yan, H. Wang, T. & Seeman, N. C. *Paranemic Crossover DNA: A Generalized Holliday Structure with Applications in Nanotechnology.* Journal of the American Chemical Society. Vol. 126.6. 2004. pp. 1666-1674. DOI: 10.1021/ja038381e.

[47] Reishus, D. Shawn, B., Brun, Y. Chelyapov, N. & Adleman, L. *Self-Assembly of DNA Double-Double Crossover Complexes into High-Density, Doubly Connected, Planar Structures.* Journal of the American Chemical Society. Vol. 127:50. 2005. pp. 17590-17591. DOI: 10.1021/ja0557177.

[48] Yan, H., Park, S. H., Finkelstein, G., Reif, J. H. & LaBean, T. H. *DNA-Templated Self-Assembly of Protein Arrays and Highly Conductive Nanowires.* Science. Vol. 301:5641. 2003. pp. 1882-1884. DOI: 10.1126/science.1089389.

[49] He, Y., Chen, Y., Liu, H., Ribbe, A. E. & Mao, C. *Self-Assembly of Hexagonal DNA Two-Dimensional (2D) Arrays.* Journal of the American Chemcial Society. Vol. 127:35. 2005. pp. 12202-12203. DOI: 10.1021/ja0541938.

[50] Zhang, C., Su, M., He, Y. Zhao, X., Fang, P-A., Ribbe, A. E., Jiang, W. & Mao, C. *Conformational flexibility facilitates self-assembly of*

complex DNA nanostructures. Proceedings of the National Academy of Sciences of the United States of America. Vol. 105:31. 2008. pp. 10665-10669. DOI: 10.1073/pnas.0803841105.

[51] He, Y., Tian, Y., Ribbe, A. E. & Mao, C. *Highly Connected Two-Dimensional Crystals of DNA Six-Point Stars.* Journal of the American Chemical Society. Vol. 128:50. 2008. pp. 15978-15979. DOI: 10.1021/ja0665141.

[52] Hamada, S. & Murata, S. *Substrate-Assisted Assembly of Interconnected Single-Duplex DNA Nanostructures.* Angewandte Chemie. Vol. 121:37. 2009. pp. 6952-6955. DOI: 10.1002/ange.200902662.

[53] Liu, D., Wang, M., Deng, Z., Walulu, R. & Mao, C. *Tensegrity: Construction of Rigid DNA Triangles with Flexible Four-Arm DNA Junctions.* Journal of the American Chemical Society. Vol. 126:8. 2004. pp. 2324-2325. DOI: 10.1021/ja031754r.

[54] Zheng, J., Birktoft, J. J., Chen, Y. Wang, T., Sha, R., Constantinou, P. E., Ginell, S. L., Mao, C. & Seeman, N. C. *From molecular to macroscopic via the rational design of a self-assembled 3D DNA crystal.* Nature. Vol. 461:7260. 2009. pp. 74-77. DOI: 10.1038/nature08274.

[55] LaBean, T. H. & Li, H. *Constructing novel materials with DNA.* Nano Today. Vol. 2:2. 2007. pp. 26-35. DOI: 10.1016/S1748-0132(07)70056-7.

[56] Chen, J. & Seeman, N. C. *Synthesis from DNA of a molecule with the connectivity of a cube.* Nature. Vol. 350:6319. 1991. pp. 631-633. DOI: 10.1038/350631a0.

[57] Zhang, Y. & Seeman, N. C. *Construction of a DNA-Truncated Octahedron.* Journal of the American Chemical Society. Vol. 116:5. 1994. pp. 1661-1669. DOI: 10.1021/ja00084a006.

[58] Goodman, R. P., Schaap, I. A. T., Tardin, C. F., Erben, C. M., Berry, R. M., Schmidt, C. F. & Turberfield, A. J. *Rapid Chiral Assembly of Rigid DNA Building Blocks for Molecular Nanofabrication.* Science. Vol. 310:5754. 2005. pp. 1661-1665. DOI: 10.1126/science.1120367.

[59] Saccà, B. & Niemeyer, C. M. *DNA Origami: The Art of Folding DNA.* Angewandte Chemie International Edition. Vol.51:1. 2012. pp. 58-66. DOI: 10.1002/anie.201105846.

[60] Wang, P., Meyer, T. A., Pan, V., Dutta, P. K. & Ke, Y. *The Beauty and Utility of DNA Origami.* Chem. Vol. 2:3. 2017. pp. 359-382. DOI: 10.1016/j.chempr.2017.02.009.

[61] Kuzuya, A. & Komiyama, M. *DNA origami: Fold, stick, and beyond.* Nanoscale. Vol. 2:3. 2010. pp. 310-322. DOI: 10.1039/b9nr00246d.

[62] Castro, C. E., Kilchherr, F., Kim, D-N, Shiao, E. L., Wauer, T., Wortmann, P., Bathe, M. & Dietz, H. *A primer to scaffolded DNA origami.* Nature Methods. Vol. 8:3. 2011. pp. 221-229. DOI: 10.1038/NMETH.1570.

[63] Tørring, T., Voigt, N. V., Nangreave, J., Yan, H. & Gothelf, K. V. *DNA origami: a quantum leap for self-assembly of complex structures.* Chemical Society Reviews. Vol. 40:12. 2011. pp. 5636-5646. DOI: 10.1039/c1cs15057j.

[64] Nangreave, J., Han, D., Liu, Y. & Yan, H. *DNA origami: a history and current perspective.* Current Opinion in Chemical Biology. Vol. 14:5. 2010. pp. 608-615. DOI: 10.1016/j.cbpa.2010.06.182.

[65] Yang, Y., Han, D., Nangreave, J., Liu, Y. & Yan, H. *DNA Origami with Double-Stranded DNA As a Unified Scaffold.* ACS Nano. Vol. 6:9. 2012. pp. 8209-8215. DOI: 10.1021/nn302896c.

[66] Zhang, G., Surwade, S. P., Zhou, F. & Liu, H. *DNA nanostructures meets nanofabrication.* Chemical Society Reviews. Vol. 42:7. 2013. pp. 2488-2496. DOI: 10.1039/c2cs35302d.

[67] Pound, E., Ashton, J. R., Becerril, H. A. & Woolley, A. T. *Polymerase Chain Reaction Based Scaffold Preparation for the Production of Thin, Branched DNA Origami Nanostructures of Arbitrary Sizes.* Nano Letters. Vol. 9:12. 2009. pp. 4302-4305. DOI: 10.1021/nl902535q.

[68] Zhang, H., Chao, J., Pan, D., Liu, H., Huang, Q. & Fan, C. *Folding super-sized DNA origami with scaffold strands from long-range PCR.* Chemical Communications. Vol. 48:51. 2012. pp. 6405-6407. DOI: 10.1039/c2cc32204h.

[69] Said, H., Schüller, V. J, Eber, F. J., Wege, C., Liedl, T. & Richert, C. *M1.3 - a small scaffold for DNA origami.* Nanoscale.Vol. 5:1. 2013. pp. 284-290. DOI: 10.1039/c2nr32393a.

[70] Veneziano, R., Ratanalert, S., Zhang, K., Zhang, F., Yan, H., Chiu, W. & Bathe, M. *Designer nanoscale DNA assemblies programmed from the top down.* Science. Vol. 352:6293. 2016. no. 1534. DOI: 10.1126/science.aaf4388.

[71] Högberg, B., Liedl, T. & Shih, W. M. *Folding DNA Origami from a Double-Stranded Source of Scaffold.* Journal of the American Chemical Society. Vol. 131:26. 2009. pp. 9154-9155. DOI: 10.1021/ja902569x.

[72] Zhao, Z., Yan, H. & Liu, Y. *A Route to Scale Up DNA Origami Using DNA Tiles as Folding Staples.* Angewandte Chemie International Edition. Vol. 49:8. 2010. pp. 1414-1417. DOI: 10.1002/anie.200906225.

[73] Zhao, Z., Liu, Y. & Yan, H. *Organizing DNA Origami Tiles into Larger Structures Using Preformed Scaffold Frames.* Nano Letters. Vol. 11:7. 2011. pp. 2997-3002. DOI: 10.1021/nl201603a.

[74] Liu, W., Zhong, H., Wang, R. & Seeman, N. C. *Crystalline Two-Dimensional DNA-Origami Arrays.* Angewandte Chemie. Vol. 123:1. 2011. pp.278-281. DOI: 10.1002/ange.201005911.

[75] Wang, P., Gaitanaros, S., Lee, S., Bathe, M., Shih, W. M. & Ke, Y. *Programming Self-Assembly of DNA Origami Honeycomb Two-Dimensional Lattices and Plasmonic Metamaterials.* Journal of the American Chemical Society. Vol. 138:24. 2016. pp. 7733-7740. DOI: 10.1021/jacs.6b03966.

[76] Endo, M., Sugita, T., Katsuda, Y., Hidaka, K. & Sugiyama, H. *Programmed-Assembly System Using DNA Jigsaw Pieces.* Chemistry - A European Journal. Vol. 16:18. 2010. pp. 5362-5368. DOI: 10.1002/chem.200903057.

[77] Endo, M., Sugita, T., Rajendran, A., Katsuda, Y., Emura, T., Hidaka, K. & Sugiyama, H. *Two-dimensional DNA origami assemblies using a four-way connector.* Chemical Communications. Vol. 47:11. 2011. pp. 3213-3215. DOI: 10.1039/c0cc05306f.

[78] Rajendran, A., Endo, M., Katsuda, Y., Hidaka, K. & Sugiyama, H. *Programmed Two-Dimensional Self-Assembly of Multiple DNA Origami Jigsaw Pieces.* ACS Nano. Vol. 5:1. 2011. pp. 665-671. DOI: 10.1021/nn1031627.

[79] Douglas, S. M., Dietz, H., Liedl, T., Högberg, B., Graf, F. & Shih, W. M. *Self-assembly of DNA into nanoscale three-dimensional shapes.* Nature. Vol. 459:7245. 2009. pp. 414-418. DOI: 10.1038/nature08016.

[80] Iinuma, R., Ke, Y., Jungmann, R., Schlichthaerle, T., Woehrstein, J. B. & Yin, P. *Polyhedra Self-Assembled from DNA Tripods and Characterized with 3D DNA-PAINT.* Science. Vol. 344:6179. 2014. pp. 65-69. DOI: 10.1126/science.1250944.

[81] Woo, S. & Rothemund, P. W. K. *Programmable molecular recognition based on the geometry of DNA nanostructures.* Nature Chemistry. Vol. 3:8. 2011. pp. 620-627. DOI: 10.1038/nchem.1070.

[82] Gerling, T., Wagenbauer, K. F., Neuner, A. M. & Dietz, H. *Dynamic DNA devices and assemblies formed by shape-complementary, non-base pairing 3D components.* Science. Vol. 347:6229. 2015. pp. 1446-1452. DOI: 10.1126/science.aaa5372.

[83] Wagenbauer, K. F., Sigl, C. & Dietz, H. *Gigadalton-scale shape-programmable DNA assemblies.* Nature. 2017. Vol. 552:7683. pp. 78-83. DOI: 10.1038/nature24651.

[84] Tikhomirov, G., Petersen, P. & Qian, L. *Programmable disorder in random DNA tilings.* Nature Nanotechnology. Vol. 12:3. 2017. pp. 251-259. DOI: 10.1038/nnano.2016.256.

[85] Tikhomirov, G., Petersen, P. & Qian, L. *Fractal assembly of micrometre-scale DNA origami arrays with arbitrary patterns.* Nature. Vol. 552:7683. 2017. pp. 67-71. DOI: 10.1038/nature24655.

[86] Gothelf, K. V. *LEGO-like DNA structures.* Science. Vol. 338:6111. 2012. pp. 1159-1160. DOI: 10.1126/science.1229960.

[87] Rothemund, P. W. K. & Andersen, E. S. *Nanotechnology: The importance of being modular.* Nature. Vol. 485:7400. 2012. pp. 584-585. DOI: 10.1038/485584a.

[88] Marchi, A. N., Saaem, I., Vogen, B. N., Brown, S. & LaBean, T. H. *Toward Larger DNA Origami.* Nano Letters. Vol. 14:10. 2014. pp. 5740-5747. DOI: 10.1021/nl502626s.

[89] Pinheiro, A. V., Han, D., Shih, V. M. & Yan, H. *Challenges and opportunities for structural DNA nanotechnology.* Nature Nanotechnology. Vol. 6:12. 2011. pp. 763-772. DOI: 10.1038/nnano.2011.187.

[90] Linko, V., Ora, A. & Kostiainen, M. A. *DNA Nanostructures as Smart Drug-Delivery Vehicles and Molecular Devices.* Trends in Biotechnology. Vol. 33:10. 2015. pp. 586-594. DOI: 10.1016/j.tibtech.2015.08.001.

[91] Praetorius, F., Kick, B., Behler, K. L., Honemann, M. N., Weuster-Botz, D. & Dietz, H. *Biotechnological mass production of DNA origami.* Nature. Vol. 552:7683. 2017. pp. 84-87. DOI: 10.1038/nature24650.

[92] Liedl, T., Högberg, B., Tytell, J., Ingber, D. E. & Shih, W. M. *Self-assembly of three-dimensional prestressed tensegrity structures from DNA.* Nature Nanotechnology. Vol. 5:7. 2010. pp. 520-524. DOI: 10.1038/nnano.2010.107.

[93] Andersen, E. S., Dong, M., Nielsen, M. M., Jahn, K., Subramani, R., Mamdouh, W., Golas, M. M., Sander, B., Stark, H., Oliveira, C. L. P., Pedersen, J. S., Birkedal, V., Besenbacher, F., Gothelf, K. V. & Kjems, J. *Self-assembly of a nanoscale DNA box with a controllable lid.* Nature. Vol. 459:7243. 2009. pp. 73-76. DOI: 10.1038/nature07971.

[94] Ke, Y., Sharma, J., Liu, M., Jahn, K., Liu, Y. & Yan, H. *Scaffolded DNA Origami of a DNA Tetrahedron Molecular Container.* Nano Letters. Vol. 9:6. 2009. pp. 2445-2447. DOI: 10.1021/nl901165f.

[95] Han, D., Pal, S., Nangreave, J., Deng, Z., Liu, Y. & Yan, H. *DNA Origami with Complex Curvatures in Three-Dimensional Space.* Science. Vol. 332:6027. 2011. pp. 342-346. DOI: 10.1126/science.1202998.

[96] Ke, Y., Douglas, S. M., Liu, M., Sharma, J., Cheng, A., Leung, A., Liu, Y., Shih, W. M. & Yan, H. *Multilayer DNA Origami Packed on a Square Lattice.* Journal of the American Chemical Society. Vol. 131:43. 2009. pp. 15903-15908. DOI: 10.1021/ja906381y.

[97] Ke, Y., Voigt, N. V., Gothelf, K. V. & Shih, W. M. *Multilayer DNA Origami Packed on Hexagonal and Hybrid Lattices.* Journal of the American Chemical Society. Vol. 134:3. 2012. pp. 1770-1774. DOI: 10.1021/ja209719k.

[98] Dietz, H., Douglas, S. M. & Shih, W. M. *Folding DNA into Twisted and Curved Nanoscale Shapes.* Science. Vol. 325:5941. 2009. pp. 725-730. DOI: 10.1126/science.1174251.

[99] Andersen, E. S., Dong, M., Nielsen, M. M., Jahn, K., Lind-Thomsen, A., Mamdouh, W., Gothelf, K. V., Besenbacher, F. & Kjems, J. *DNA*

Origami Design of Dolphin-Shaped Structures with Flexible Tails. ACS Nano. Vol. 2:6. 2008. pp. 1213-1218. DOI: 10.1021/nn800215j.

[100] Douglas, S. M., Marblestone, A. H., Teerapittayanon, S., Vazquez, A., Church, G. M. & Shih, W. M. *Rapid prototyping of 3D DNA-origami shapes with caDNAno.* Nucleic Acids Research. Vol. 37:15. 2009. pp. 5001-5006. DOI: 10.1093/nar/gkp436.

[101] Kim, D-N., Kilchherr, F., Dietz, H. & Bathe, M. *Quantitative prediction of 3D solution shape and flexibility of nucleic acid nanostructures.* Nucleic Acids Research. Vol. 40:7. 2012. pp. 2862-2868. DOI: 10.1093/nar/gkr1173.

[102] Linko, V. & Kostiainen, M. A. *Automated design of DNA origami.* Nature Biotechnology. Vol. 34:8. 2016. pp. 826-827. DOI: 10.1038/nbt.3647.

[103] Benson, E., Mohammed, A., Gardell, J., Masich, S., Czeizler, E., Orponen, P. & Högberg, B. *DNA rendering of polyhedral meshes at the nanoscale.* Nature. Vol. 523:7561. 2015. pp. 441-444. DOI: 10.1038/nature14586.

[104] Ramakrishnan, S., Krainer, G., Grundmeier, G., Schlierf, M. & Keller, A. *Structural stability of DNA origami nanostructures in the presence of chaotropic agents.* Nanoscale. Vol. 8:19. 2016. pp. 10398-10405. DOI: 10.1039/c6nr00835f.

[105] Martin, T. G. & Dietz, H. *Magnesium-free self-assembly of multi-layer DNA objects.* Nature Communications. Vol. 3. 2012. p. 1103. DOI: 10.1038/ncomms2095.

[106] Bald, I. & Keller, A. *Molecular Processes Studied at a Single-Molecule Level Using DNA Origami Nanostructures and Atomic Force Microscopy.* Molecules. Vol. 19:9. 2014. pp. 13803-13823. DOI: 10.3390/molecules190913803.

[107] Jungmann, R., Liedl, T., Sobey, T. L., Shih, W. & Simmel, F. C. *Isothermal Assembly of DNA Origami Structures Using Denaturing Agents.* Journal of the American Chemical Society. Vol. 130:31. 2008. pp. 10062-10063. DOI: 10.1021/ja8030196.

[108] Sobczak, J-P. J., Martin, T. G., Gerling, T. & Dietz, H. *Rapid Folding of DNA into Nanoscale Shapes at Constant Temperature.* Science. Vol. 338:6113. 2012. pp. 1458-1461. DOI: 10.1126/science.1229919.

[109] Myhrvold, C., Dai, M., Silver, P. A. & Yin, P. *Isothermal Self-Assembly of Complex DNA Structures under Diverse and Biocompatible Conditions.* Nano Letters. Vol. 13:9. 2013. pp. 4242-4248. DOI: 10.1021/nl4019512.

[110] Stahl, E., Martin, T. G., Praetorius, F. & Dietz, H. *Facile and Scalable Preparation of Pure and Dense DNA Origami Solutions.* Angewandte Chemie International Edition. Vol. 53:47. 2014. pp. 12735-12740. DOI: 10.1002/anie.201405991.

[111] Lin, C., Perrault, S. D., Kwak, M., Graf, F. & Shih, W. M. *Purification of DNA-origami nanostructures by rate-zonal centrifugation.* Nucleic Acids Research. Vol. 41:2. 2013. No. e40. DOI: 10.1093/nar/gks1070.

[112] Bellot, G., McClintock, M. A., Lin, C. & Shih, W. M. *Recovery of intact DNA nanostructures following agarose-gel-based separation.* Nature Methods. Vol. 8:3. 2011. pp. 192-194. DOI: 10.1038/nmeth0311-192.

[113] Douglas, S. M., Bachelet, I. & Church, G. M. *A Logic-Gated Nanorobot for Targeted Transport of Molecular Payloads.* Science. Vol. 335:6070. 2012. pp. 831-834. DOI: 10.1126/science.1214081.

[114] Wickham, S. F. J., Endo, M., Katsuda, Y., Hidaka, K., Bath, J., Sugiyama, H. & Turberfield, A. J. *Direct observation of stepwise movement of a synthetic molecular transporter.* Nature Nanotechnology. Vol.6:3. 2011. pp. 166-169. DOI: 10.1038/nnano.2010.284.

[115] Tan, S. J., Campolongo, M. J., Luo, D. & Cheng, W. *Building plasmonic nanostructures with DNA.* Nature Nanotechnology. Vol. 6:5. 2011. pp. 268-276. DOI: 10.1038/nnano.2011.49.

[116] Pilo-Pais, M., Acuna, G. P., Tinnerfeld, P. & Liedl, T. *Sculpting light by arranging optical components with DNA nanostructures.* MRS Bulletin. Vol. 42:12. 2017. pp. 936-942. DOI: 10.1557/mrs.2017.278.

[117] Linko, V., Nummelin, S., Aarnos, L., Tapio, K., Toppari, J. J. & Kostiainen, M. A. *DNA-Based Enzyme Reactors and Systems.* Nanomaterials. Vol. 6:8. 2016. no. 139. DOI: 10.3390/nano6080139.

[118] Li, J., Fan, C. Pei, H., Shi, J. & Huang, Q. *Smart Drug Delivery Nanocarriers with Self-Assembled DNA Nanostructures.* Advanced Materials. Vol: 25:32. 2013. pp. 4386-4396. DOI: 10.1002/adma.201300875.

[119] Sharma, J., Chhabra, R., Andersen, C. S., Gothelf, K. V., Yan, H. & Liu, Y. *Toward Reliable Gold Nanoparticle Patterning On Self-Assembled DNA Nanoscaffold.* Journal of the American Chemical Society. Vol. 130:25. 2008. pp. 7820-7821. DOI: 10.1021/ja802853r.

[120] Ding, B., Deng, Z., Yan, H., Cabrini, S., Zuckermann, R. N. & Bokor, J. *Gold Nanoparticle Self-Similar Chain Structure Organized by DNA Origami.* Journal of the American Chemical Society. Vol. 132:10. 2010. pp. 3248-3249. DOI: 10.1021/ja9101198.

[121] Pilo-Pais, M., Goldberg, S., Samano, E., LaBean, T. H. & Finkelstein, G. *Connecting the Nanodots: Programmable Nanofabrication of Fused Metal Shapes on DNA Templates.* Nano Letters. Vol. 11:8. 2011. pp. 3489-3492. DOI: 10.1021/nl202066c.

[122] Gür, F. N., Schwarz, F. W., Ye, J., Diez, S. & Schmidt, T. L. *Toward Self-Assembled Plasmonic Devices: High-Yield Arrangement of Gold Nanoparticles on DNA Origami Templates.* ACS Nano. Vol. 10:5. 2016. pp. 5374-5382. DOI: 10.1021/acsnano.6b01537.

[123] Shen, X., Song, C., Wang, J., Shi, D., Wang, Z., Liu, N. & Ding, B. *Rolling Up Gold Nanoparticle-Dressed DNA Origami into Three-Dimensional Plasmonic Chiral Nanostructures.* Journal of the American Chemical Society. Vol. 134:1. 2011. pp. 146-149. DOI: 10.1021/ja209861x.

[124] Kuzyk, A., Schreiber, R., Fan, Z., Pardatscher, G., Roller, E-M., Högele, A., Simmel, F. C., Govorov, A. O. & Liedl, T. *DNA-based self-assembly of chiral plasmonic nanostructures with tailored optical response.* Nature. Vol. 483:7389. 2012. pp. 311-314. DOI: 10.1038/nature10889.

[125] Urban, M. J., Dutta, P. K. Wang, P., Duan, X., Shen, X., Ding, B., Ke, Y. & Liu, N. *Plasmonic Toroidal Metamolecules Assembled by DNA Origami.* Journal of the American Chemical Society. Vol. 138:17. 2016. pp. 5495-5498. DOI: 10.1021/jacs.6b00958.

[126] Zhao, Z., Jacovetty, E. L., Liu, Y. & Yan, H. *Encapsulation of Gold Nanoparticles in a DNA Origami Cage.* Angewandte Chemie International Edition. Vol. 50:9. 2011. pp. 2041-2044. DOI: 10.1002/anie.201006818.

[127] Shen, C., Lan, X., Lu, X., Meyer, T. A., Ni W., Ke, Y. & Wang, Q. *Site-Specific Surface Functionalization of Gold Nanorods Using DNA*

Origami Clamps. Journal of the American Chemical Society. Vol. 138:6. 2016. pp. 1764-1767. DOI: 10.1021/jacs.5b11566.

[128] Pal, S., Deng, Z., Ding, B., Yan, H. & Liu, Y. *DNA-Origami-Directed Self-Assembly of Discrete Silver-Nanoparticle Architectures.* Angewandte Chemie International Edition. Vol. 49:15. 2010. pp. 2700-2704. DOI: 10.1002/anie.201000330.

[129] Eskelinen, A-P., Moerland, R. J., Kostiainen, M. A. & Törmä, P. *Self-Assembled Silver Nanoparticles in a Bow-Tie Antenna Configuration.* Small. Vol. 10:6. 2014. pp. 1057-1062. DOI: 10.1002/smll.201302046.

[130] Bui, H., Onodera, C., Kidwell, C., Tan, Y., Graugnard, E., Kuang, W., Lee, J., Knowlton, W. B., Yurke, B. & Hughes, W. L. *Programmable Periodicity of Quantum Dot Arrays with DNA Origami Nanotubes.* Nano Letters. Vol. 10:9. 2010. pp. 3367-3372. DOI: 10.1021/nl101079u.

[131] Deng, Z., Samanta, A., Nangreave, J., Yan, H. & Liu, Y. *Robust DNA-Functionalized Core/Shell Quantum Dots with Fluorescent Emission Spanning from UV-vis to Near-IR and Compatible with DNA-Directed Self-Assembly.* Journal of the American Chemical Society. Vol. 134:42. 2012. pp. 17424-17427. DOI: 10.1021/ja3081023.

[132] Maune, H. T., Han, S-P., Barish, R. D., Bockrath, M., Goddard III, W. A., Rothemund, P. W. K. & Winfree, E. *Self-assembly of carbon nanotubes into two-dimensional geometries using DNA origami templates.* Nature Nanotechnology. Vol. 5:1. 2010. pp. 61-66. DOI: 10.1038/nnano.2009.311.

[133] Eskelinen, A-P., Kuzyk, A., Kaltiaisenaho, T. K., Timmermans, M. Y., Nasibulin, A. G., Kauppinen, E. I. & Törmä, P. *Assembly of Single-Walled Carbon Nanotubes on DNA-Origami Templates through Streptavidin-Biotin Interactions.* Vol. 7:6. 2011. pp. 746-750. DOI: 10.1002/smll.201001750.

[134] Samanta, A. & Medintz, I. L. *Nanoparticles and DNA - a powerful and growing functional combination in bionanotechnology.* Nanoscale. Vol. 8:17. 2016. pp. 9037-9095. DOI: 10.1039/C5NR08465B.

[135] Gothelf, K. V. *Chemical modifications and reactions in DNA nanostructures.* MRS Bulletin. Vol. 42:12. 2017. pp. 897-903. DOI: 10.1557/mrs.2017.276.

[136] Niemeyer, C. M. *Semisynthetic DNA-Protein Conjugates for Biosensing and Nanofabrication.* Angewandte Chemie International Edition. Vol. 49:7. 2010. pp. 1200-1216. DOI: 10.1002/anie.200904930.

[137] Grossi, G., Jaekel, A., Sloth Andersen, E. & Saccà, B. *Enzyme-functionalized DNA nanostructures as tools for organizing and controlling enzymatic reactions.* MRS Bulletin. Vol. 42:12. 2017. pp. 920-923. DOI: 10.1557/mrs.2017.269.

[138] Stephanopoulos, N., Liu, M., Tong, G. J., Li, Z., Liu, Y., Yan, H. & Francis, M. B. *Immobilization and One-Dimensional Arrangement of Virus Capsids with Nanoscale Precision Using DNA Origami.* Nano Letters. Vol. 10:7. 2010. pp. 2714-2720. DOI: 10.1021/nl1018468.

[139] Schüller, V. J., Heidegger, S., Sandholzer, N., Nickels, P. C., Suhartha, N. A, Endres, S., Bourquin, C. & Liedl, T. *Cellular Immunostimulation by CpG-Sequence-Coated DNA Origami Structures.* ACS Nano. Vol. 5:12. 2011. pp. 9696-9702. DOI: 10.1021/nn203161y.

[140] Zhao, Y-X., Shaw, A., Zeng, X. Benson, E., Nystöm, A. M. & Högberg, B. *DNA Origami Delivery System for Cancer Therapy with Tunable Release Properties.* ACS Nano. Vol. 6:10. 2012. pp. 8684-8691. DOI: 10.1021/nn3022662.

[141] Perrault, S. D. & Shih, W. M. *Virus-Inspired Membrane Encapsulation of DNA Nanostructures To Achieve In Vivo Stability.* ACS Nano. Vol. 8:5. 2014. pp. 5132-5140. DOI: 10.1021/nn5011914.

[142] Mikkilä J., Eskelinen, A-P., Niemelä, E. H., Linko, V., Frilander, M. J., Törmä, P. & Kostiainen, M. A. *Virus-Encapsulated DNA Origami Nanostructures for Cellular Delivery.* Nano Letters. Vol. 14:4. 2014. pp. 2196-2200. DOI: 10.1021/nl500677j.

[143] Kiviaho, J. K., Linko, V., Ora, A., Tiainen, T., Järvihaavisto, E., Mikkilä, J., Tenhu, H., Nonappa & Kostiainen, M. A. *Cationic polymers for DNA origami coating - examining their binding efficiency and tuning the enzymatic reaction rates.* Nanoscale. Vol. 8:22. 2016. pp. 11674-11680. DOI: 10.1039/C5NR08355A.

[144] Auvinen, H., Zhang, H., Nonappa, Kopilow, A., Niemelä, E. H., Nummelin, S., Correia, A., Santos, H. A., Linko, V. & Kostiainen, M. A. *Protein Coating of DNA Nanostructures for Enhanced Stability and Immunocompatibility.* Advanced Healthcare Materials. Vol. 6:18. 2017. No. 1700692. DOI: 10.1002/adhm.201700692.

[145] Helmi, S., Ziegler, C., Kauert, D. J. & Seidel, R. *Shape-Controlled Synthesis of Gold Nanostructures Using DNA Origami Molds.* Nano Letters. Vol. 14:11. 2014. pp. 6693-6698. DOI: 10.1021/nl503441v.

[146] Sun, W., Boulais, E., Hakobyan, Y., Wang, W. L., Guan, A., Bathe, M. & Yin, P. *Casting inorganic structures with DNA molds.* Science. Vol. 346:6210. 2014. no. 1258361. DOI: 10.1126/science.1258361.

[147] Bayrak, T., Helmi, S., Ye, J., Kauert, D., Kelling, J, Schönherr, T., Weichelt, R., Erbe, A. & Seidel, R. *DNA-Mold Templated Assembly of Conductive Gold Nanowires.* Nano Letters. Vol. 18:3. 2018. pp. 2116-2123. DOI: 10.1021/acs.nanolett.8b00344.

[148] Shen, B., Linko, V., Tapio, K., Kostiainen, M. A. & Toppari, J. J. *Custom-shaped metal nanostructures based on DNA origami silhouttes.* Nanoscale. Vol. 7:26. 2015. pp. 11267-11272. DOI: 10.1039/C5NR02300A.

[149] Shen, B., Linko, V., Tapio, K., Pikker, S., Lemma, T., Gopinath, A., Gothelf, K. V., Kostiainen, M. A. & Toppari, J. J. *Plasmonic nanostructures through DNA-assisted lithography.* Science Advances. Vol. 4:2. 2018. no. eaap8978. DOI: 10.1126/sciadv.aap8978.

[150] Graugnard, E., Hughes, W. L., Jungmann, R., Kostiainen, M. A. & Linko, V. *Nanometrology and super-resolution imaging with DNA.* MRS Bulletin. Vol. 42:12. 2017. pp. 951-959. DOI: 10.1557/mrs.2017.274.

[151] Korpelainen, V., Linko, V., Seppä, J., Lassila, A. & Kostiainen, M. A. *DNA origami structures as calibration standards for nanometrology.* Measurement Science and Technology. Vol. 28:3. 2017. No. 034001. DOI: 10.1088/1361-6501/28/3/034001.

[152] Jungmann, R., Steinhauer, C., Scheible, M., Kuzyk, A., Tinnefeld, P. & Simmel, F. C. *Single-Molecule Kinetics and Super-Resolution Microscopy by Fluorescence Imaging of Transient Binding on DNA Origami.* Nano Letters. Vol. 10:11. 2010. pp. 4756-4761. DOI: 10.1021/nl103427w.

[153] Schnitzbauer, J., Strauss, M. T., Schlichthaerle, T., Schueder, F. & Jungmann, R. *Super-resolution microscopy with DNA-PAINT.* Nature Protocols. Vol 12:6. 2017. pp. 1198-1228. DOI: 10.1038/nprot.2017.024.

[154] Bathe, M. & Rothemund, P. W. K. *DNA nanotechnology: A foundation for programmable nanoscale materials.* MRS Bulletin. Vol. 42:12. 2017. pp. 882-888. DOI: 10.1557/mrs.2017.279.

[155] GATTAquant DNA Nanotechnologies. http://www.gattaquant.com. (accessed February 9, 2018)

[156] Kostiainen, M. A., Hiekkataipale, P., Laiho, A., Lemieux, V., Seisonen, J., Ruokolainen, J. & Ceci, P. *Electrostatic assembly of binary nanoparticle superlattices using protein cages.* Nature Nanotechnology. Vol. 8:1. 2013. pp. 52-56. DOI: 10.1038/nnano.2012.220.

[157] Smith, A. M., Lee, A. A. & Perkin, S. *The Electrostatic Screening Length in Concentrated Electrolytes Increases with Concentration.* The Journal of Physical Chemistry Letters. Vol. 7:12. 2016. pp. 2157-2163. DOI: 10.1021/acs.jpclett.6b00867.

[158] Liljestöm, V., Ora, A. Hassinen, J., Rekola, H., Nonappa, Heilala, M., Joensuu, J., Ras, R. H. A., Törmä, P., Ikkala, O. & Kostiainen, M. A. *Cooperative colloidal self-assembly of metal-protein superlattice wires.* Nature Communications. Vol. 8:1. 2017. no. 671. DOI: 10.1038/s41467-017-00697-z.

[159] Künzle, M., Eckert, T. & Beck, T. *Binary Protein Crystals for the Assembly of Inorganic Nanoparticle Superlattices.* Journal of the American Chemical Society. Vol. 138:39. 2016. pp. 12731-12734. DOI: 10.1021/jacs.6b07260.

[160] Velev, O. D. *Self-assembly of unusual nanoparticle crystals.* Science. Vol. 312:5772. 2006. pp. 376-377. DOI: 10.1126/science.1125800.

[161] Liljeström, V. *Electrostatic Self-assembly - From Proteins, Viruses, and Nanoparticles to Functional Materials.* Doctoral dissertation. Aalto University, School of Science, Department of Applied Physics. 2017. 86 pp. ISBN: 978-952-60-7535-8.

[162] Khan, A. A., Fox, E. K., Górzny, M. Ł., Nikulina, E., Brougham, D. F., Wege, C. & Bittner, A. M. *pH Control of the Electrostatic Binding of Gold and Iron Oxide Nanoparticles to Tobacco Mosaic Virus.* Langmuir. Vol. 29:7. 2013. pp. 2094-2098. DOI: 10.1021/la3044126.

[163] Westerlund, F. & Bjørnholm, T. *Directed assembly of gold nanoparticles.* Current Opinion in Colloid & Interface Science. Vol.14:2. 2009. pp. 126-134. DOI: 10.1016/j.cocis.2008.07.002.

[164] Ghosh, S. K. & Pal, T. *Interparticle Coupling Effect on the Surface Plasmon Resonance of Gold Nanoparticles: From Theory to Applications.* Chemical Reviews. Vol. 107:11. 2007. pp. 4797-4862. DOI: 10.1021/cr0680282.

[165] Daniel, M-C. & Astruc, D. *Gold Nanoparticles: Assembly, Supramolecular Chemistry, Quantum-Size-Related Properties, and Applications toward Biology, Catalysis, and Nanotechnology.* Chemical Reviews. Vol. 104:1. 2004. pp. 293-346. DOI: 10.1021/cr030698+.

[166] Eustis, S. & El-Sayed, M. A. *Why gold nanoparticles are more precious than pretty gold: Noble metal surface plasmon resonance and its enhancement of the radiative and nonradiative properties of nanocrystals of different shapes.* Chemical Society Reviews. Vol. 35:3. 2006. pp. 209-2017. DOI: 10.1039/b514191e.

[167] Zeng, S., Yong, K-T, Roy, I., Dinh, X-Q., Yu, X. & Luan, F. *A Review on Functionalized Gold Nanoparticles for Biosensing Applications.* Plasmonics. Vol. 6:3. 2011. pp. 491-506. DOI: 10.1007/s11468-011-9228-1.

[168] Zhao, W., Brook, M. A. & Li, Y. *Design of Gold Nanoparticle-Based Colorimetric Biosensing Assays.* ChemBioChem. Vol. 9:15. 2008. pp. 2363-2371. DOI: 10.1002/cbic.200800282.

[169] Shipway, A. N., Lahav, M., Gabal, R. & Willner, I. *Investigations into the Electrostatically Induced Aggregation of Au Nanoparticles.* Langmuir. Vol. 16:23. 2000. pp. 8789-8795. DOI: 10.1021/la000316k.

[170] Bohren, C. F. & Huffman, D. R. *Absorption and Scattering of Light by Small Particles.* Weinheim: Wiley-VCH Verlag GmbH & Co. KGaA. 1983, reprinted 2004. 530 pp. ISBN: 978-0-471-29340-8.

[171] Mie, G. *Beiträge zur Optik trüber Medien, speziell kolloidaler Metallösungen.* Annalen der Physik. Vol. 330:3. 1908. pp. 377-445. DOI: 10.1002/andp.19083300302.

[172] Grzelczak, M., Pérez-Juste, J., Mulvaney, P. & Liz-Marzán, L. M. *Shape control in gold nanoparticle synthesis.* Chemical Society Reviews. Vol. 37:9. 2008. pp. 1783-1791. DOI: 10.1039/B711490G.

[173] Giljohann, D. A., Seferos, D. S., Daniel, W. L, Massich, M. D., Patel, P. C. & Mirkin, C. A. *Gold Nanoparticles for Biology and Medicine.*

Angewandte Chemie International Edition. Vol. 49:19. 2010. pp. 3280-3294. DOI: 10.1002/anie.200904359.

[174] Dreaden, E. C., Alkilany, A. M., Huang, X., Murphy, C. J. & El-Sayed, M. A. *The golden age: gold nanoparticles for biomedicine.* Chemical Society Reviews. Vol. 41:7. 2012. pp. 2740-2779. DOI: 10.1039/c1cs15237h.

[175] Zhao, P., Li, N. & Astruc, D. *State of the art in gold nanoparticle synthesis.* Coordination Chemistry Reviews. Vol. 257:3-4. 2013. pp. 638-665. DOI: 10.1016/j.ccr.2012.09.002.

[176] Willets, K. A. & Van Duyne, R. P. *Localized Surface Plasmon Resonance Spectroscopy and Sensing.* Annual Review of Physical Chemistry. Vol. 58. 2007. pp. 267-297. DOI: 10.1146/annurev.physchem.58.032806.104607.

[177] Rosi, N. L. & Mirkin, C. A. *Nanostructures in Biodiagnostics.* Chemical Reviews. Vol. 105:4. 2005. pp. 1547-1562. DOI: 10.1021/cr030067f.

[178] Ghosh, P., Han, G., De, M., Kim, C. K. & Rotello, V. M. *Gold nanoparticles in delivery applications.* Advance Drug Delivery Reviews. Vol. 60:11. 2008. pp. 1307-1315. DOI: 10.1016/j.addr.2008.03.016.

[179] Samanta, A., Banerjee, S. & Liu, Y. *DNA nanotechnology for nanophotonic applications.* Nanoscale. Vol. 7;6. 2015. pp. 2210-2220. DOI: 10.1039/C4nr06283c.

[180] Shipway, A. N., Katz, E. & Willner, I. *Nanoparticle Arrays on Surfaces for Electronic, Optical, and Sensor Applications.* ChemPhysChem. Vol. 1:1. 2000. pp. 18-52. DOI: 10.1002/1439-7641(20000804)1:1<18::AID-CPHC18>3.0.CO;2-L.

[181] Lohse, S. E. & Murphy, C. J. *Applications of Colloidal Inorganic Nanoparticles: From Medicine to Energy.* Journal of the American Chemical Society. Vol. 134:38. 2012. pp. 15607-15620. DOI: 10.1021/ja307589n.

[182] Mirkin, C. A., Letsinger, R. L., Mucic, R. C. & Storhoff, J. J. *A DNA-based method for rationally assembling nanoparticles into macroscopic materials.* Nature. Vol. 382:6592. 1996. pp. 607-609. DOI: 10.1038/382607a0.

[183] Alivisatos, A. P., Johnsson, K. P., Peng, X., Wilson, T. E., Loweth, C. J., Bruchez Jr, M. P. & Schultz, P. G. *Organization of 'nanocrystal molecules' using DNA.* Nature. Vol. 382:6592. 1996. pp. 609-611. DOI: 10.1038/382609a0.

[184] Loweth, C. J., Caldwell, W. B., Peng, X., Alivisatos, A. P. & Schultz, P. G. *DNA-Based Assembly of Gold Nanocrystals.* Angewandte Chemie International Edition. Vol. 38:12.1999. pp. 1808-1812. DOI: 10.1002/(SICI)1521-3773(19990614)38:12<1808::AID-ANIE1808>3.0.CO;2-C.

[185] Jones, M. R., Osberg, K. D., Macfarlane, R. J., Langille, M. R. & Mirkin, C. A. *Templated Techniques for the Synthesis and Assembly of Plasmonic Nanostructures.* Chemical Reviews. Vol. 111:6. 2011. pp. 3736-3827. DOI: 10.1021/cr1004452.

[186] Park, S. Y., Lytton-Jean, A. K. R., Lee, B., Weigand, S., Schatz, G. C. & Mirkin, C. A. *DNA-programmable nanoparticle crystallization.* Nature. Vol. 451:7178. 2008. pp. 553-556. DOI: 10.1038/nature06508.

[187] Nykypanchuk, D., Maye, M. M., van der Lelie, D. & Gang, O. *DNA-guided crystallization of colloidal nanoparticles.* Nature. Vol. 451:7178. 2008. pp. 549-552. DOI: 10.1038/nature06560.

[188] Macfarlane, R. J., O'Brien, M. N., Petrosko, S. H. & Mirkin, C. A. *Nucleic Acid-Modified Nanostructures as Programmable Atom Equivalents: Forging a New "Table of Elements".* Angewandte Chemie International Edition. Vol. 52:22. 2013. pp. 5688-5698. DOI: 10.1002/anie.201209336.

[189] Macfarlane, R. J., Lee, B., Jones, M. J., Harris, N., Schatz, G. C. & Mirkin, C. A. *Nanoparticle Superlattice Engineering with DNA.* Science. Vol. 334:6053. 2011. pp. 204-208. DOI: 10.1126/science.1210493.

[190] Li, H., Park, S. H., Reif, J. H., LaBean, T. H. & Yan, H. *DNA-Templated Self-Assembly of Protein and Nanoparticle Linear Arrays.* Journal of the American Chemical Society. Vol. 126:2. 2004. pp. 418-419. DOI: 10.1021/ja0383367.

[191] Beyer, S., Nickels, P. & Simmel, F. C. *Periodic DNA Nanotemplates Synthesized by Rolling Circle Amplification.* Nano Letters. Vol. 5:4. 2005. pp. 719-722. DOI: 10.1021/nl050155a.

[192] Sharma, J., Chhabra, R., Cheng, A., Brownell, J., Liu, Y. & Yan, H. *Control of Self-Assembly of DNA Tubules Through Interaction of Gold Nanoparticles.* Science. Vol. 323:5910. 2009. pp. 112-116. DOI: 10.1126/science.1165831.

[193] Liu, F., Sha, R. & Seeman, N. C. *Modifying the Surface Features of Two-Dimensional DNA Crystals.* Journal of the American Society. Vol. 121:5. 1999. pp. 917-922. DOI: 10.1021/ja982824a.

[194] Lo, P. K., Karam, P., Aldaye, F. A., McLaughlin, C. K., Hamblin, G. D., Cosa, G. & Sleiman, H. F. *Loading and selectively release of cargo in DNA nanotubes with longitudinal variation.* Nature Chemistry. Vol. 2:4. 2010. pp. 319-328. DOI: 10.1038/nchem.575.

[195] Lo, P. K., Altvater, F. & Sleiman, H. F. *Templated Synthesis of DNA Nanotubes with Controlled, Predetermined Lengths.* Journal of the American Chemical Society. Vol. 132:30. 2010. pp. 10212-10214. DOI: 10.1021/ja1017442.

[196] Lau, K. L., Hamblin, G. D. & Sleiman, H. F. *Gold Nanoparticle 3D-DNA Building Blocks: High Purity Preparation and Use for Modular Access to Nanoparticle Assemblies.* Small. Vol. 10:4. 2014. pp. 660-666. DOI: 10.1002/smll.201301562.

[197] Hamblin, G. D., Hariri, A. A., Carneiro, K. M. M., Lau, K. L., Cosa, G. & Sleiman, H. F. *Simple Design for DNA Nanotubes from a Minimal Set of Unmodified Strands: Rapid, Room-Temperature Assembly and Readily Tunable Structure.* ACS Nano. Vol. 7:4. 2013. pp. 3022-3028. DOI: 10.1021/nn4006329.

[198] DeVries, G. A., Brunnbauer, M., Hu, Y., Jackson, A. M., Long, B., Neltner, B. T., Uzun, O., Wunsch, B. H. & Stellacci, F. *Divalent Metal Nanoparticles.* Science. Vol. 315:5810. 2007. pp. 358-361. DOI: 10.1126/science.1133162.

[199] Ohya, Y., Miyoshi, N. Hashizume, M., Tamaki, T., Uehara, T., Shingubara, S & Kuzuya, A. *Formation of 1D and 2D Gold Nanoparticle Arrays by Divalent DNA-Gold Nanoparticle Conjugates.* Small. Vol. 8:15. 2012. pp. 2335-2340. DOI: 10.1002/smll.201200092.

[200] Lan, X., Lu, X., Shen, C., Ke, Y., Ni, W. & Wang, Q. *Au Nanorod Helical Superstructures with Designed Chirality.* Journal of the American Chemical Society. Vol. 137:1. 2014. pp. 457-462. DOI: 10.1021/ja511333q.

[201] Tian, Y., Wang, T., Liu, W., Xin, H. L., Li H., Ke, Y., Shih, W. M. & Gang, O. *Prescribed nanoparticle cluster architectures and low-dimensional arrays built using octahedral DNA origami frames.* Nature Nanotechnology. Vol. 10:7. 2015. pp. 637-644. DOI: 10.1038/nnano.2015.105.

[202] Schreiber, R., Santiago, I., Ardavan, A. & Turberfield, A. J. *Ordering Gold Nanoparticles with DNA Origami Nanoflowers.* ACS Nano. Vol. 10:8. 2016. pp. 7303-7306. DOI: 10.1021/acsnano.6b03076.

[203] Liu, W., Halverson, J., Tian, Y., Tkachenko, A. V. & Gang, O. *Self-organized architectures from assorted DNA-framed nanoparticles.* Nature Chemistry. Vol. 8:9. 2016. pp. 867-873. DOI: 10.1038/nchem.2540.

[204] Maeda, Y., Tabata, H. & Kawai, T. *Two-dimensional assembly of gold nanoparticles with a DNA network template.* Applied Physics Letters. Vol. 79:8. 2001. pp. 1181-1183. DOI: 10.1063/1.1396630.

[205] Xiao, S., Liu, F., Rosen, A. E., Hainfeld, J. F., Seeman, N. C., Musier-Forsyth, K. & Kiehl, R. A. *Selfassembly of metallic nanoparticle arrays by DNA scaffolding.* Journal of Nanoparticle Research. Vol. 4:4. 2002. pp. 313-317. DOI: 10.1023/A:1021145208328.

[206] Le, J. D., Pinto, Y., Seeman, N. C., Musier-Forsyth, K., Taton, T. A. & Kiehl, R. A. *DNA-Templated Self-Assembly of Metallic Nanocomponent Arrays on a Surface.* Nano Letters. Vol. 4:12. 2004. pp. 2343-2347. DOI: 10.1021/nl048635+.

[207] Pinto, Y. Y., Le, J. D., Seeman, N. C., Musier-Forsyth, K., Taton, T. A. & Kiehl, R. A. *Sequence-Encoded Self-Assembly of Multiple-Nanocomponent Arrays by 2D DNA Scaffolding.* Nano Letters. Vol. 5:12. 2005. pp. 2399-2402. DOI: 10.1021/nl0515495.

[208] Sharma, J., Ke, Y., Lin, C., Chhabra, R., Wang, Q., Nangreave, J., Liu, Y. & Yan, H. *DNA-Tile-Directed Self-Assembly of Quantum Dots into Two-Dimensional Nanopatterns.* Angewandte Chemie International Edition. Vol. 47:28. 2008. pp. 5157-5159. DOI: 10.1002/anie.200801485.

[209] Ke, Y., Ong, L. L., Sun, W., Song, J., Dong, M., Shih, W. M. & Yin, P. *DNA brick crystals with prescribed depths.* Nature Chemistry. Vol. 6:11. 2014. pp. 994-1002. DOI: 10.1038/nchem.2083.

[210] Ke, Y., Ong, L. L., Shih, W. M. & Yin, P. *Three-Dimensional Structures Self-Assembled from DNA Bricks.* Science. Vol. 338:6111. 2012. pp. 1177-1183. DOI: 10.1126/science.1227268.

[211] Zhang, J., Liu, Y., Ke, Y. & Yan, H. *Periodic Square-Like Gold Nanoparticle Arrays Templated by Self-Assembled 2D DNA Nanogrids on a Surface.* Nano Letters. Vol. 6:2. 2006. pp. 248-251. DOI: 10.1021/nl052210l.

[212] Carter, J. D. & LaBean, T. H. *Organization of Inorganic Nanomaterials via Programmable DNA Self-Assembly and Peptide Molecular Recognition.* ACS Nano. Vol. 5:3. 2011. pp. 2200-2205. DOI: 10.1021/nn1033983.

[213] Park, S. H., Yin, P., Liu, Y., Reif, J. H., LaBean, T. H. & Yan, H. *Programmable DNA Self-Assemblies for Nanoscale Organizations of Ligands and Proteins.* Nano Letters. Vol. 5:4. 2005. pp. 729-733. DOI: 10.1021/nl050175c.

[214] Sharma, J., Chhabra, R., Liu, Y., Ke, Y. & Yan, H. *DNA-Templated Self-Assembly of Two-Dimensional and Periodical Gold Nanoparticle Arrays.* Angewandte Chemie International Edition. Vol. 45:5. 2006. pp. 730-735. DOI: 10.1002/anie.200503208.

[215] Zheng, J., Constantinou, P. E., Micheel, C., Alivisatos, A. P., Kiehl, R. A. & Seeman, N. C. *Two-Dimensional Nanoparticle Arrays Show the Organizational Power of Robust DNA Motifs.* Nano Letters. Vol. 6:7. 2006. pp. 1502-1504. DOI: 10.1021/nl060994c.

[216] Schreiber, R., Do, J., Roller, E-M., Zhang, T., Schüller, V. J., Nickels, P. C., Feldmann, J. & Liedl, T. *Hierarchical assembly of metal nanoparticles, quantum dots and organic dyes using DNA origami scaffolds.* Nature Nanotechnology. Vol. 9:1. 2014. pp. 74-78. DOI: 10.1038/nnano.2013.253.

[217] Liu, W., Tagawa, M., Xin, H. L., Wang, T., Emamy, H., Li, H., Yager, K. G., Starr, F. W., Tkachenko, A. V. & Gang, O. *Diamond family of nanoparticle superlattices.* Science. Vol. 351:6273. 2016. pp. 582-586. DOI: 10.1126/science.aad2080.

[218] Tian, Y., Zhang, Y., Wang, T., Xin, H. L., Li, H. & Gang, O. *Lattice engineering through nanoparticle-DNA frameworks.* Nature Materials. Vol. 15:6. 2016. pp. 654-661. DOI: 10.1038/nmat4571.

[219] Zhang, T., Hartl, C., Fischer, S., Frank, K., Nickels, P., Heuer-Jungemann, A., Nickel, B. & Liedl, T. *3D DNA origami crystals.* arXiv preprint. 2017. Preprint available at arXiv: https://arxiv.org/abs/1706.06965.

[220] Liu, W., Mahynski, N. A., Gang, O., Panagiotopoulos, A. Z. & Kumar, S. K. *Directionally Interacting Spheres and Rods Form Ordered Phases.* ACS Nano. Vol. 11:5. 2017. pp. 4950-4959. DOI: 10.1021/acsnano.7b01592.

[221] Yonezawa, T. Onoue, S-Y. & Kimizuka, N. *Metal Coating of DNA Molecules by Cationic, Metastable Gold Nanoparticles.* Chemistry Letters. Vol. 31:12. 2002. pp. 1172-1173. DOI: 10.1246/cl.2002.1172.

[222] Nakao, H., Shiigi, H., Yamamoto, Y., Tokonami, S., Nagaoka, T., Sugiyama, S. & Ohtani, T. *Highly Ordered Assemblies of Au Nanoparticles Organized on DNA.* Nano Letters. Vol. 3:10. 2003. pp. 1391-1394. DOI: 10.1021/nl034620k.

[223] Wang, G. & Murray, R. W. *Controlled Assembly of Monolayer-Protected Gold Clusters by Dissolved DNA.* Nano Letters. Vol. 4:1. 2004. pp. 95-101. DOI: 10.1021/nl034922m.

[224] Woehrle, G. H., Warner, M. G. & Hutchison, J. E. *Molecular-Level Control of Feature Separation in One-Dimensional Nanostructure Assemblies Formed by Biomolecular Nanolithography.* Langmuir. Vol. 20:14. 2004. pp. 5982-5988. DOI: 10.1021/la049491h.

[225] Hassinen, J., Liljeström, V., Kostiainen, M. A. & Ras, R. H. A. *Rapid Cationization of Gold Nanoparticles by Two-Step Phase Transfer.* Angewandte Chemie International Edition. Vol. 54:27. 2015. pp. 7990-7993. DOI: 10.1002/anie.201503655.

[226] Jiang, T., Meyer, T. A., Modlin, C., Zuo, X., Conticello, V. P. & Ke, Y. *Structurally Ordered Nanowire Formation from Co-Assembly of DNA Origami and Collagen-Mimetic Peptides.* Journal of the American Chemical Society. Vol. 139:40. 2017. pp. 14025-14028. DOI: 10.1021/jacs.7b08087.

[227] Linko, V., Shen, B., Tapio, K., Toppari, J. J., Kostiainen, M. A. & Tuukkanen, S. *One-step large-scale deposition of salt-free DNA origami nanostructures.* Scientific Reports. Vol. 5. 2015. 15634. DOI: 10.1038/srep15634.

[228] Wilson, K. & Walker, J. *Principles and Techniques of Biochemistry and Molecular Biology.* 6th ed. New York: Cambridge University Press, 2005. 783 pp. ISBN: 0-521-53581-6.

[229] Hung, A. M., Micheel, C. M., Bozano, L. D., Osterbur, L. W., Wallraff, G. M. & Cha, J. N. *Large-area spatially ordered arrays of gold nanoparticles directed by lithographically confined DNA origami.* Nature Nanotechnology. Vol.5:2. 2010. pp. 121-126. DOI: 10.1038/nnano.2009.450.

[230] Brust, M., Walker, M., Bethell, D., Schiffrin, D. J. & Whyman, R. *Synthesis of Thiol-derivatised Gold Nanoparticles in a Two-phase Liquid-Liquid System.* Journal of the Chemical Society, Chemical Communications. Vol. 7. 1994. pp. 801-802. DOI: 10.1039/C39940000801.

[231] Storhoff, J. J., Elghanian, R., Mucic, R., Mirkin, C. A. & Letsinger, R. L. *One-Pot Colorimetric Differentiation of Polynucleotides with Single Base Imperfections Using Gold Nanoparticle Probes.* Journal of the American Chemical Society. Vol. 120:9. 1998. pp. 1959-1964. DOI: 10.1021/ja972332i.

[232] Schnablegger, H. & Singh, Y. *The SAXS guide: Getting acquainted with the principles.* 3rd ed. Graz: Anton Paar GmbH, 2013. 122 pp. ISBN: 18012013.

[233] Mastronarde, D. N. *SerialEM: A Program for Automated Tilt Series Acquisition on Tecnai Microscopes Using Prediction of Specimen Position.* Microscopy and Microanalysis. Vol. 9:S02. 2003. pp. 1182-1183. DOI: 10.1017/S1431927603445911.

[234] Kremer, J. R., Mastronarde, D. N. & McIntosh, J. R. *Computer Visualization of Three-Dimensional Image Data Using IMOD.* Journal of Structural Biology. Vol. 116:1. 1996. pp. 71-76. DOI: 10.1006/jsbi.1996.0013.

[235] Engelhardt, P. *Electron Tomography of Chromosome Structure.* Encyclopedia of Analytical Chemistry. Vol. 6. 2006. pp. 4948-4984. DOI: 10.1002/9780470027318.a1405.

[236] Kewalramani, S., Guerrero-García, G. I., Moreau, L. M., Zwanikken, J. W., Mirkin, C. A., Olvera de la Cruz, M. & Bedzyk, M. J. *Electrolyte-Mediated Assembly of Charged Nanoparticles.* ACS Central Science. Vol. 2:4. 2016. pp. 219-224. DOI: 10.1021/acscentsci.6b00023.

[237] Kraus, W. & Nolze, G. *POWDER CELL - a program for the representation and manipulation of crystal structures and calculation of the resulting X-ray powder patterns.* Journal of Applied Crystallography. Vol. 29:3. 1996. pp. 301-303. DOI: 10.1107/S0021889895014920.

[238] Pedersen, J. S. *Determination of Size Distributions from Small-Angle Scattering Data for Systems with Effective Hard-Sphere Interactions.* Journal of Applied Crystallography. Vol. 27:4. 1994. pp. 595-608. DOI: 10.1107/S0021889893013810.

[239] Niemeyer, C. M. *Self-assembled nanostructures based on DNA: towards the development of nanobiotechnology.* Current Opinion in Chemical Biology. Vol. 4:6. 2000. pp. 609-618. DOI: 10.1016/S1367-5931(00)00140-X.

Appendix A

Staple strands for DNA origami 6HB

A complete list of the 170 staple strands required for the DNA origami 6HB structure are listed below. The DNA origami 6HB design is with some adjustments adapted from Bui *et al.* [130]. In the new design, the extended staple strands in the original design have been replaced with shorter staple strands of normal length.

No.	Sequence	Bases
1	GCCAGAGGGGGTAAAGACTCCTTATTACAACG-CAAAGACACC	42
2	CAATACTGCGGAATAACGCAATAATAACATAG-AAAATTCATA	42
3	AAATGCTTTAAACATAAGCAGATAGCCGCGAC-ATTCAACCGA	42
4	AAAAATCAGGTCTTAAATAGCAATAGCTAAATT-ATTCATTAA	42
5	GCGGATTGCATCAACAAGAATTGAGTTAGCCA-TTTGGGAATT	42
6	CAAATATCGCGTTTAGTCAGAGGGTAATTTACC-ATTAGCAAG	42
7	GGAAGCAAACTCCAGAAGCGCATTAGACATAG-CAGCACCGTA	42
8	TTGCTCCTTTTGATTGAAAATAGCAGCCTTAGC-GTCAGACTG	42
9	GCTTAATTGCTGAACCCAATCCAAATAAATAGC-CCCCTTATT	42

10	ATATGCAACTAAAGGCCTAATTTGCCAGTCACC-GGAACCAGA	42
11	AACAGTTGATTCCCTTTATCCTGAATCTCCGCC-ACCCTCAGA	42
12	ACCATTAGATACATCCTTAAATCAAGATGAGCC-GCCACCAGA	42
13	TATATTTTCATTTGAGGCGTTTTAGCGAACAGG-AGTTAGACT	42
14	TCTACTAATAGTAGCAAATCAGATATAGATCCT-TTGCCCGAA	42
15	GCAAGGCAAAGAATTTTATTTTCATCGTATTAT-CATTTTGCG	42
16	GCATAAAGCTAAATATTAAACCAAGTACATTAT-CATCATATT	42
17	TAATACTTTTGCGGATCAATAATCGGCTAATAT-AATCCTGAT	42
18	AAAATTTTTAGAACAAAAATAATATCCCAGGGT-TAGAACCTA	42
19	GTAATGTGTAGGTAAGAACGCGCCTGTTAGAA-ATAAAGAAAT	42
20	GACAGTCAAATCACTCTGTCCAGACGACTGAAT-ATACAGTAA	42
21	TGATAAATTAATGCAGTAATAAGAGAATAACG-GATTCGCCTG	42
22	TACAAAGGCTATCAAACAACGCCAACATGCGCA-GAGGCGAAT	42
23	AAGAGAATCGATGACCAACGCTCAACAGAGAT-GATGAAACAA	42
24	CATATGTACCCCGGTTTAGTATCATATGTAACA-ATTTCATTT	42
25	GAAGATTGTATAAGATAAGAATAAACACATAA-ATCAATATAT	42
26	TTTGTTAAAATTCGTAATGGTTTGAAATCGTCG-CTATTAATT	42
27	TTTTAACCAATAGGTTTCAAATATATTTAGCGA-TAGCTTAGA	42
28	CCTTCCTGTAGCCATGATGCAAATCCAAATTTA-TCAAAATCA	42
29	TATCATAACCCTCGCGTCTTTCCAGACGGTACA-AACTACAAC	42

30	CATAACGCCAAAAGTTGCTAAACAACTTCCAAT-AGGAACCCA	42
31	TCAGTTGAGATTTAAAGGAACAACTAAACCACC-CTCAGAGCC	42
32	AACGAACTAACGGATGAAAATCTCCAAAGGTT-TAGTACCGCC	42
33	TATACCAGTCAGGAGTATCGGTTTATCAATATA-AGTATAGCC	42
34	ATCATTGTGAATTAAGCTTGATACCGATTTTTG-CTCAGTACC	42
35	CGAGTAGTAAATTGGCCCACGCATAACCAGAG-GCTGAGACTC	42
36	TCATTCAGTGAATAGAGTTAAAGGCCGCTGCC-TATTTCGGAA	42
37	AGAACCGGATATTCAAAGACAGCATCGGGTGC-CTTGAGTAAC	42
38	GGCGCATAGGCTGGTTGAGGACTAAAGAGATG-ATACAGGAGT	42
39	TGACCAACTTTGAAGGGTAAAATACGTATCTCT-GAATTTACC	42
40	GCCGGAACGAGGCGCGAAAGAGGCAAAACAAA-CAAATAAATC	42
41	GATAAATTGTGTCGCCCAGCGATTATACAGAA-GTAGTTGAGG	42
42	TTTGCGTATTGGGCTCTTTTCACCAGTGTAATA-GATTAGAGC	42
43	CCAGCTGCATTAATCGCCTGGCCCTGAGTTGAG-GAAGGTTAT	42
44	GTTGCGCTCACTGCTTGCCCCAGCAGGCAATCA-ATATCTGGT	42
45	AGCCTGGGGTGCCTATCGGCAAAATCCCATCTA-AAGCATCAC	42
46	CACAATTCCACACAGGGTTGAGTGTTGTGCCT-GCAACAGTGC	42
47	ATCATGGTCATAGCAAGAACGTGGACTCAGCA-GAAGATAAAA	42
48	GTCGACTCTAGAGGCAGGGCGATGGCCCTAGC-CCTAAAACAT	42
49	CGTTGTAAAACGACTTTTTGGGGTCGAGCAAT-ATTTTTGAAT	42

50	AGGCGATTAAGTTGAAAGGGAGCCCCCGAGAA-CCCTTCTGAC	42
51	TCTTCGCTATTACGAACGTGGCGAGAAACACAC-GACCAGTAA	42
52	TTCAGGCTGCGCAAGCTAGGGCGCTGGCAATC-GTCTGAAATG	42
53	ACCGCTTCTGGTGCACCACACCCGCCGCAACAG-GAAAAACGC	42
54	GTATCGGCCTCAGGTATGGTTGCTTTGACTTG-CTGGTAATAT	42
55	GCATCGTAACCGTGAGAATCAGAGCGGGAATA-ACATCACTTG	42
56	GGATTGACCGTAATTTTAGACAGGAACGATCA-CGCAAATTAA	42
57	ATCTAAAGTTTTGTTTTACCAGACGACGGCAAA-AGAAGTTTT	42
58	ATGAATTTTCTGTATGGGATTGAATTACGAGG-CATGACTGGATAGCGTC	49
59	TTTCAGCGGAGTGAGAATAGAGGAATACCACA-TTCATTGAATCCCCCTC	49
60	CGAATAATAATTTTTTCACGTACAACATTATTA-CAAATGACCATAAATC	49
61	AGGAGCCTTTAATTCGTTGGGAAGAAAATAGT-CAGAAGCAAA	42
62	TGAATTTCTTAAACCCTTATGCGATTTTAGCCC-GAAAGACTT	42
63	TGACAACAACCATCGGCTTGAGATGGTTAAGC-GAACCAGACC	42
64	CTGAGGCTTGCAGGAGGCTTGCCCTGACGAGA-GTACCTTTAA	42
65	CACCCTCAGCAGCGATTACCCAAATCAAGCGGA-TGGCTTAGA	42
66	CGGCTACAGAGGCTCTGACCTTCATCAATCAAC-ATGTTTTAA	42
67	AGTTTCCATTAAACAGAGGACAGATGAAGTTT-CATTCCATAT	42
68	GCACCAACCTAAAACAGACGGTCAATCAGTAG-ATTTAGTTTG	42
69	ACTCATCTTTGACCAAATCCGCGACCTGATAAC-CTGTTTAGC	42

70	GAAACAAAGTACAATGGTTTTGCCAGGGCGGA-GATAAGGTGGCATCAAT	49
71	CAACAGCTGATTGCCCTTCACGAATCGGCCAAC-GCAATAAATCATACAG	49
72	CAGCAAGCGGTCCACGCTGGTCCGCTTTCCAGT-CGAATAAAGCCTCAGA	49
73	ATGGTGGTTCCGAAAATGAGTGAGCTAAACAT-TATGACCCTG	42
74	AATAGCCCGAGATAACATACGAGCCGGATCAA-CGCAAGGATA	42
75	AGAGTCCACTATTATGTTTCCTGTGTGAAATGC-AATGCCTGA	42
76	GAAAAACCGTCTATATCCCCGGGTACCGTGAG-AAAGGCCGGA	42
77	CACCCAAATCAAGTGGCCAGTGCCAAGCTCAAC-CGTTCTAGC	42
78	TAAATCGGAACCCTGGTAACGCCAGGGTATTT-TTGAGAGATC	42
79	GGGGAAAGCCGGCGCCAGCTGGCGAAAGAGTC-TGGAGCAAAC	42
80	CGAAAGGAGCGGGCCTGTTGGGAAGGGCACTA-GCATGTCAAT	42
81	CGCTGCGCGTAACCCGGAAACCAGGCAAAGCC-CCAAAAACAG	42
82	GCGCCGCTACAGGGCGCGTACAAGATCGCACT-CCAGTAAACGTTAATAT	49
83	GTATAACGTGCTTTCCTCGTTCATCTGCCAGTT-TGTAAATCAGCTCATT	49
84	CAGGAGGCCGATTAAAGGGATGGGATAGGTCA-CGTTAATTCGCGTCTGG	49
85	TGAGAAGTGTTTTTCGTCGGATTCTCCGTAAAT-GTGAGCGAG	42
86	GCCTGTAGCATTCCCAACATATAAAAGAGCAGT-ATGTTAGCA	42
87	TGTACCGTAACACTTTTTGTCACAATCAGGAAT-ACCCAAAAG	42
88	ACCACCCTCATTTTCAAAGACAAAAGGGAACAA-AGTTACCAG	42
89	ACCCTCAGAACCGCGTAAATATTGACGGATCTT-ACCGAAGCC	42

90	CGGAATAGGTGTATCGTCACCGACTTGAAGCCCAATAATAAG	42
91	AGGCGGATAAGTGCCACCAGTAGCACCATGAGCGCTAATATC	42
92	CTCAAGAGAAGGATCAATGAAACCATCGGGGAGAATTAACTG	42
93	CCTATTATTCTGAAAATCAAGTTTGCCTTTTACAGAGAGAAT	42
94	AGTGCCCGTATAAACGGCATTTTCGGTCGAAACGATTTTTTG	42
95	GTACTGGTAATAAGTTTCATAATCAAAATTACAAAATAAACA	42
96	GTTCCAGTAAGCGTCGCCTCCCTCAGAGTACCAACGCTAACG	42
97	CTCATTAAAGCCAGAGCCACCACCCTCATAGTTGCTATTTTG	42
98	CAGGTCAGACGATTCGCCGCCAGCATTGACCTCCCGACTTGC	42
99	CGTCAATAGATAATACAACTCGTATTAAAAGGCTTATCCGGT	42
100	CTAAAATATCTTTAAAAGTTTGAGTAACAGGAATCATTACCG	42
101	CAGTTGGCAAATCACCAGAAGGAGCGGACGCACTCATCGAGA	42
102	CTTGCTGAACCTCAGATGGCAATTCATCGTCTTTCCTTATCA	42
103	CACGCTGAGAGCCATTCTGAATAATGGAATCCTAATTTACGA	42
104	CAGAGGTGAGGCGGTTTGCACGTAAAACTATCAACAATAGAT	42
105	CGCCATTAAAAATAGGTTTAACGTCAGAGACAATAAACAACA	42
106	GGCTATTAGTCTTTTCGGGAGAAACAATATAAAGTACCGACA	42
107	CTGAAAGCGTAAGACAAGTTACAAAATCGTAATTTAGGCAGA	42
108	TAAAAGGGACATTCACCTGAGCAAAAGATAGGGCTTAATTGA	42
109	GATTATTTACATTGAAATTAATTACATTCGTTATACAAATTC	42

110	TCATGGAAATACCTAATGGAAACAGTACCGGA-ATCATAATTA	42
111	CCAGAACAATATTATTGCTTCTGTAAATACCGA-CCGTGTGAT	42
112	CCTGAGTAGAAGAAATCCTTGAAAACATTAGT-TAATTTCATC	42
113	CCGTTGTAGCAATAAGAGTCAATAGTGATCGC-AAGACAAAGA	42
114	TGAGGCCACCGAGTTACCTTTTTAACCTGTTGG-GTTATATAA	42
115	ACGGAATAAGTTTAGAGTTTCGTCACCATTAGT-AA	35
116	TGGTTTACCAGCGCCAGGGATAGCAAGCTCAA-CAG	35
117	TTGAGGGAGGGAAGCACCCTCAGAACCGGGAA-TTG	35
118	AGGTGAATTATCACCACCGTACTCAGGAAAAA-AGGCTCCAAA	42
119	AGAGCCAGCAAAATCGTCGAGAGGGTTGGCTT-GCTTTCGAGG	42
120	GCCGGAAACGTCACTAGGATTAGCGGGGAGTT-GCGCCGACAA	42
121	ATCAGTAGCGACAGACATGAAAGTATTAGATA-TATTCGGTCG	42
122	TAGCGCGTTTTCATCAGTTAATGCCCCCTTTTG-CGGGATCGT	42
123	AGCGTTTGCCATCTTTTTAACGGGGTCAAACGA-GGGTAGCAA	42
124	GCCACCACCGGAACCATACATGGCTTTTCTTTT-TCATGAGGA	42
125	ACCGCCACCCTCAGAATGGAAAGCGCAGATGC-CACTACGAAG	42
126	ACCACCACCAGAGCGGCCTTGATATTCAGAATA-CACTAAAAC	42
127	TTACAAACAATTCGACATTTGAGGATTTCAAGC-GC	35
128	CGTTATTAATTTTAGGAGCACTAACAACAGACG-GG	35
129	GAACAAAGAAACCAACAGTTGAAAGGAAAGAG-TTG	35

130	CCTGATTATCAGATAATATCAAACCCTCGAAAA-TCCTGTTTG	42
131	TGTTTGGATTATACGCAGCAAATGAAAATTAT-AAATCAAAAG	42
132	CCATATCAAAATTATCAGTATTAACACCTCCAG-TTTGGAACA	42
133	TGCGTAGATTTTCACCGAACGAACCACCCAACG-TCAAAGGGC	42
134	CAGTACCTTTTACAAATGCGCGAACTGAACTAC-GTGAACCAT	42
135	ATTGCTTTGAATACATACGTGGCACAGAGTGC-CGTAAAGCAC	42
136	TATTCATTTCAATTTGGCCAACAGAGATATTTA-GAGCTTGAC	42
137	ACATCAAGAAAACAGCAGATTCACCAGTGGAA-GGGAAGAAAG	42
138	GAATTACCTTTTTTACATTTTGACGCTCAAGTG-TAGCGGTCA	42
139	GTGAGTGAATAACCCCGCCAGCCATTGCGCTTA-AT	35
140	AATTTTCCCTTAGACTCAAACTATCGGCCGAGC-AC	35
141	TTAAGACGCTGAGACTTCTTTGATTAGTAGCTA-AA	35
142	TAGGTCTGAGAGACAAAAGAGTCTGTCCGTAC-GCCAGAATCC	42
143	AACTGGCATGATTATAGTAAAATGTTTAAGTA-AGAGCAACAC	42
144	AAGGAAACCGAGGACGTCATAAATATTCAACT-AATGCAGATA	42
145	CTTTTTAAGAAAAGGTTCAGAAAACGAGGGTA-GAAAGATTCA	42
146	AGCAAGAAACAATGTACCCTGACTATTAATCTA-CGTTAATAA	42
147	AGAGAGATAACCCAAAAGATTAAGAGGAAAGA-ACTGGCTCAT	42
148	AACACCCTGAACAATAATTCGAGCTTCATAATT-TCAACTTTA	42
149	AACATAAAAACAGGACAGGTCAGGATTAGAGA-AACACCAGAA	42

150	TTTAACGTCAAAAAAAGAGGTCATTTTTCGTAA-CAAAGCTGC	42
151	GCCATATTATTTATTATAATGCTGTAGCGAGTA-ATCTTGACA	42
152	AGCGTCTTTCCAGATACGGTGTCTGGAACGGT-GTACAGACCA	42
153	CACCCAGCTACAATAATTCTGCGAACGATAAGG-GAACCGAAC	42
154	GGGAGGTTTTGAAGTTCGCAAATGGTCACTCC-ATGTTACTTA	42
155	ATTCTAAGAACGCGGGGCGCGAGCTGAATTGT-ATCATCGCCT	42
156	CGCCCAATAGCAAGTAGCATTAACATCCGCGG-GGAGAGGCGG	42
157	ACAAGCAAGCCGTTTAGCAAAATTAAGCGGAA-ACCTGTCGTG	42
158	TTCCAAGAACGGGTCGGTTGTACCAAAACTCAC-ATTAATTGC	42
159	GCATGTAGAAACCAGAGAAGCCTTTATTAGCA-TAAAGTGTAA	42
160	AAGTCCTGAACAAGCCTCATATATTTTAAATTG-TTATCCGCT	42
161	TGTTCAGCTAATGCAAGATTCAAAAGGGAGCT-CGAATTCGTA	42
162	AAAGGTAAAGTAATCATCAATATGATATTTGCA-TGCCTGCAG	42
163	GGCATTTTCGAGCCCGGAGAGGGTAGCTTTTC-CCAGTCACGA	42
164	GAATCGCCATATTTGGTCATTGCCTGAGGGGG-ATGTGCTGCA	42
165	TTACCAGTATAAAGACGGTAATCGTAAAGATC-GGTGCGGGCC	42
166	CTAGAAAAAGCCTGTTGATAATCAGAAAAGCG-CCATTCGCCA	42
167	AAATAAGGCGTTAACAAATATTTAAATTGCCAG-CTTTCCGGC	42
168	TTCTGACCTAAATTCATTAAATTTTTGTAGGGG-ACGACGACA	42
169	ACGCGAGAAAACTTAACGCCATCAAAAATGGT-GTAGATGGGC	42

170	CTATATGTAAATGCGCTTTCATCAACATTGGGA-ACAAACGGC	42

Appendix B

AuNP binding properties of DNA origami nanostructures

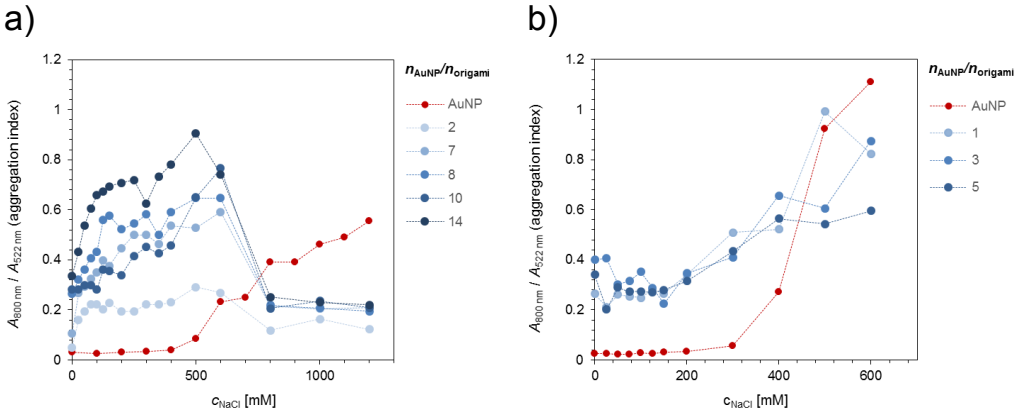

Figure B.1: Colloidal stability of the AuNPs when also DNA origami structures are present in the solution. The colloidal stability is measured by UV/Vis spectroscopy and determined as a function of the ionic strength by the aggregation index, $A_{800\text{nm}}/A_{520\text{nm}}$. The AuNP concentration is kept constant ($c_{\text{AuNP}} = 6$ nM), but the DNA origami concentration varied bet ween the series and is given as the AuNP to DNA origami ratio ($n_{\text{AuNP}}/n_{\text{origami}}$) in the legend. a) DNA origami 24HB and middle-sized AuNPs ($D_{\text{core}} = 10.9$ nm) b) DNA origami 60HB and large AuNPs ($D_{\text{core}} = 12.4$ nm).

Appendix C

DNA origami 6HB and small AuNP

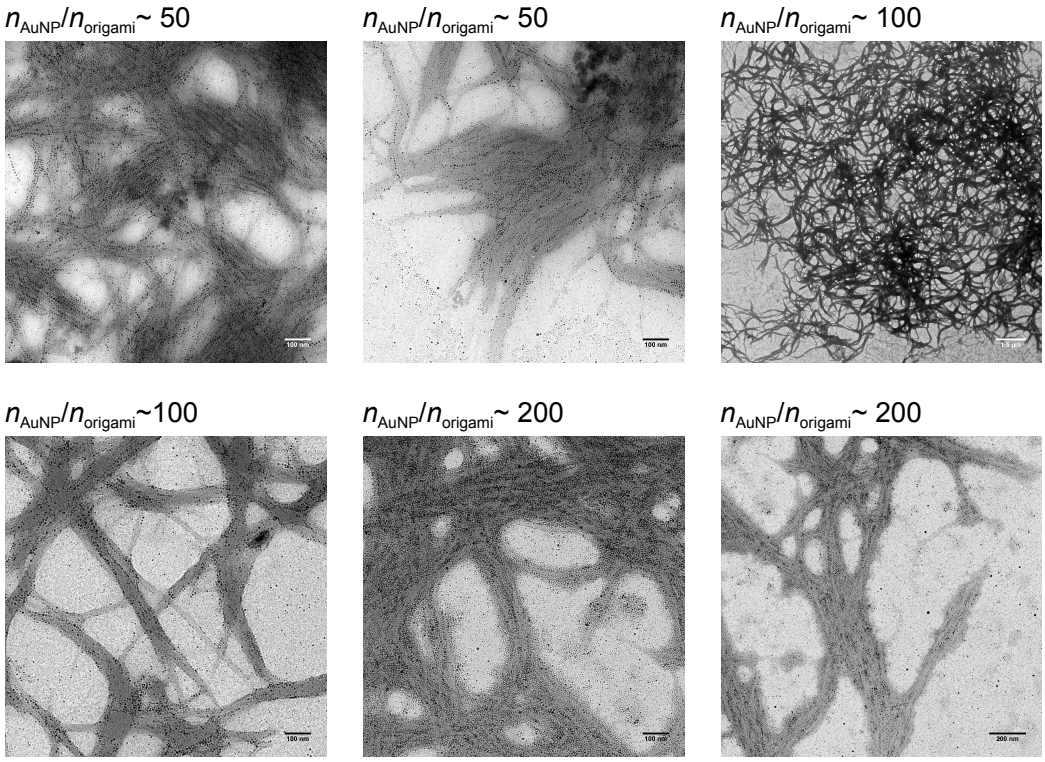

Figure C.1: Electrostatic self-assembly of DNA origami 6HB structures and small AuNPs ($D_{\text{core}} = 2.5$ nm) yielded well-ordered superlattice structures.

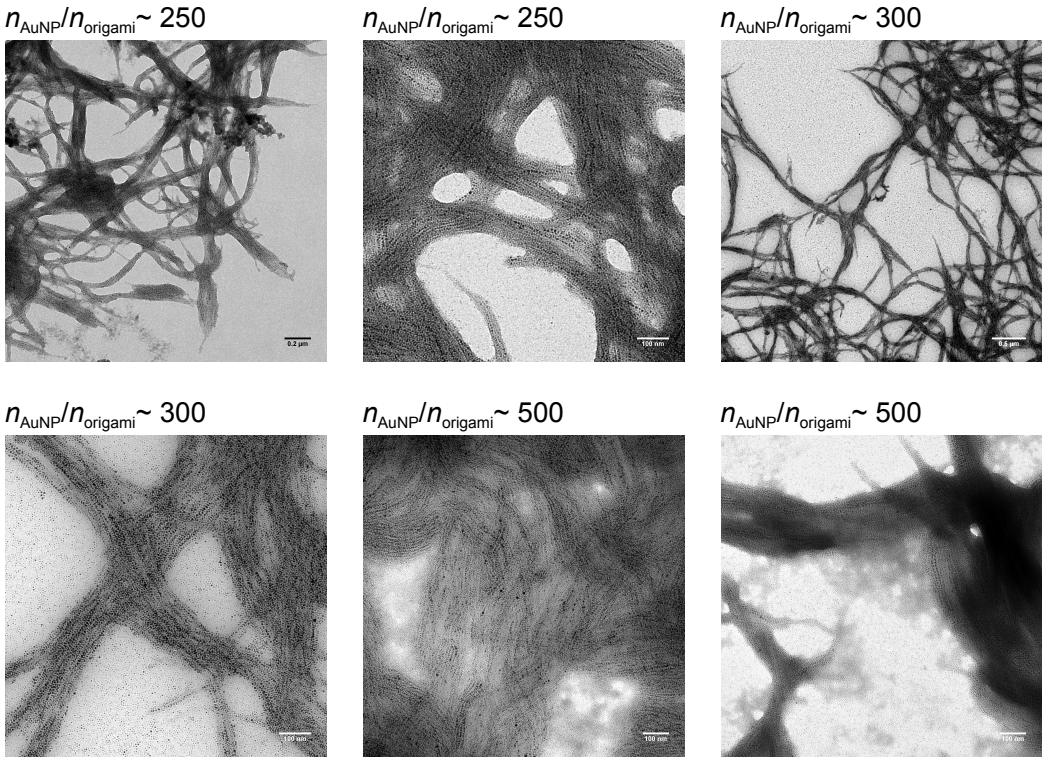

Figure C.2: Electrostatic self-assembly of DNA origami 6HB structures and small AuNPs ($D_{\text{core}} = 2.5$ nm) yielded well-ordered superlattice structures.

Appendix D

DNA origami 6HB and middle-sized AuNP

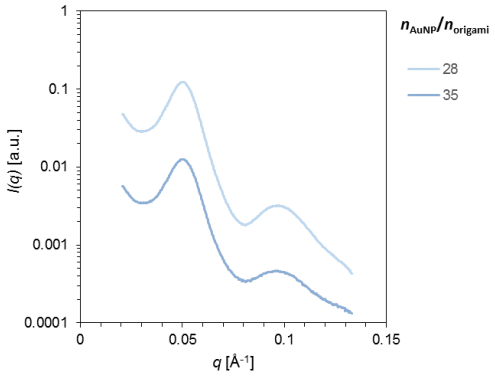

Figure D.1: SAXS data measured from samples having different stoichiometric ratios between middle-sized AuNPs ($D_{\mathrm{core}} = 10.9$ nm) and DNA origami 6HB structures ($n_{\mathrm{AuNP}}/n_{\mathrm{origami}}$).

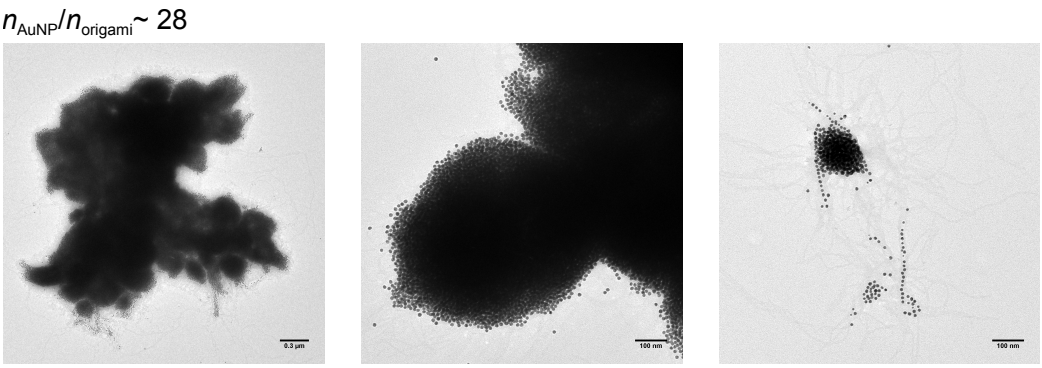

Figure D.2: Electrostatic self-assembly of DNA origami 6HB structures and middle-sized AuNPs ($D_{\mathrm{core}} = 10.9$ nm) yielded amorphous aggregates.

Appendix E

DNA origami 24HB and middle-sized AuNP

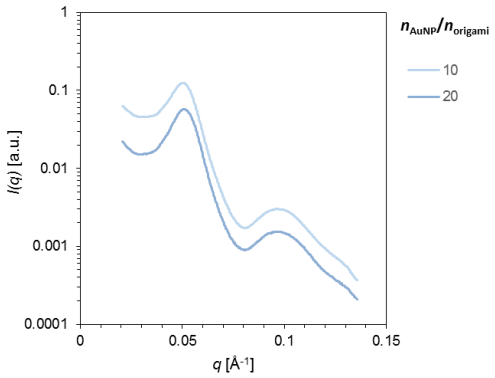

Figure E.1: SAXS data measured from samples having different stoichiometric ratios between middle-sized AuNPs ($D_{\mathrm{core}} = 10.9$ nm) and DNA origami 24HB structures ($n_{\mathrm{AuNP}}/n_{\mathrm{origami}}$).

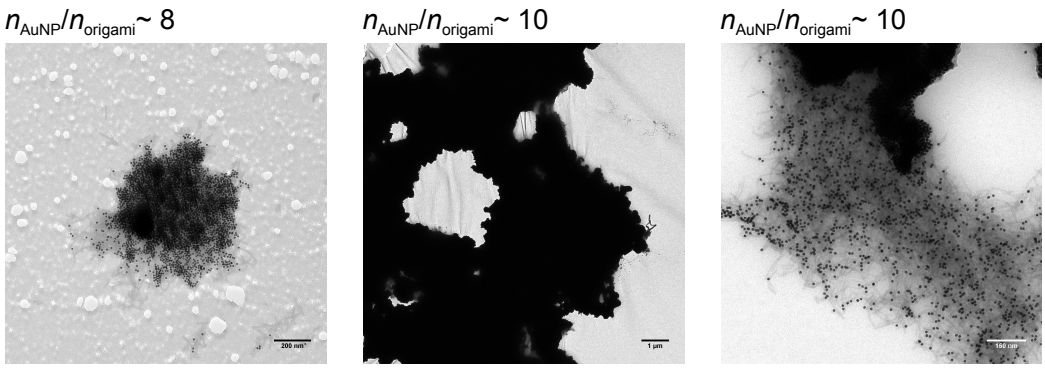

Figure E.2: Electrostatic self-assembly of DNA origami 24HB structures and middle-sized AuNPs ($D_{\mathrm{core}} = 10.9$ nm) yielded amorphous aggregates.

Appendix F

DNA origami 60HB and large AuNP

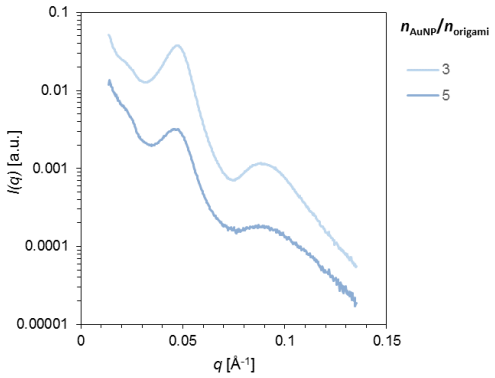

Figure F.1: SAXS data measured from samples having different stoichiometric ratios between large AuNPs ($D_{\mathrm{core}} = 12.4$ nm) and DNA origami 60HB structures ($n_{\mathrm{AuNP}}/n_{\mathrm{origami}}$).

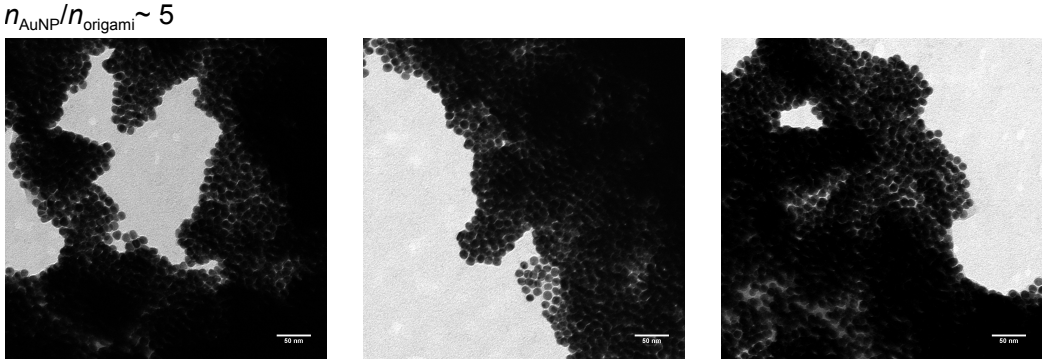

Figure F.2: Electrostatic self-assembly of DNA origami 60HB structures and large AuNPs ($D_{\text{core}} = 12.4$ nm) yielded amorphous aggregates.